NASA CR - 145167
(SER - 50983)

STUDY TO INVESTIGATE DESIGN, FABRICATION AND TEST OF LOW COST CONCEPTS FOR LARGE HYBRID COMPOSITE HELICOPTER FUSELAGE - PHASE II

by

K. M. Adams and J. J. Lucas

April 1977

Prepared under Contract No. NASI-13479

by

Sikorsky Aircraft

Division of United Technologies Corporation,

Stratford, Conn.

for

NASA

National Aeronautics and Space Administration

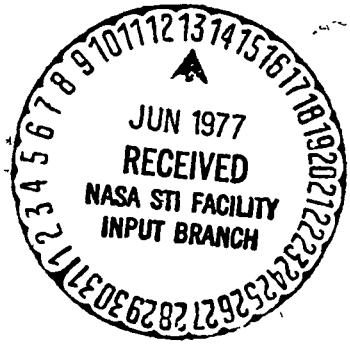

NASA CR - 145167
(SER - 50983)

STUDY TO INVESTIGATE DESIGN, FABRICATION AND TEST OF LOW COST CONCEPTS FOR LARGE HYBRID COMPOSITE HELICOPTER FUSELAGE - PHASE II

by

K. M. Adams and J. J. Lucas

April 1977

Prepared under Contract No. NASI-13479

by

Sikorsky Aircraft

Division of United Technologies Corporation,

Stratford, Conn.

for

National Aeronautics and
Space Administration

FOREWORD

This report was prepared by Sikorsky Aircraft, Division of United Technologies Corporation, under NASA contract NAS1-13479 and covers the work performed during the period September 1975 through October 1976. This report is the final Phase II report and summarizes the Phase II activity. This program was jointly funded by the Materials Division of NASA-Langley Research Center and the U. S. Army Air Mobility Research and Development Laboratory (Langley Directorate). The NASA-Langley Technical Monitor for this contract was Dr. R. L. Foye. The Sikorsky Aircraft Program Manager was J. J. Lucas.

The authors wish to acknowledge the contributions of the following Sikorsky personnel: S. Svensson, Materials Engineering; D. Lowry, Structures Engineering; C. Cooper and F. Tarulli, Test Engineering; and K. Schneider, Manufacturing Engineering.

UNITS

Dimensional information is presented in the International System of Units (S.I.). The equivalent values in the U. S. customary system are shown in parentheses. All calculations were performed in the customary system and converted to the S.I. units.

TABLE OF CONTENTS

LIST OF ILLUSTRATIONS

LIST OF ILLUSTRATIONS (Cont'd)

LIST OF ILLUSTRATIONS (Cont'd)

LIST OF ILLUSTRATIONS (Cont'd)

LIST OF TABLES

STUDY TO INVESTIGATE THE DESIGN, FABRICATION, AND TEST OF LOW COST CONCEPTS FOR LARGE HYBRID COMPOSITE HELICOPTER FUSELAGE PHASE II

by

K.M. Adams and J.J. Lucas

Sikorsky Aircraft
Division of United Technologies
Stratford, Connecticut

SUMMARY

The development of a frame/stringer/skin fabrication technique for composite airframe construction promises to provide a low cost approach to the manufacturer of large helicopter airframe components. This low cost fabrication technique is dependent on the development of a single cure of the assembled composite structure, the selection of cure compatible constituent materials which comprise that structure, and the utilization of an economical and reliable tooling concept to produce the structure.

A center cabin aluminum airframe section of the Sikorsky CH-53D, a typical current production transport helicopter, was selected for evaluation as a composite structure. The design, as developed, is composed of a woven KEVLAR ^{R}-49/epoxy skin and graphite/epoxy frames and stringers. The single cure concept is made possible by the utilization of pre-molded foam cores, over which the graphite/epoxy pre-impregnated frame and stringer reinforcements are positioned. Bolted composite channel sections were selected as the optimum joint construction.

This report summarizes the work accomplished in Phase II of a three phase effort. In Phase I, reported in NASACR-132731 (Ref. 1), manufacturing and materials studies were conducted to evaluate materials and manufacturing methods suitable for the manufacture of a low cost composite airframe structure utilizing a single cure concept to produce a frame/stringer/skin fuselage section. Tooling studies were conducted to evaluate and choose a tooling concept suited to the single cure concept. Representative frame/stringer/skin sections were selected, analyzed, and designed for composite fabrication.

Individual frame and stringer test specimens were fabricated from the selected materials, utilizing the tooling concepts developed, and statically tested. The predicted failure loads were in good to excellent agreement with test data.

To verify the applicability of the single cure concept to larger realistic curved airframe sections, and the durability of the composite structure in a realistic spectrum fatigue environment, the work described in this Phase II report was accomplished.

Utilizing all of the techniques developed in the Phase I study, a detail design for a fuselage composite shell section was prepared. In this design the frame elements consisted of a straight (test) section, with a curved section at each end. The curved areas incorporated into the design simulate the maximum curvature of a CH-53D cabin section. The actual 102 cm (40 in.) x 173 cm (68 in.) shell section fabricated consisted of a Kevlar-49/epoxy composite skin, four graphite/epoxy reinforced frame elements and five graphite/epoxy and Kevlar-49/epoxy reinforced stringer-elements. A shell tool, the concept for which was developed in Phase I of this program was designed and fabricated to manufacture the composite shell sections.

Two composite shell sections were fabricated, one for frame fatigue tests and one for frame splice joint fatigue tests. Each shell section was cut to provide four single frame specimens for fatigue testing and display.

Each test specimen was subjected to a realistic accelerated 4000 hour spectrum fatigue test, and then if structurally intact, statically loaded in compression and bending to fracture to determine the residual strength.

Failure analysis was conducted on each specimen to establish fracture modes and evaluate design adequacy. Evaluation of test results indicate the basic design concept to be valid, the tooling concept good, and the fabrication technique to be acceptable for the manufacture of low cost composite airframe sections by the single cure method. No problems were encountered with the joint design, however, radial compressive loads in curved sections caused initial problems that necessitated some design modifications.

A weight reduction of 18 percent, compared to a conventional aluminum skin/stringer/frame airframe was calculated for the composite CH-53D airframe. Acquisition cost of a production composite CH-53D aircraft is reduced by 0.3 percent, and when coupled with the increased vehicle productivity due to the weight reduction of the composite vehicle, fleet size is reduced, and a savings of 6.5 percent is realized in the 10 year life cycle cost to provide comparable mission capabilities.

In Phase III of this program, an additional study will be conducted to demonstrate the practicality of the low cost concept as applied to the design and fabrication of highly loaded attachments such as encountered in the transmission to fuselage attachment area.

SECTION 1.0 INTRODUCTION

Many paper studies have been generated, which show impressive savings in cost and weight through the use of composite materials. A significant number of these concepts have been proven to be less than successful during the gestation period between conception and production, when savings, performance and reliability improvements vanished. Other concepts were carried through to reality only to find that the resulting product was marked more by change than accomplishment of the original goals of product improvement or cost reduction. Although much valuable information and experience has been obtained in these programs, the only major accomplishment was to prove that composite materials are adaptable as a replacement for conventional metallic materials.

The objective of the Phase II effort described herein is to structurally evaluate one single cure concept as applied to the manufacture of composite airframe sections, composed of frame, skin and stringer elements. Phase I demonstrated the static strength capability of this construction. This phase demonstrates the feasibility of manufacture of large curved sections, as shown in Figure 1, and verifies the structural characteristics of both frame and frame splice joint sections under a realistic accelerated spectrum fatigue test of these components.

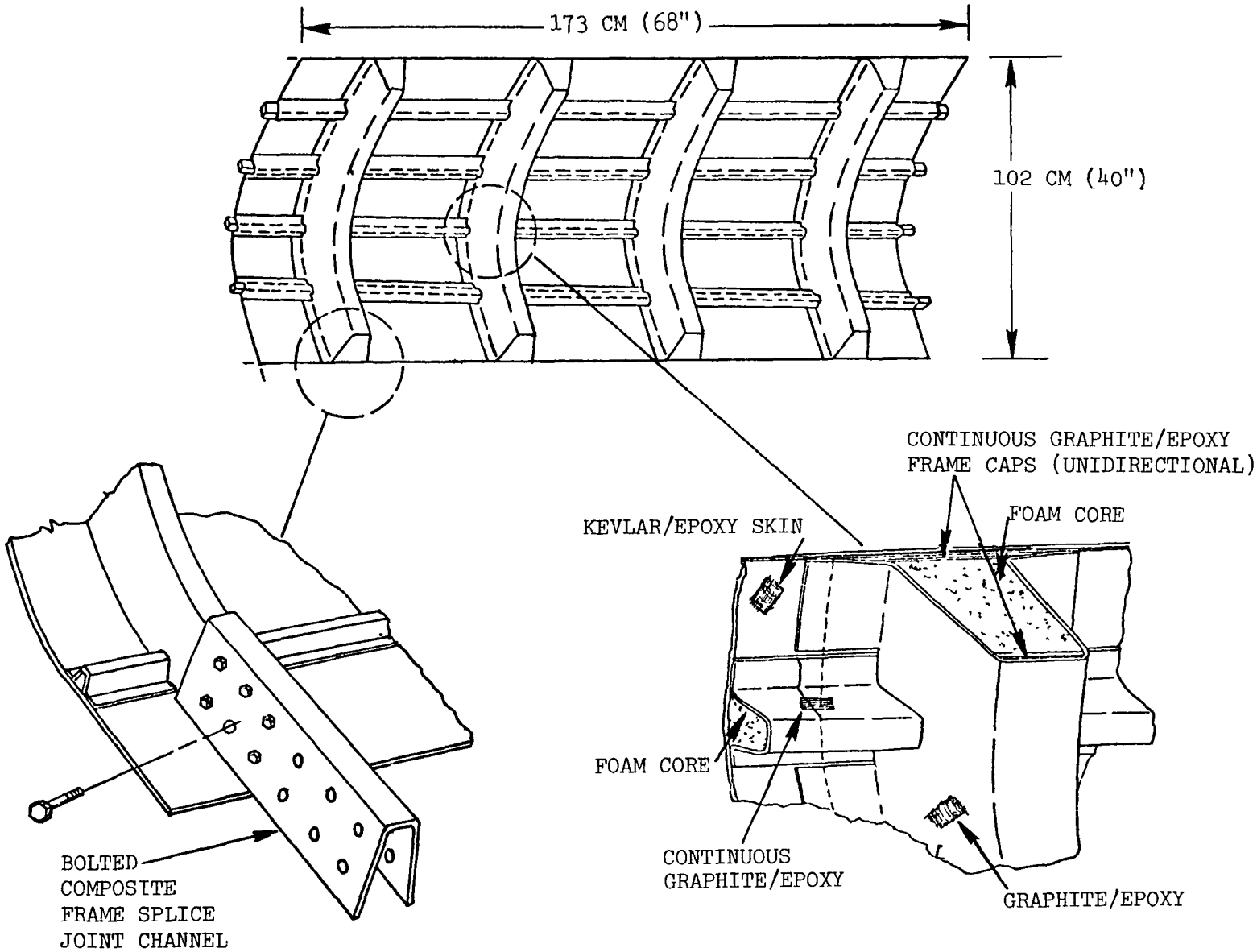

FIGURE 1. THE SINGLE CURE CONCEPT PERMITS FABRICATION OF SKIN/STRINGER/ FRAME SHELL SECTIONS IN ONE SINGLE OPERATION.

SECTION 2.0 DESIGN OF CURVED FUSELAGE SECTION

Design and analysis of the basic frame, stringer and joint attachment areas were accomplished under Phase I of this program, and are reported in Reference 1. Since the original tests conducted on individual straight frames and stringers were proven to be structurally adequate, no changes were incorporated into the curved fuselage section.

The curved fuselage shell section design, EWR 32381 (Figure 2a and 2b), was intended to be representative of a typical section of the cabin area of the CH-53D. A frame spacing of 50.8 cm (20.0 in.) and a stringer spacing of 15.2 cm (6.0 in.) is similar to that currently found in the cabin area of conventional aircraft. The laminate configuration specified in Figure 2b was proven to be structurally adequate by static testing of individual straight frame and stringer members in Phase I of this program. The basic frame design consists of $\pm 45^{\circ}$ and 0° and 90° graphite/epoxy plies in the web to react shear loads and provide bending stability in the frame/stringer intersection areas. Upper and lower 0° unidirectional graphite/epoxy caps are located at the top and bottom of the frame cross section to react compression and tensile loads. A foam core provides shape definition for the layup of these members and stabilization of the fabricated frame. The stringer members consist of 0° unidirectional graphite/epoxy plies and one woven $\pm 45^{\circ}$ KEVLAR-49 ply over a shape defining foam core. Woven KEVLAR-49 plies oriented at $\pm 45^{\circ}$ compose the basic skin structure. The design was based upon a layup or fabrication sequence which would produce the required structural configuration with the least number of manufacturing steps.

Curved frames were incorporated into the design to present a configuration which would best demonstrate the feasibility of, and expose the difficulties in fabrication of deep curved hat section frame members, and to assess the practicality of producing the shell type laminating tool selected for fabrication of the shell section. The radius of curvature of the frame ends is similar to the maximum frame curvature in the CH-53D airframe. Figure 2b shows the built-up non aircraft attachment joints utilized to test the frame. The aircraft splice joint channel is the same as the earlier design from Phase I, and is detailed in Reference 3.

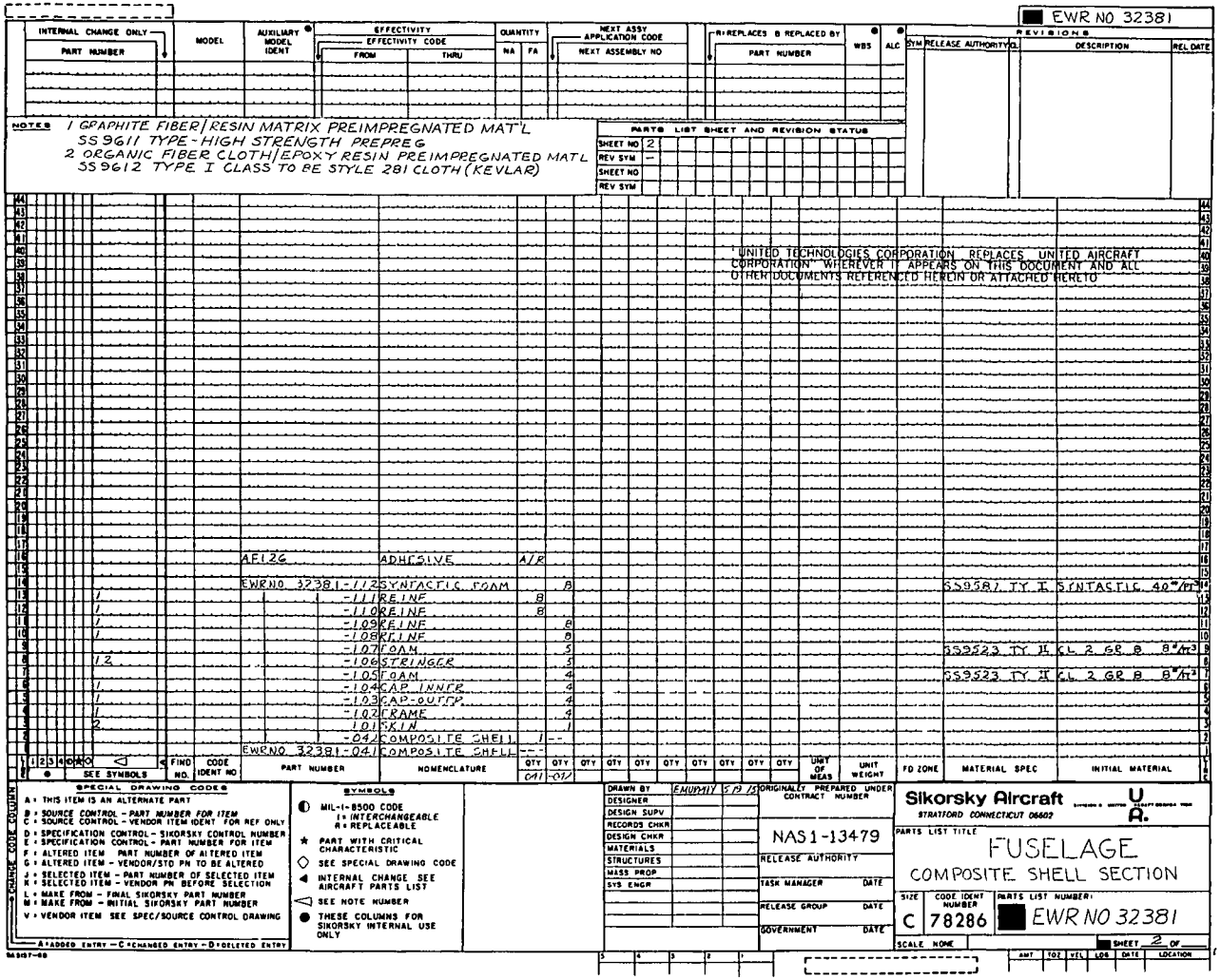

FIGURE 2a EWR 32381 FUSELAGE, COMPOSITE SHELL SECTION DRAWING, SHEET #2

Page
Intentionally
Left Blank

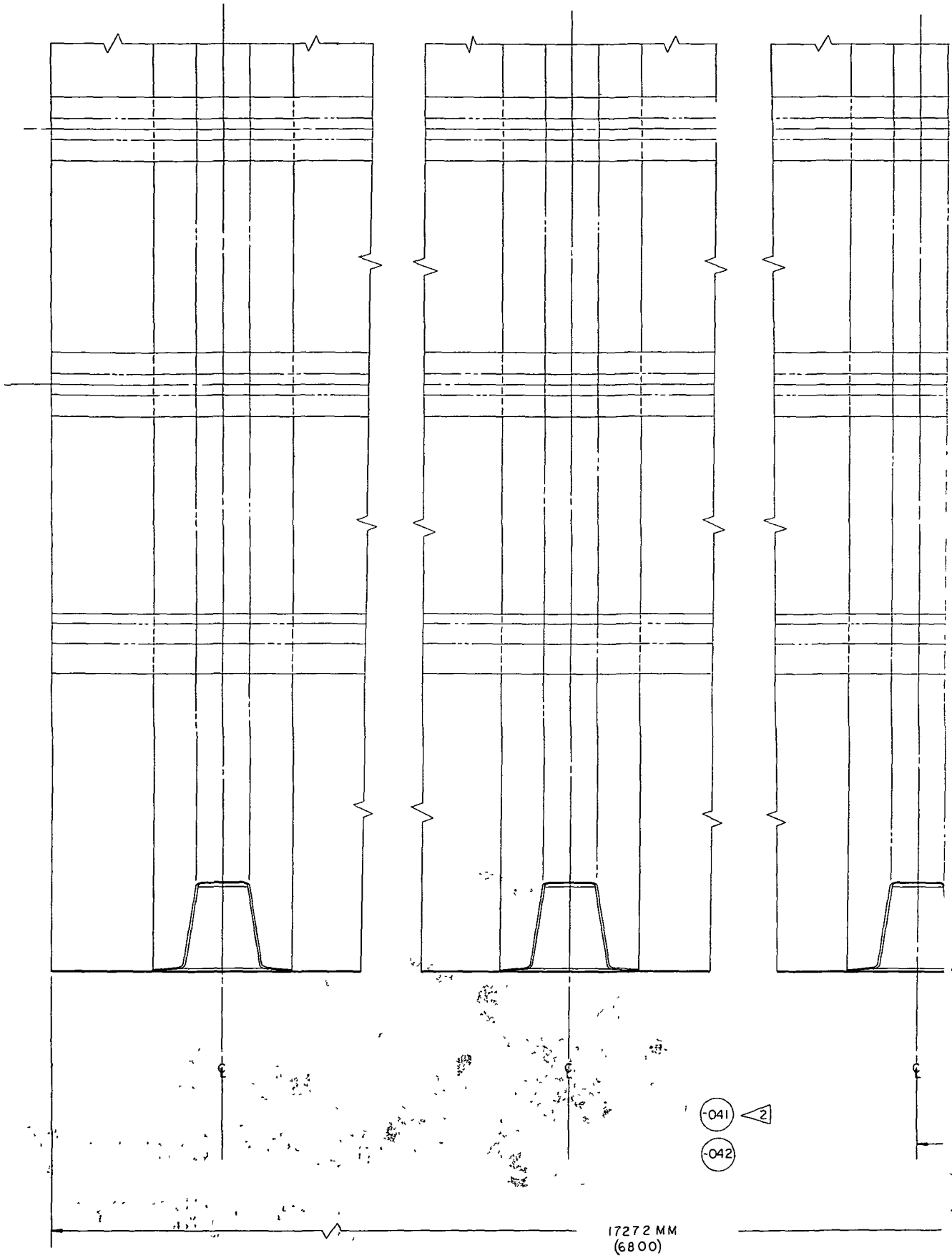

FIGURE 2b. EWR 32381 FUSELAGE, COMPOSITE SHELL SECTION DRAWING, SHEET #3.

Page
Intentionally
Left Blank

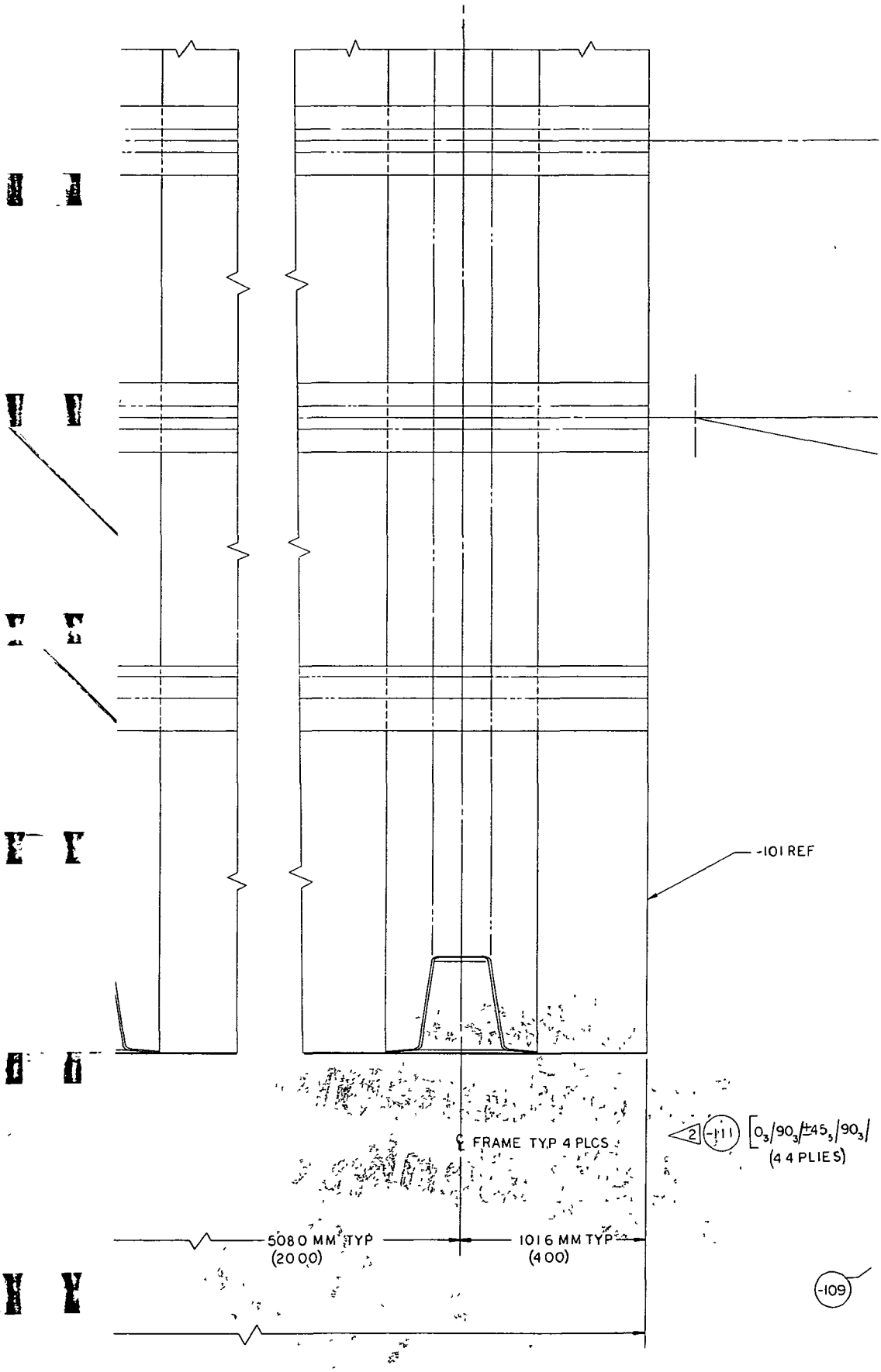
-101 REF
℄ FRAME TYP 4 PLCS
2 -111 [0₃/90₃/±45₅/90₃/
(44 PLIES)
5080 MM TYP
(200)
1016 MM TYP
(400)
-109

DWG NO
EW

Page
Intentionally
Left Blank

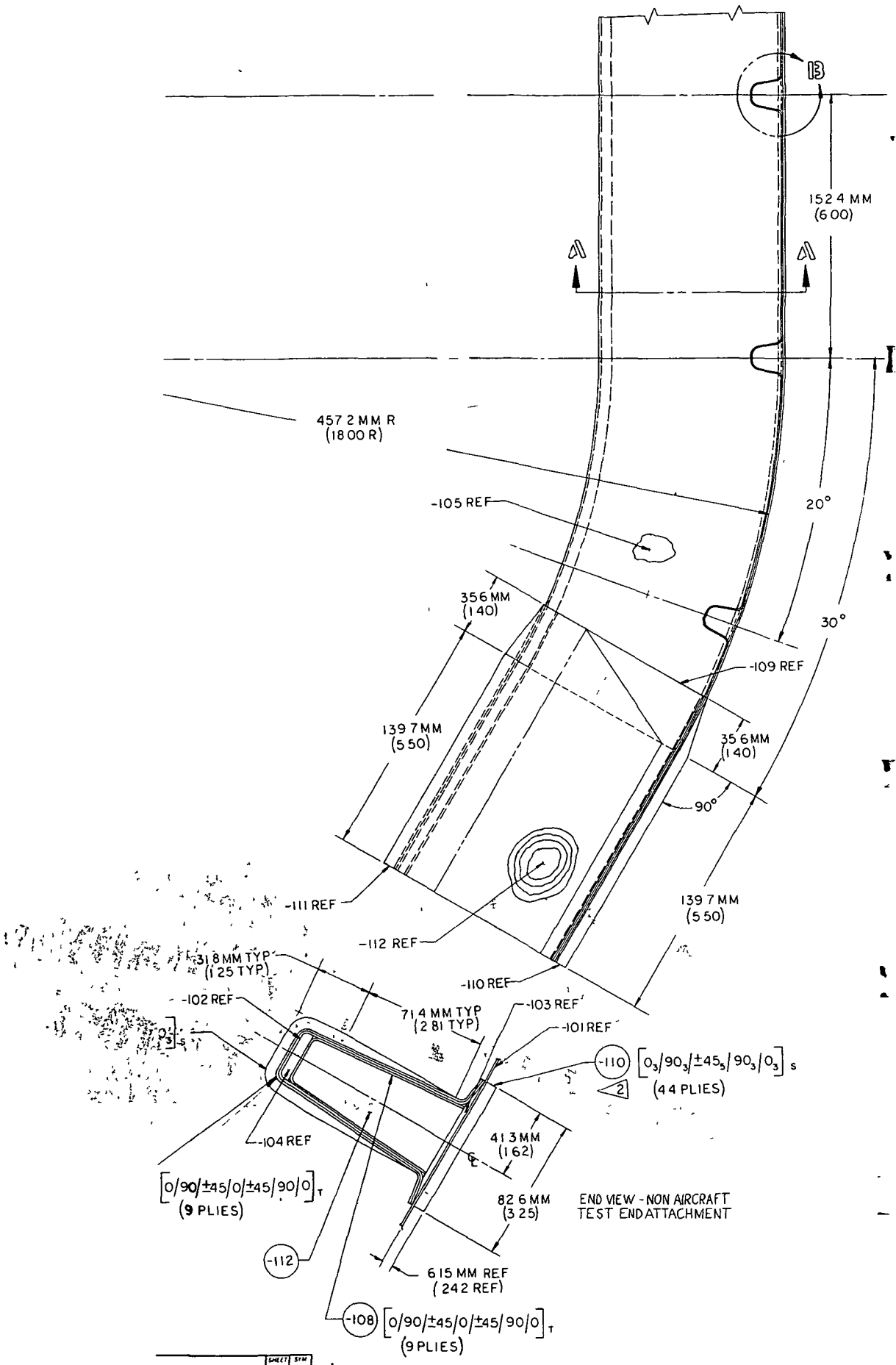

/R NO 32381 | SHEET 3 | SYM –

Page
Intentionally
Left Blank

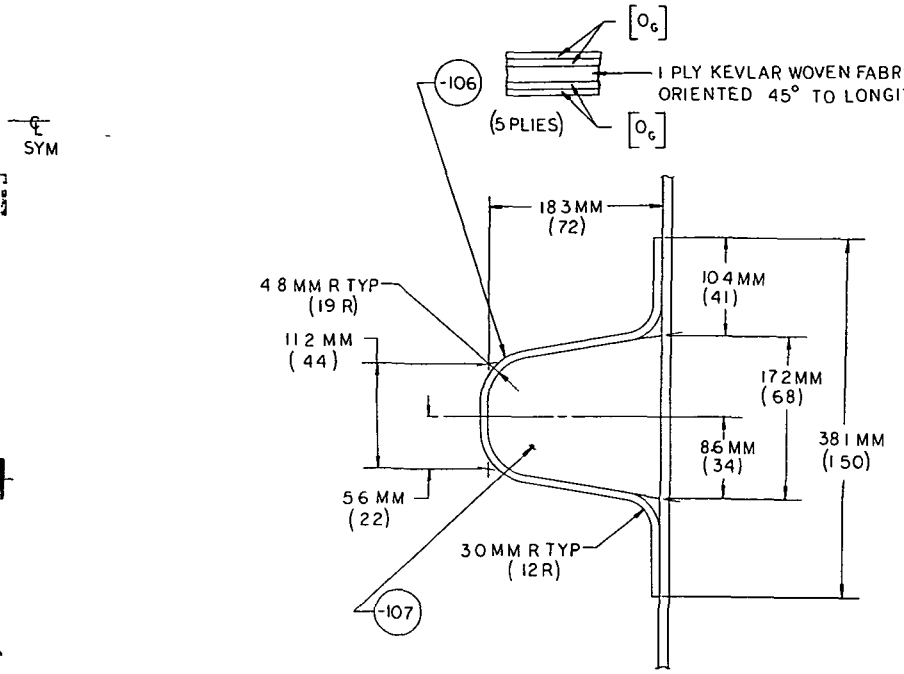

DETAIL [3] TYP
SCALE 4/1

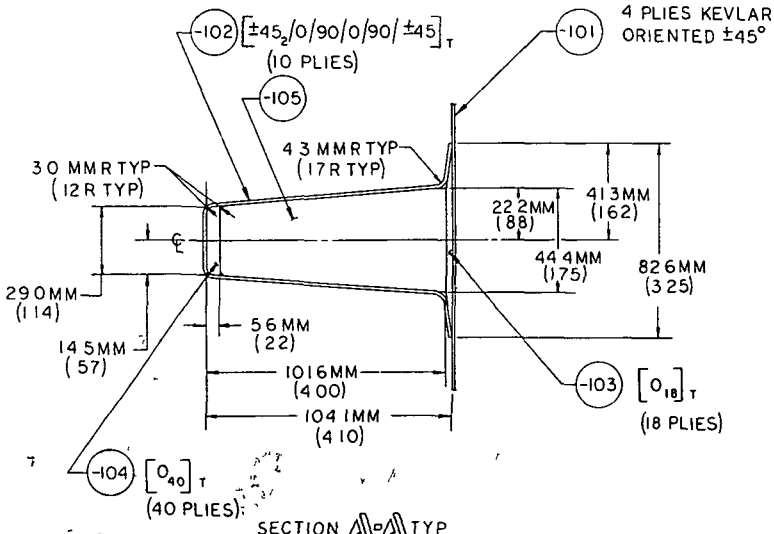

SECTION [1]-[1] TYP
FULL SIZE

APPLICATION OF PROTECTIVE FINISHES					
TYPE	DASH NO'S APPLICABLE				
FN #1					
FN #2					
FN #3					
FN #4					
SPEC	TREATMENT	FN #1	FN #2	FN #3	FN #4
MIL-A-8625	ANODIZE				
TT-P-1757	PRIMER				
SS8486	CHEM SURFACE TREAT				
QQ-P-416	CADMIUM PLATE (CL 2 TYPE II)				
SS8630	INSULATE DISSIMILAR METALS ON ASSY/INSTL				
	TOUCH UP ON ASSY/INSTL				

DASH NO	MAGNETIC MIL-I-6868		FLUORESCENT MIL-I-6868			
	YES	NO	YES	NO	YES	NO
ALL		✓		✓		✓

INSPECTION REQUIREMENTS

SYMBOLS & A
SS — SIKORSKY
SEE — SIKORSKY
SES — SIKORSKY
EO — ENGINEERIN
RTL — REQUEST T
△ — PART MAR
◁ — SEE NOTE
○ — TORQUE

AXIS

WOVEN FABRIC
TO LONGITUDINAL AXIS

NOTES

1 TOLERANCE ON DIMENSIONS IN MILLIMETERS
X ± 79 MM
XX ± 25 MM
2 BOND WITH AF 126 ADHESIVE PER SS8669 CLASS II B
3 SEE SHEET 4 FOR FULL SIZE CONTOUR

SEE SEPARATE PARTS LIST

ABBREVIATIONS
STANDARD OR SPEC
ENGRG REPORT
NGRG SPEC
G ORDER
O ENGRG
ING
NO

UNLESS OTHERWISE SPECIFIED
TOLERANCES
ANGULAR ± 0° 30'
LINEAR (EXCEPT HOLES)
.XX ± .03 .XXX ± .010
HOLES PER SS5100
TORQUE ALL BOLTS AND NUTS PER SS9300
PART MARKING PER SS8798
DRAWING INTERPRETATION PER MIL STD-100
DIMENSIONS IN INCHES
ADVANCE PROCUREMENT E I

DRAWN BY E MURPHY 5-16-75
DESIGNER
DESIGN SUPV
DESIGN CHKR
RECORD CHKR
STRUCT ANAL
STRUCT SUPV
MATERIAL
FINISH
MASS PROP
SYS ENGR

ORIGINALLY PREPARED UNDER CONTRACT NUMBER
NAS1-13479
RELEASE AUTHORITY
TASK MANAGER DATE
RELEASE GROUP DATE
GOVERNMENT DATE

Sikorsky Aircraft U A.
STRATFORD, CONNECTICUT 06602
DRAWING TITLE
FUSELAGE
COMPOSITE SHELL SECTION
SIZE J
CODE IDENT NUMBER 78286
DRAWING NUMBER EWR NO 32381
SCALE 1 NOTED
SHEET 3 OF

5 4 3 2 1

AMT YOE VEL LOG DATE LOCATION

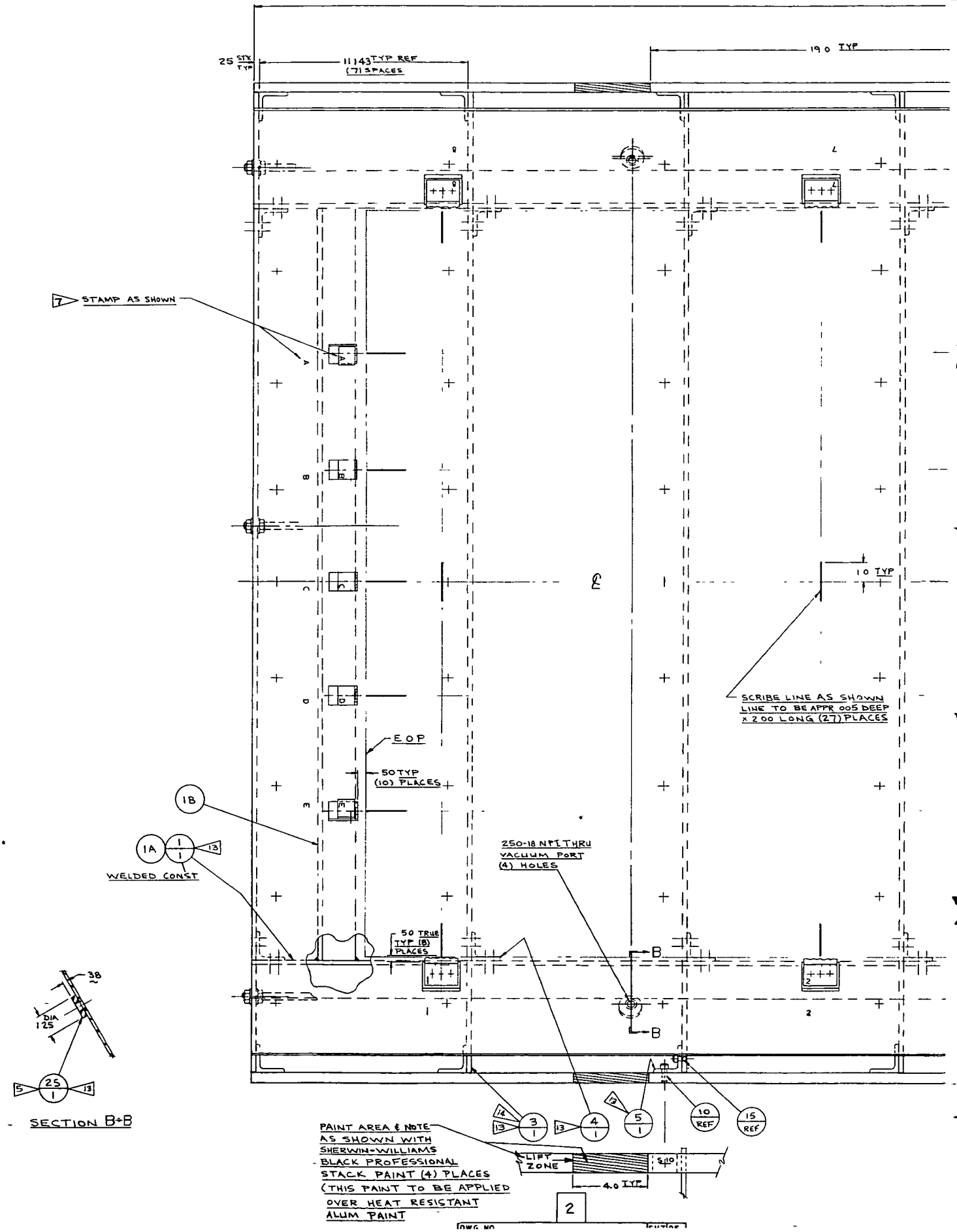

FIGURE 3. 32381-042T60, BONDING FIXTURE, FUSELAGE COMPOSITE SHELL SECTION DRAWING, SHEET #

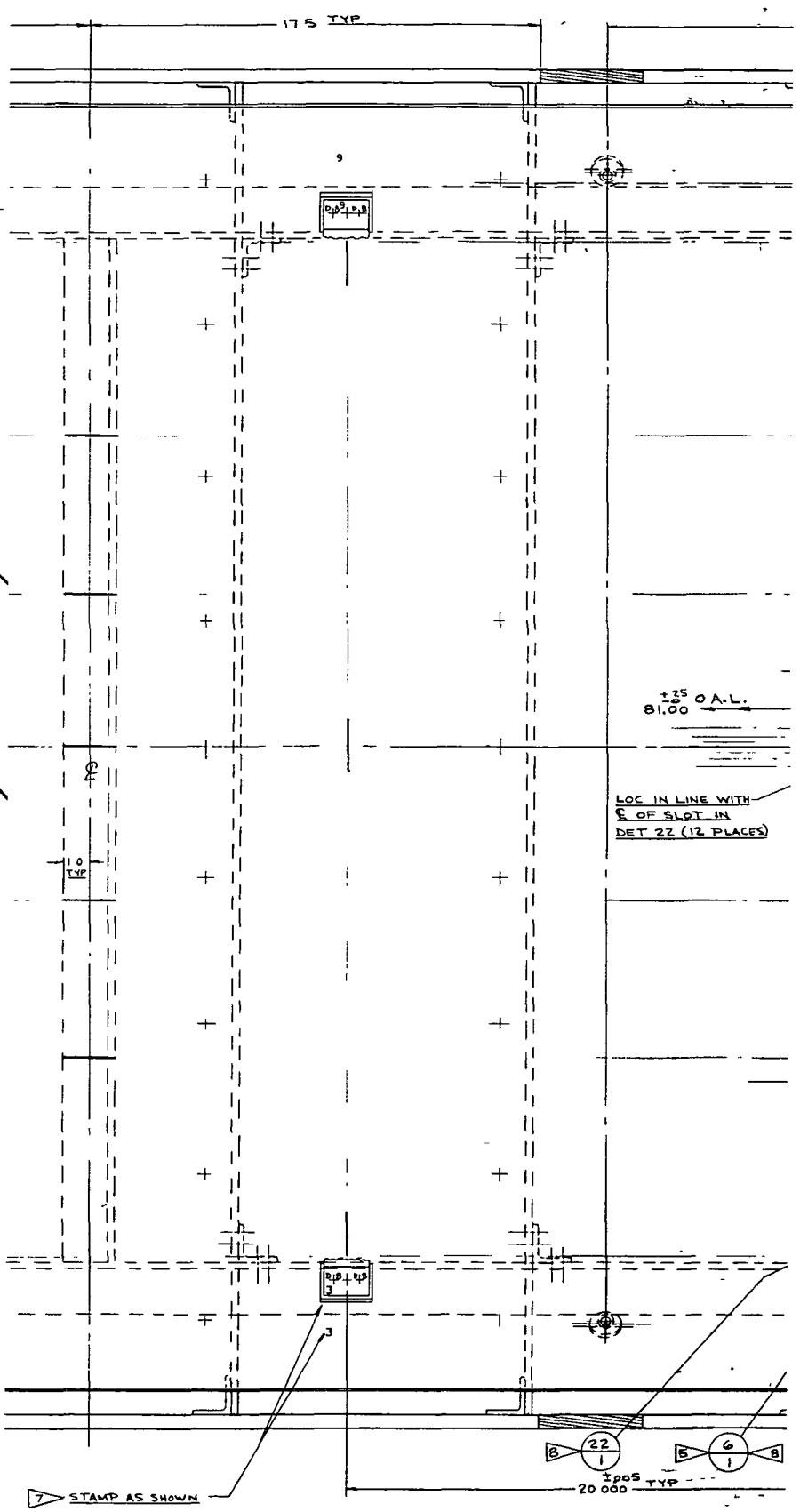
80 0
17 5 TYP
9
+35
81.00 O.A.L.
LOC IN LINE WITH
℄ OF SLOT IN
DET 22 (12 PLACES)
10
TYP
3
7 STAMP AS SHOWN
22
1
6
1
1005 TYP
20 000

'1.

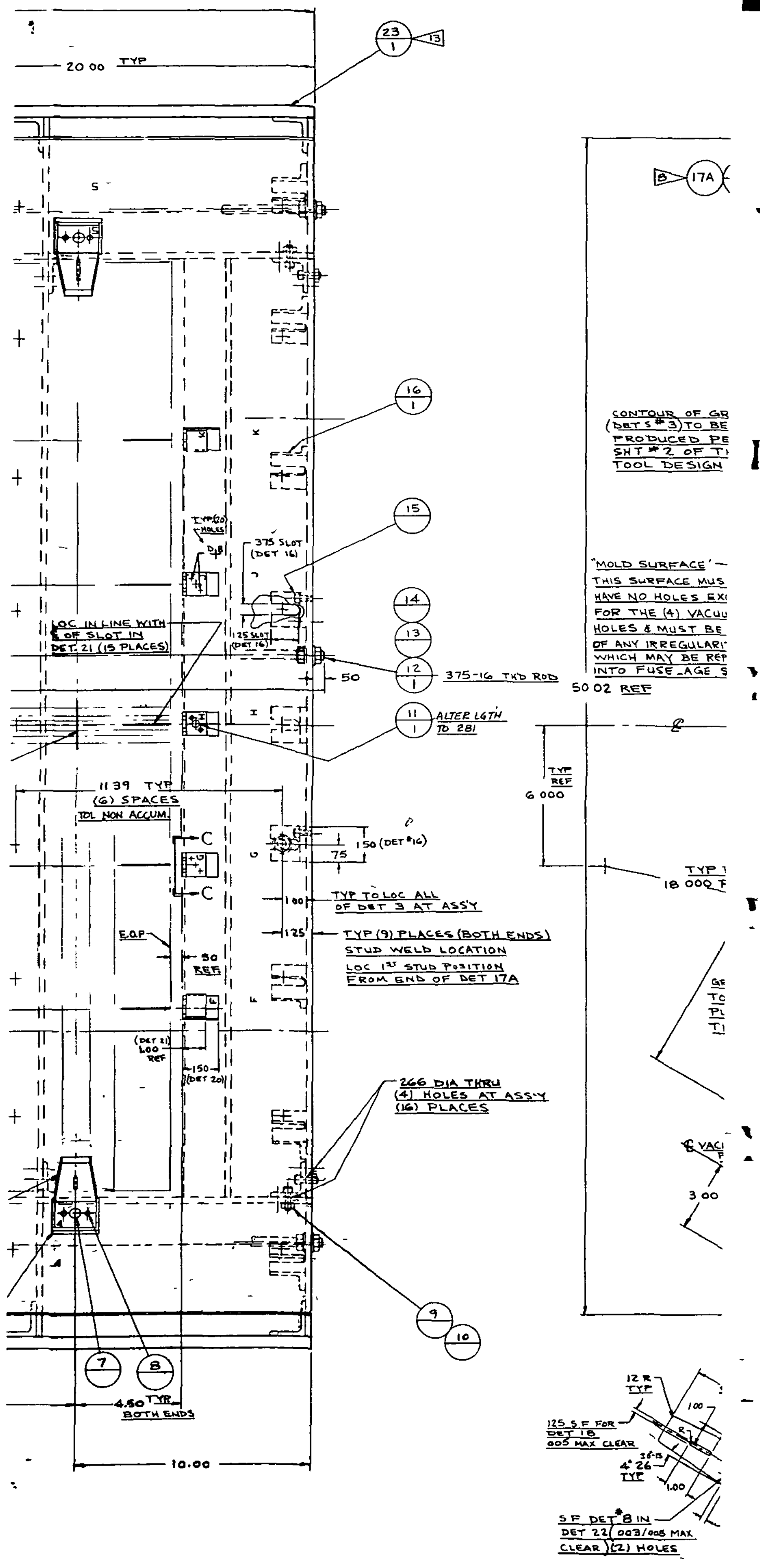

20 00 TYP
23
1
13
17A
16
1
15
CONTOUR OF GR
(DETS #3) TO BE
PRODUCED PE
SHT #2 OF T
TOOL DESIGN
TYP (20) HOLES
375 SLOT (DET 16)
"MOLD SURFACE" —
THIS SURFACE MUS
HAVE NO HOLES EX
FOR THE (4) VACUU
HOLES & MUST BE
OF ANY IRREGULARI
WHICH MAY BE REP
INTO FUSE_AGE S
14
13
12
1
LOC IN LINE WITH
℄ OF SLOT IN
DET. 21 (15 PLACES)
125 SLOT (DET 16)
50
375-16 THD ROD
50 02 REF
11
1
ALTER LGTH TO 281
TYP REF
6 000
1139 TYP
(6) SPACES
TOL NON ACCUM.
C
C
150 (DET #16)
75
TYP 1
18 000
100
TYP TO LOC ALL
OF DET 3 AT ASS'Y
125
TYP (9) PLACES (BOTH ENDS)
STUD WELD LOCATION
LOC 1ST STUD POSITION
FROM END OF DET 17A
E.O.P.
50
REF
(DET 21)
LOO
REF
150
(DET 20)
266 DIA THRU
(4) HOLES AT ASS'Y
(16) PLACES
℄ VAC
3 00
9
10
7
8
4.50 TYP
BOTH ENDS
10.00
12 R
TYP
100
125 S F FOR
DET 18
005 MAX CLEAR
4° 26'
TYP
1.00
S F DET #8 IN
DET 22 (003/008 MAX
CLEAR) (2) HOLES

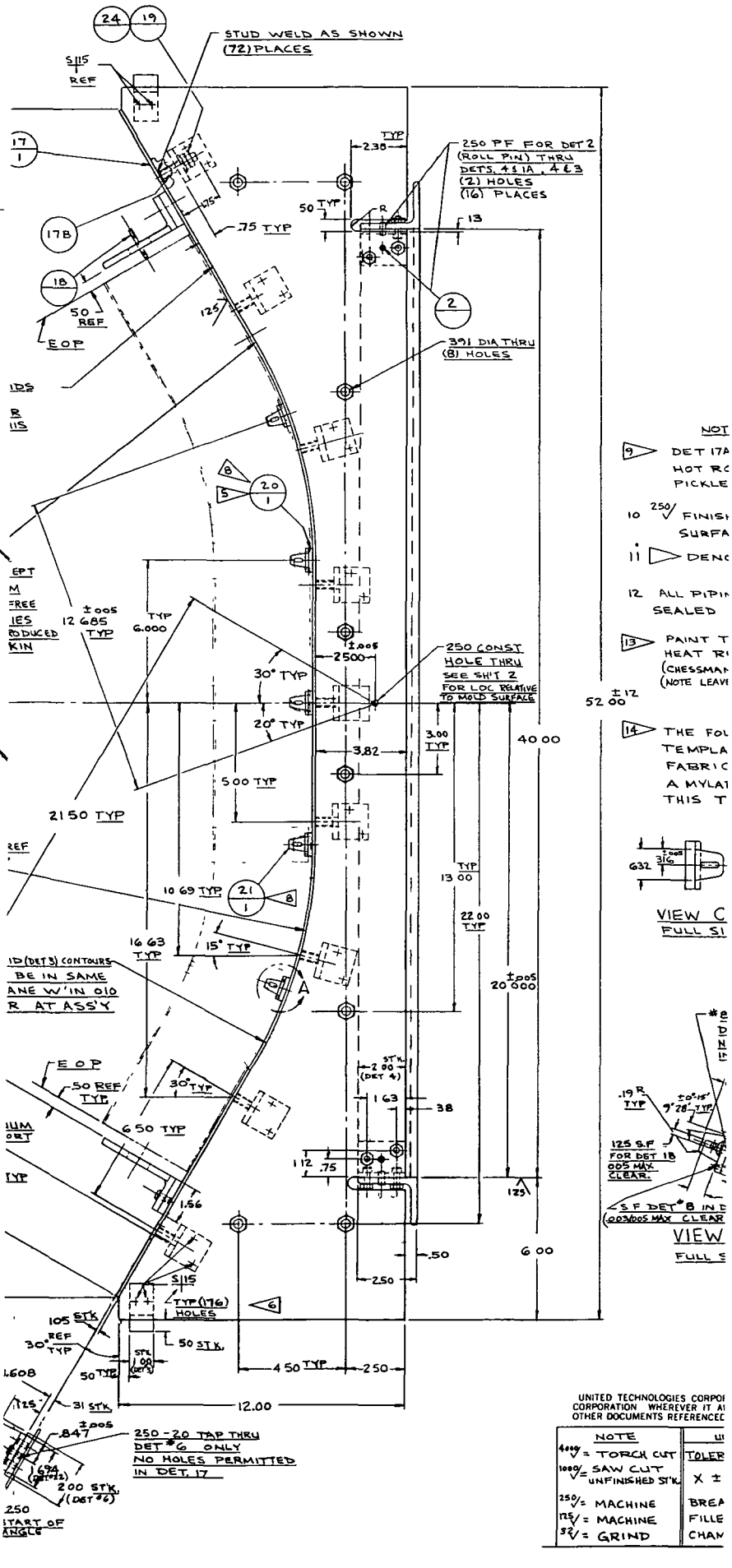

NOT

9 DET 17A HOT RC PICKLE

10 250 FINISH SURFA

11 DENC

12 ALL PIPIN SEALED

13 PAINT T HEAT RI (CHESSMAN (NOTE LEAVI

14 THE FOL TEMPLA FABRIC A MYLAT THIS T

UNITED TECHNOLOGIES CORPOR CORPORATION WHEREVER IT AI OTHER DOCUMENTS REFERENCED

NOTE	
400 = TORCH CUT	TOLER
1000 = SAW CUT UNFINISHED ST'K.	X ±
250 = MACHINE	BREA
125 = MACHINE	FILLE
32 = GRIND	CHAM

ER EWR 32381-042 T060
CH'G "O

1. PURCHASE STANDARD ITEMS PER B/M OR EQUIVALENT UNLESS OTHERWISE NOTED
2. ALL WELDMENTS CASTINGS, BOILER PLATE, ETC., TO BE NORMALIZED OR STRESS RELIEVED AS NECESSARY
   TOOL VENDORS MUST SUBMIT WRITTEN VERIFICATION THAT THEY HAVE COMPLIED WITH THIS AND OTHER NOTES
3. MARK ALL LOOSE AND REMOVEABLE PIECES WITH TOOL AND DETAIL NUMBER ALL DETAILS MENTIONED IN OPERATING INSTRUCTIONS WITH DETAIL NUMBER, ALSO ALL BUSHINGS WITH SIZE
4. STAMP TOOL EWR-32381-042 T060

TOOL DESIGN REV —

ENG DWG EWR-32381 REV ~ (ADV SHTS)

A/F

5. BOND DET'S 64.20 TO DET. 17A ~ & DETS 17A & 25 WITH EA 934 ADHESIVE PURCHASE FROM HYSOL DIV OF DEXTOR PITTSBURGH, CAL.
6. SCR & DOWEL AS SHOWN IN F/D LOCATION & HOLE PREPARATION MUST SUIT GOOD TOOLMAKING PRACTICES DOWELS TO BE PF UNLESS OTHERWISE NOTED

SYMBOL DEFINITION. SCR OR DOWEL (S OR D) — DET NO

7. FILL STAMPINGS WITH SHERWIN-WILLIAMS BLACK PROFESSIONAL COATING STACK PAINT OR EQUIV.
8. ON THIS DETAIL, NO SHARP EDGES OR CORNERS ARE PERMITTED WHICH MAY CAUSE PUNCTURES TO VACUUM BAG

(NOTES CONT'D LEFT)

ES CONT'D

, TO BE MADE FROM
)LLED STEEL, LOW CARBON,
D & OILED SH'T STOCK

I ON ALL UNSPECIFIED
CES

)TES SEE NOTE NO

IG FOR VACUUM TO BE
AIR TIGHT

HIS DET WITH #1202
ESISTANT ALUM PAINT
ELIOT BROOKLYN N Y)
WORKING SURFACES CLEAR)

LOWING TOOLS AND/OR
TES ARE REQUIRED FOR
ATION OF THIS FIXTURE:
R COPY OF SHT # 2 OF
OOL DESIGN

£

'C
ZE

)-32 TAP THRU
ET #20 ONLY
O HOLES PERMITTED
DET #17

573

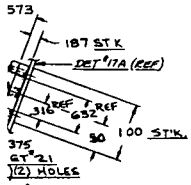

+A
IZE

DET	QTY	NAME	ZONE / SHT	MAT'L	STOCK SIZE
25	4	PAD		PES 10	125 DIA x 50
24	72	WASHER		STD	FOR 312 BOLT
23	2	GUARD RAIL		PES 10	50 x 100 x 80.12
22	8	ANGLE (LOCATOR)		ST'L	4.00 x 3.00 x 26 x 1.75
21	10	ANGLE (LOCATOR)		ST'L	100 x 75 x 12 x 100
20	10	PAD		PES 10	187 x 100 x 1.62
19	144	JAM NUT		STD	312-18
18	18	(DOWEL) LOC PIN		STD.	125 DIA x 1.60
17B	72	(THD ROD) STUD		ST'L	312-18 x 1.87
17A	1	PLATE		9	105 x 54 x 80.12
17	1	WORK REST		~	WELDMENT
16	72	ANGLE		ST'L	150 x 150 x 25 x 150
15	176	SOC HD CAP SCR		STD	250-20 x 50
14	128	WASHER		STD	FOR 375 BOLT
13	128	HEX NUT		STD	375-16
12	8	TH'D ROD		ST'L	375-16 x 8.12
ALTER. 11	10	BUT HD CAP SCR		STD	#8-32 x 38
10	80	SOC HD CAP SCR.		STD	250-20 x 75
9	64	HEX NUT		STD	250-20
8	36	DOWEL		STD	125 DIA x 38
7	8	BUT HD. CAP SCR.		STD	.250-20 x .50
6	8	PAD		PES 10	.31 x 2.00 x 1.68
5	16	ANGLE		ST'L	1.50 x 1.50 x 1.9 x 1.12
4	16	ANGLE		ST'L.	1.50 x 1.50 x 1.9 x 2.00
3	8	GRID		PES 11	25 x 12.12 x 62.12
2	32	ROLL PIN		STD	250 DIA x .62
18	3	ANGLE		STL	2.50 x 2.00 x 25 x 80.12
1A	2	ANGLE		ST'L	250 x 2.00 x 25 x 80.00
1	1	FRAME		~	WELDMENT

Sikorsky Aircraft — U —
MANUFACTURING ENGINEERING DEPT A STRATFORD, CONN. 06602

TOOL BONDING FIXTURE (MOLD)

FUNCTION BOND FUSELAGE COMPOSITE SHELL SECTION — SCALE 1/2 & NOTED

DESIGN	CHECK	PE CONCUR	TD APPVL RO CARD
C J Doan	LAN	N A S	
DATE 7-3-75	DATE 5-17-75	DATE 7-17-75	DATE 7-17-75

EWR-32381-042 T060 — SHT 1 OF 2 — REV ~

1

RATION REPLACES UNITED AIRCRAFT
PPEARS ON THIS DOCUMENT AND ALL
HEREIN OR ATTACHED HERETO

LESS OTHERWISE SPECIFIED
ANCES ANGULAR ± 1°
.06 XX ± .03 XXX ± 010
K SHARP EDGES .005 TO .015 R.
T RADII TO BE .005 TO .030 R
FERS TO BE .030 x 45°

"Page missing from available version"

pages 1—10 of this section.

SECTION 3.0 MATERIALS

The materials utilized in the fabrication of the composite shell sections described in this report were selected as the result of an evaluation and test study conducted in the Phase I effort of this program (Reference 1). The final selection of the constituent materials from the candidate materials was based upon their applicability to the requirements established for fabrication of composite fuselage shell sections, composed of frame/stringer/skin elements, by the single layup, single cure concept. A maximum cure temperature of 121°C (250°F) was established to minimize thermal incompatibility between the composite reinforcement and the tooling, and to eliminate distortion of the foam cores during cure.

The materials selected were: Thornel T-300 unidirectional graphite, impregnated with Narmco 5209 epoxy resin for the frames and stringers.

KEVLAR-49 type III, Polyaramid fiber in the form of a woven fabric (style 281), impregnated with Narmco 5209 epoxy resin was used for the skin material and the stringer shear webs.

Stathane 8747, foam-in-place, CO_2 blown polyurethane foam with a nominal density of 221 mg/m^3 (8.0 lb/ft^3) was used for frame and stringer core sections.

Epocast 169, an epoxy resin/phenolic microballoon syntactic foam with a nominal density of 967 mg/m^3 (35.0 lb/ft^3) was used for bearing stabilization of the frame members in areas of attachment.

SECTION 4.0 SELECTION OF COMPOSITE SHELL TOOLING

In Phase I of the subject program, a tooling investigation and evaluation was conducted to determine the lowest cost acceptable tooling approach for fabrication of representative curved fuselage composite shell sections. The basic tooling philosophy of providing a female shell tool to the outside mold surface of the aircraft skin, with locator angles and floating pin restraints to position both frame and stringer elements was proven successful.

In the detail design of the EWR 32381-042 T60 molding tool shown in Figure 3, four main areas of consideration governed the selection of materials and the fabrication process used to produce the tool. They are:

1. Low mass to provide a fast uniform heat up rate of the tool, required to promote cure compatibility between the skin laminate in contact with the tool surface and the frame and stringer elements separated only by the vacuum bag from the heated autoclave air.

2. Maintenance of contour, surface uniformity, and continuity - necessary to produce an aerodynamic surface on the manufactured composite hardware, acceptable to contour and surface finish design tolerances. A second and equally important consideration for the requirement of surface continuity is the ability to produce a tool surface with no manufacturing breaks or mechanical attachment holes, necessary to insure vacuum integrity during the fabrication of composite hardware.

3. Positive location of the detail frame and stringer core elements as they are incorporated into the composite shell section part during the fabrication of the one step cure fuselage composite shell section.

4. The lowest possible differential thermal coefficient of expansion between the composite materials selected and the materials of construction for the tool.

4.1 TOOL DESIGN

Composite Shell Tool. The composite shell section fabrication tool shown in Figure 3 and 4 consists of two basic elements: the base, a skeleton egg crate framework consisting of steel templates machined to the contour of the frame section, joined by a series of steel rods and angles, and a hot rolled, low carbon steel skin or tool surface 0.27 cm (0.105 in.) thick, roll formed to the contour of the outside mold surface of the fuselage composite shell section.

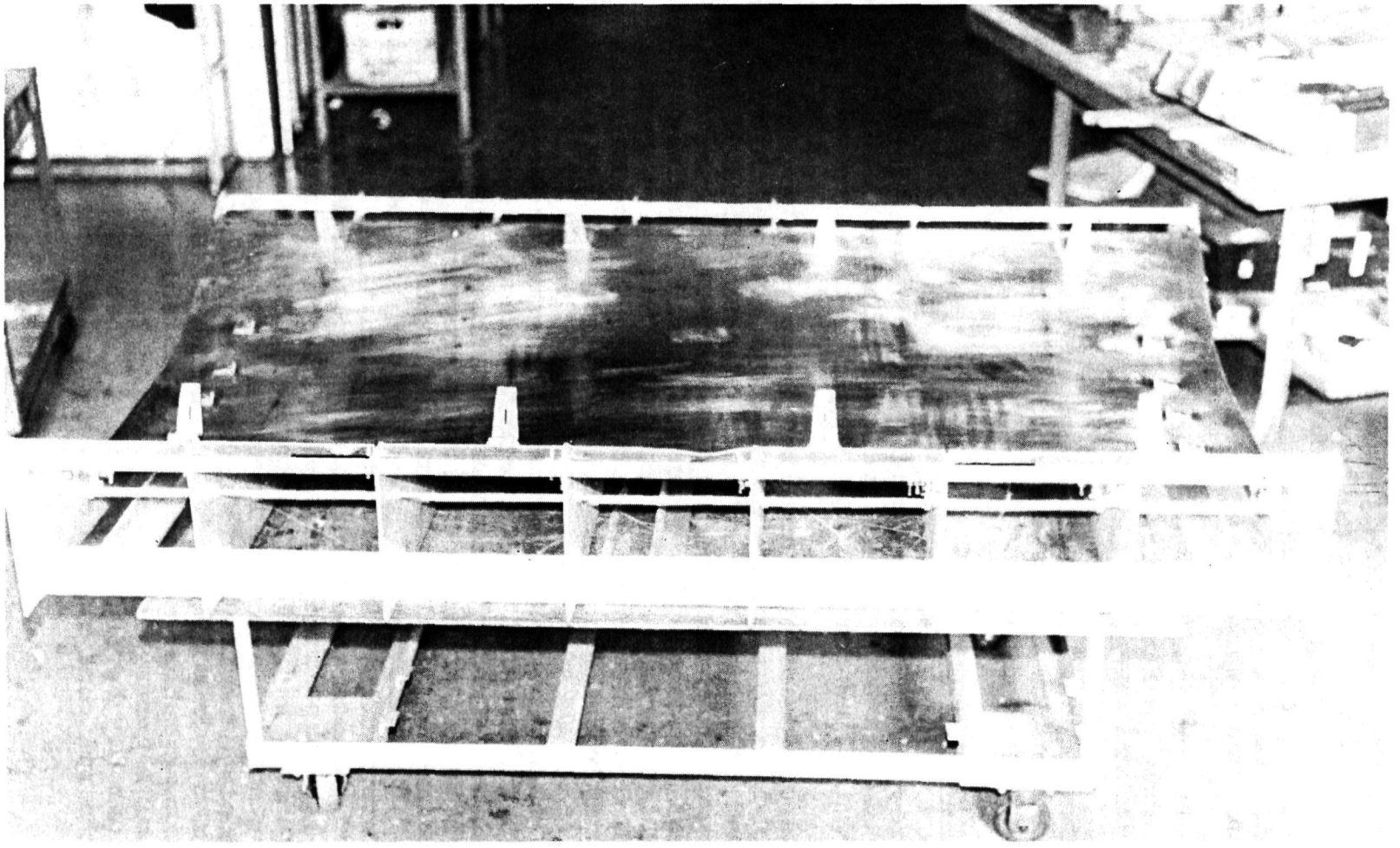

FIGURE 4. EWR 32381-T60 FUSELAGE COMPOSITE SHELL SECTION MOLDING TOOL.

Attachment provisions, for joining the skin section to the egg crate section are made by resistance welding threaded studs to the underside of the steel skin after the skin has been roll formed to produce an acceptable contour match. When the skin section of the tool is matched to the egg crate contour section, the threaded studs align with restraint angles attached to the contour templates. Each stud is individually tightened to bring the tool surface into full contact with the contour templates and adjusted as required to produce a perfect surface contour.

Foam Tooling. To fabricate the frame and stringer foam core details, female molding tools were designed to reproduce the cross sectional shape of the foam elements.

Splice Channel Tool. The male aluminum tool, designed to produce the composite splice channels tested in Phase I (Reference 1) of the program, was utilized.

4.2 TOOL FABRICATION

Fabrication of the Fuselage Shell Section layup tool was accomplished by one of the qualified tooling vendors currently fabricating tooling for Sikorsky Aircraft on a contract basis.

Initial inspection of the completed layup tool revealed localized damage to the edge of the tool surface which had occurred in shipment from the vendor to Sikorsky. During the detail inspection phase, prior to acceptance, it was found however that the damage was superficial and in no way affected the laminating surface or desired performance of the tool. Dimensional and contour checks of the tool were performed, the tool was within tolerance and was accepted.

Because of the scope and schedule of the subject program, no tooling provisions were made for the fabrication of a permanent contour silicone rubber bag similar to that successfully fabricated in Phase I (Reference 1) of the program (i.e., fabrication of a wooden mockup simulating the completed shell section). However, it was decided to utilize a concept reported by General Dynamics Corporation, Fort Worth Division, in Reference 2. In this method, bleeder and vent plies are placed directly over the completed layup, painted with a liquid room temperature vulcanizing silicone rubber, and allowed to cure. Accordingly, the completed preimpregnated shell section layup was prepared by covering with nylon peel ply material over which a series of dry glass fabric bleeder plies were positioned. A coating of Dow Corning 92-048 liquid silicone rubber thinned to a paintable consistency with Methyl Ethyl Ketone solvent was applied to the surface of the outer bleeder ply by brush. It was planned to apply succeeding coats of the silicone rubber compound to the cured surface of the

bag to build up on the surface, a sufficient thickness to produce a reusable glass reinforced vacuum bag (see Figure 5). After cure, a similar coating was to have been applied to the inner surface of the fabricated bag to encapsulate the reinforcing fabric. Unfortunately, the time frame chosen for bag fabrication was during a period of high humidity. After application of the first sealer coat, it was found that the silicone compound, which cures by reaction with moisture, had cured only on the outer surface. The solvent used to thin the silicone compound had become entrapped by the cured surface and was now causing the composite layup to soften. To prevent any damage to the completed layup, the partially completed bag was stripped from the surface of the layup. No additional attempts were made to produce a reusable bag, although it was felt that a simple change in the solvent system used would have produced an acceptable bag.

Tooling for fabrication of the EWR 32381-107 frame foam and the EWR 32381-108 stringer foam core details was produced by conventional tooling techniques. For the curved frame foam core detail, a glass reinforced epoxy female tool was fabricated to produce one-half of the required frame core section. The foaming tool for the stringer core section was fabricated from an aluminum bar milled to produce the stringer foam cavity. When casting foam sections in each of these tools, it was found that the glass reinforced tool produced a more uniform surface finish on the cast foam, with consistently fewer problems encountered in the release of the cured foam from the tool surface.

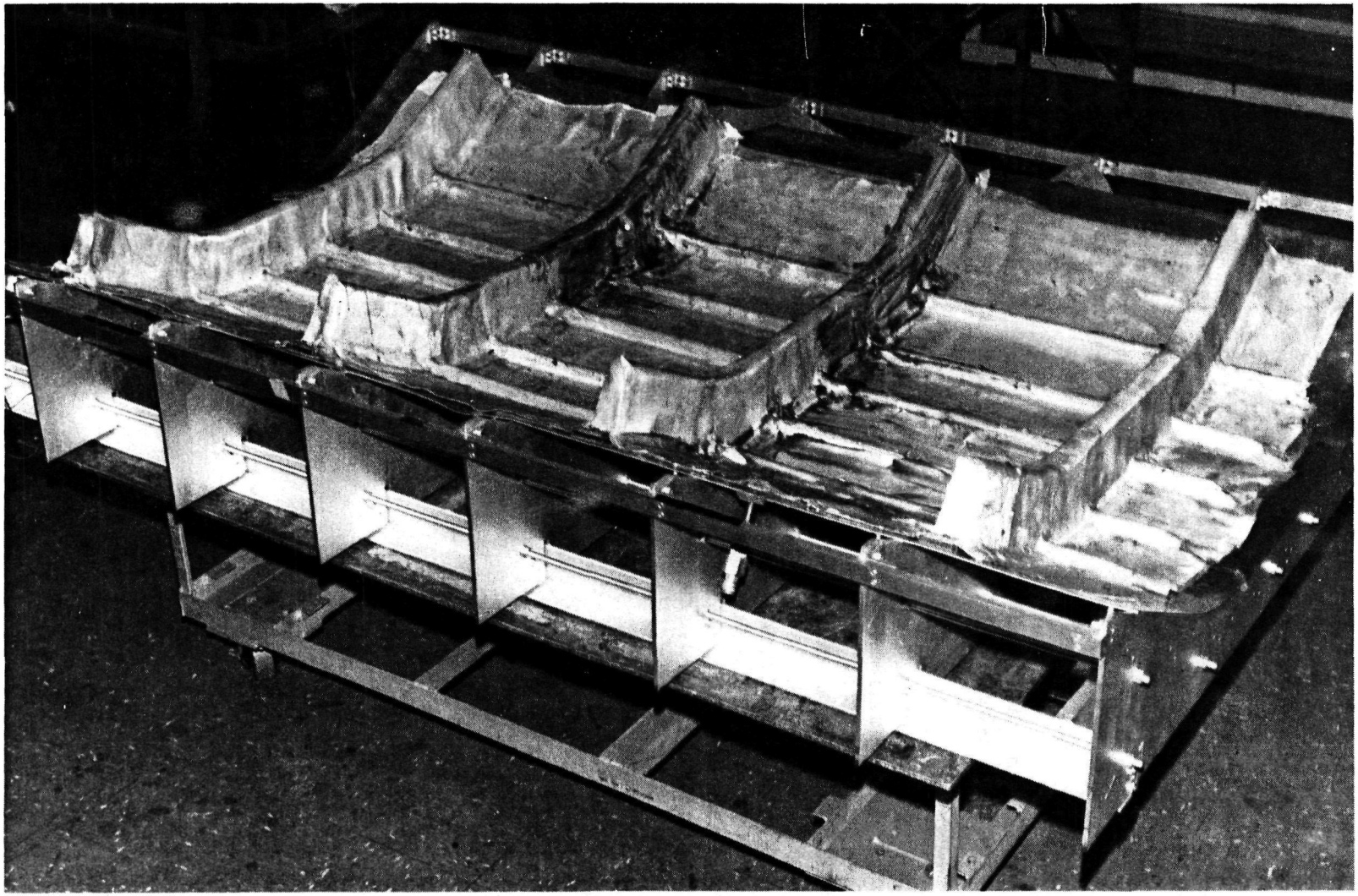

FIGURE 5. ATTEMPTED LAYUP OF REINFORCED SILICONE RUBBER CONTOUR BAG OVER COMPLETED EWR 32381 COMPOSITE SHELL SECTION LAYUP.

SECTION 5.0 HARDWARE FABRICATION

The fabrication procedures developed in Phase I for the fabrication of the straight section static test specimens were reviewed and modified to provide a basic procedure for the fabrication of both the Fuselage Frame Section Panel and the Fuselage Frame Splice Joint Section Panel.

The Fuselage Frame Section panel is representative of a main fuselage section of the center cabin area of the Sikorsky CH-53D. It consists of four frame members equally spaced at twenty inch intervals. The curved areas of the frame section are similar to the maximum frame curvature in the CH53D airframe; however, the actual shape of the frame sections was developed to produce the required geometry to facilitate the location of the test hardware in such a position so as to produce the required 6 to 1 ratio of bending load to axial compression load. Five stringers have been incorporated into the frame section panel, spaced at six inch intervals.

The Fuselage Frame Splice Joint Section Panel is similar to the frame section panel. In each frame of this panel, provisions were made to provide additional densification of the foam substrate in both the test hardware attachment areas, and the representative aircraft end attachment areas. The fabrication of the composite fuselage frame fatigue test specimens for both the frame and frame splice joint fatigue tests is accomplished in two operations:

1) Fabrication of the EWR 32381 Fuselage Composite Shell Section to verify the single cure concept.

2) Subsequent lamination of composite test doublers to provide suitable test hardware attachment areas and to insure fracture of the specimen in the desired test or gage area.

A sequential fabrication guide was established to produce the EWR 32381 Fuselage Composite Shell Section shown in Figure 6. The sequence of fabrication is as follows:

1. Fabricate foam frame and stringer core details.

2. Prepare graphite/Kevlar materials to sizes and orientations defined in process control layup sheets.

3. Inspect prepared preimpregnated materials and package in individual subassembly ply group packages. See Figure 7 for typical frame layup assembly group.

4. Layup precut patterned materials and foam details on tool in accordance with sequential process control sheets.

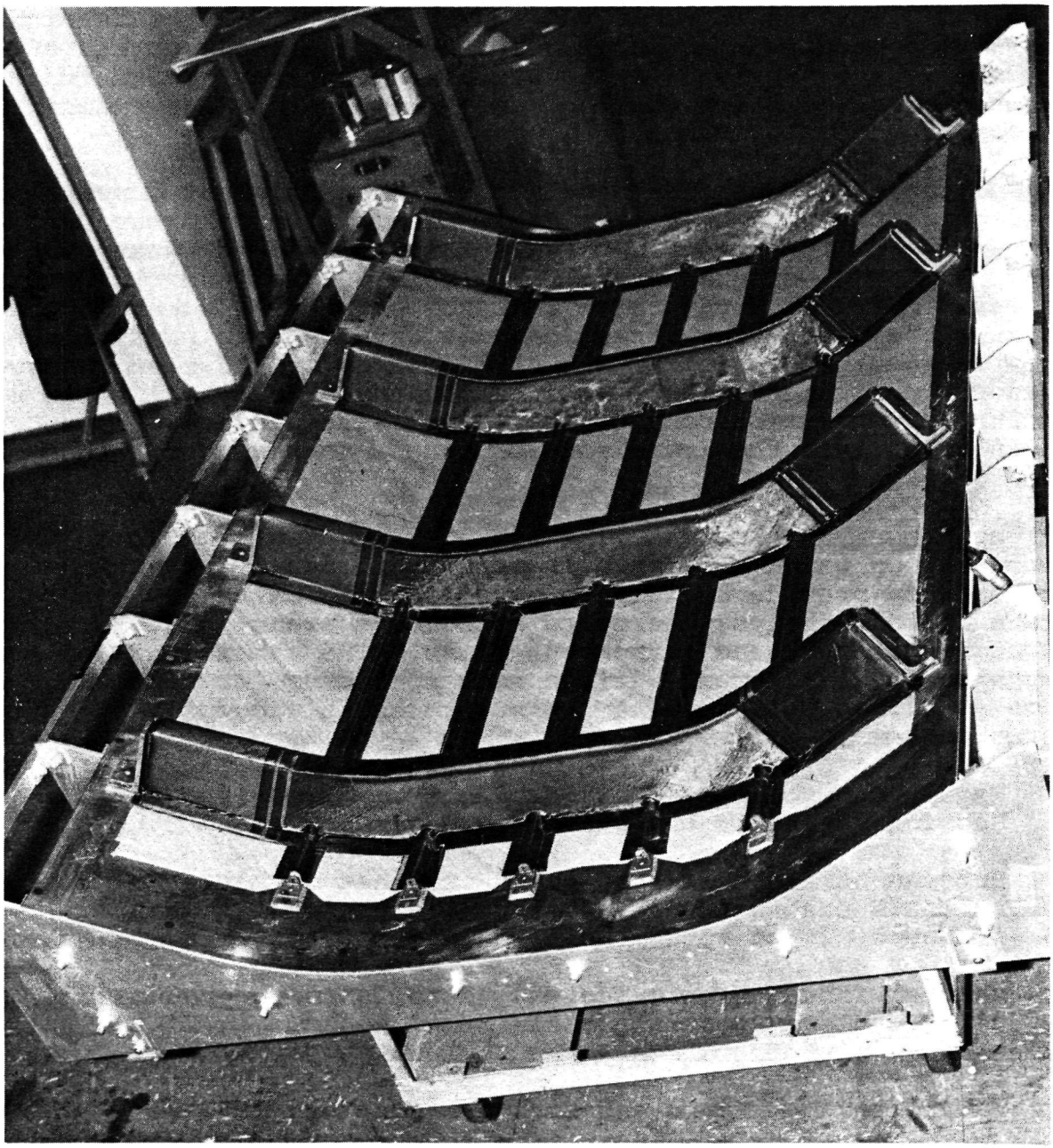

FIGURE 6. CURED EWR 32381 FUSELAGE COMPOSITE SHELL SECTION IN EWR 32381-T60 FEMALE TOOL.

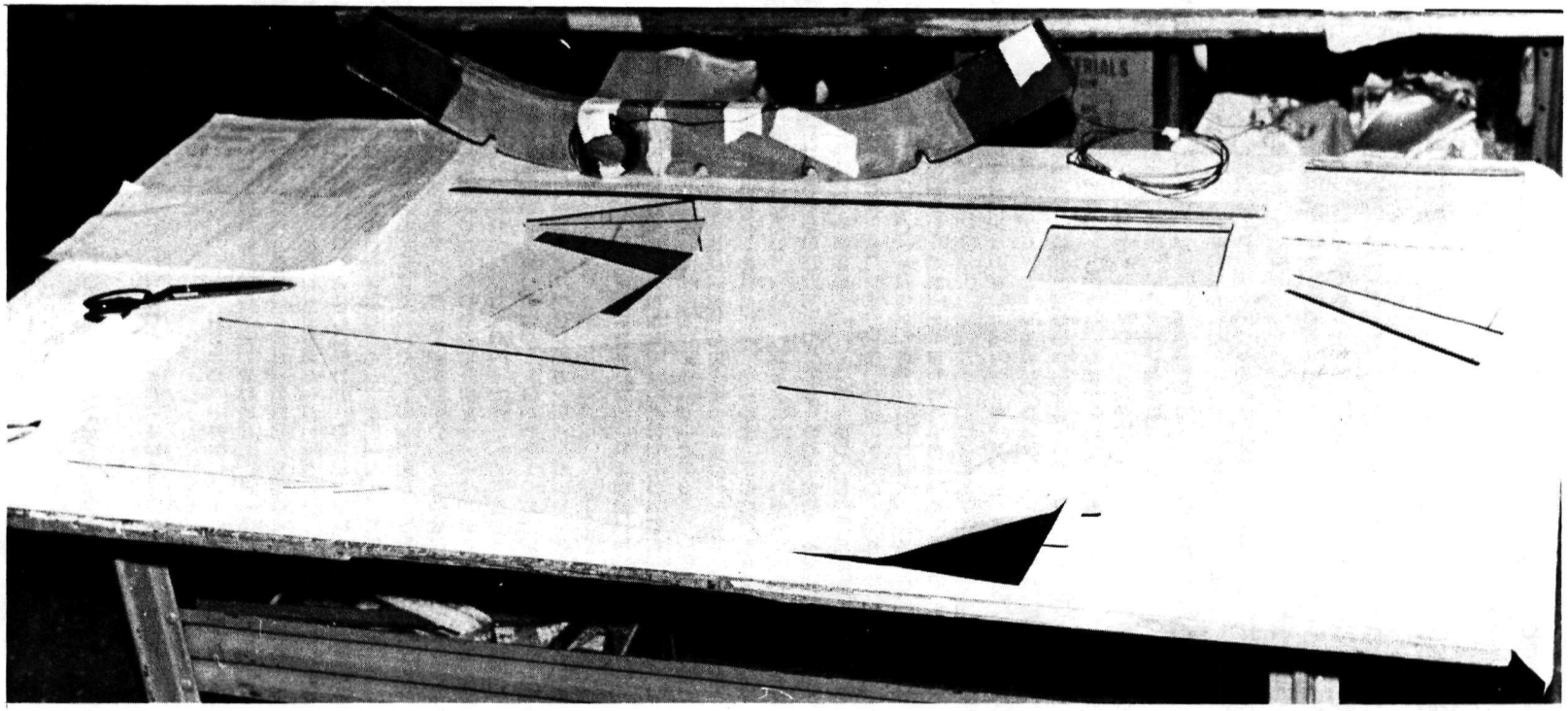

FIGURE 7 . TYPICAL FRAME LAYUP ASSEMBLY GROUP.

5. Apply peel and bleeder plies, vacuum bag and cure in autoclave at specified pressure and temperature.

6. Remove completed Fuselage Composite Shell Section from layup tool and inspect.

5.1 PREPARATION OF MATERIALS AND TOOLING

All preimpregnated materials, Narmco 5209/T300 graphite/epoxy and Narmco 5209/KEVLAR-49/epoxy, were hand cut to the prepared patterns fabricated in accordance with the EWR 32381 Fuselage Composite Shell Section drawing. The Narmco 5209/T300 graphite was purchased in the form of 12 inch wide 0° unidirectional tape. All 0° and 90° plies were cut directly from the tape. Both the lower cap reinforcement (18 plies) and the upper cap reinforcement (40 plies) were cut from sheets of 0° tape which had been preplied to the required number of plies. All off axis plies ($\pm 45^{\circ}$) were prepared by preassembling $+45^{\circ}$ and -45° pattern cut segments into one two ply sheet of sufficient size to permit the cutting of all patterns in an individual subassembly ply group. The Narmco 5209/KEVLAR-49 style 281 fabric was purchased in a 48 inch width to minimize the number of butt joints occurring in any one skin ply. (The skin plies are also oriented at $\pm 45^{\circ}$ to produce shear stability in an airframe section.) One butt splice joint was required in each skin ply to produce the Composite Fuselage Shell section pictured in Figure 6. Location of the butt splice joints were staggered 6 inches on each succeeding ply to provide shear transfer between plies. After all composite preimpregnated materials were cut, they were inspected visually for size, fiber distortion, resin coating uniformity and identification. Four individual packages containing all the materials necessary for the layup of each individual frame section and one package containing all five stringer subassembly ply groups were prepared.

The foam frame and stringer cores were molded from Stathane 8747, a rigid water blown polyester based polyurethane foam with a free rise density of 221 mg/m^3 (8 lb/cu ft). Selection of the foam was based upon its excellent compression strength at elevated temperatures. The only undesirable characteristic of the 8747 foam is its extremely short "cream" time of 30 seconds at room temperature. ("Cream" time is defined as the elapsed time between the combination of the two components and the initiation of the foaming reaction). To eliminate the problems encountered with the collapse of the foam during the cure cycle of the frame specimen encountered in Phase I of the program, the foaming process was modified as follows:

1) All foam batches were mixed for an exact period of twenty seconds.
2) The mixed foam was introduced into the female foaming tool

shown in Figure 8 through a 2 inch diameter hole in the center of the tool and allowed to distribute itself uniformly in the closed tool.

3) Each foam core 1/2 section was post-cured at 198°C (300°F) for 60 minutes.

4) After all foam details were fabricated, they were placed in a vacuum bag and exposed to the required laminate cure temperature and pressure in an autoclave to verify their compressive dimensional stability.

Utilizing this procedure, an actual density range of 152 kg/m^3 (95 lb/cu ft) to 168 kg/m^3 (10.5 lb/cu ft) was obtained. After cure temperature/pressure verification tests were completed, the foam core details were fitted to the contour of the layup tool, trimmed to size and repositioned in the foaming tool. Epocast 169, a phenolic microballoon/epoxy resin syntactic foam was then cast in the tool to produce the densified areas shown in Figure 9. For the cyclic fatigue tests to be conducted in this program, through holes are drilled in the specimens in these areas, and the mounting hardware for the test loading cylinder is attached. In an actual airframe, these areas would be the areas of attachment of the individual composite fuselage shell sections. Prior to the actual layup of the composite fuselage shell section, all frame and stringer core details were assembled in the tool, as shown in Figure 10, to provide a positive alignment check and a restraining fixture for the cold bond assembly of the frame foam core half sections. A final visual inspection of the assembled foam details was performed at this time, and receiving holes for the floating locator/lateral restraint pins were drilled in the ends of the foam details.

The -T60 shell tool was prepared for layup by cleaning the tool surface with solvent, coating the tool layup surface with two coats of Ram 225, a buffered fluorocarbon bake on type mold release and baking the release coated tool at 198°C (300°F) for two hours.

5.2 FRAME SECTION FABRICATION

Fabrication of the fuselage composite shell section was accomplished over a four day period. This time frame was predicated on the requirement for vacuum debulking or pre-compaction of each completed frame element layup, and an overnight period was selected for this operation. The four ply skin layup shown in Figure 11 was completed with no difficulty.

Each ply segment was placed in the tool individually and tightly butted to the adjacent ply segment. The pre-plied, eighteen ply lower cap reinforcements were then placed in the skin layup using the frame locator angles and an intermediate positioning bar to insure proper location. When the first lower cap rein-

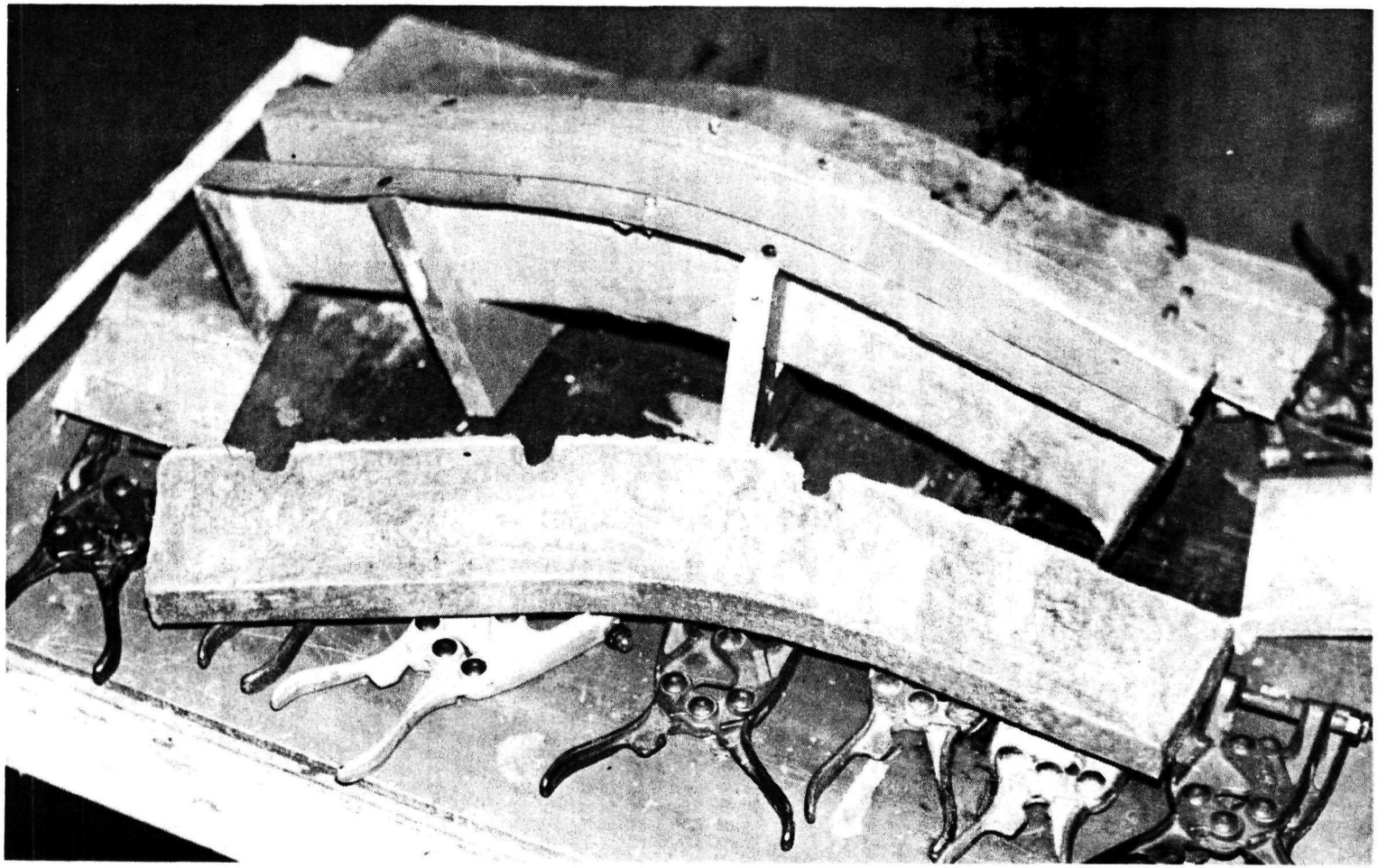

FIGURE 8 . EWR 32381 FOAMING TOOL SHOWING UNTRIMMED FOAM FRAME CORE HALF SECTION.

FIGURE 9 . COMPLETED FOAM CORE DETAILS FOR FRAME AND STRINGER ELEMENTS, SHOWING DENSIFIED AREAS AT ATTACHMENT POINTS ON THE FRAME CORE ELEMENTS.

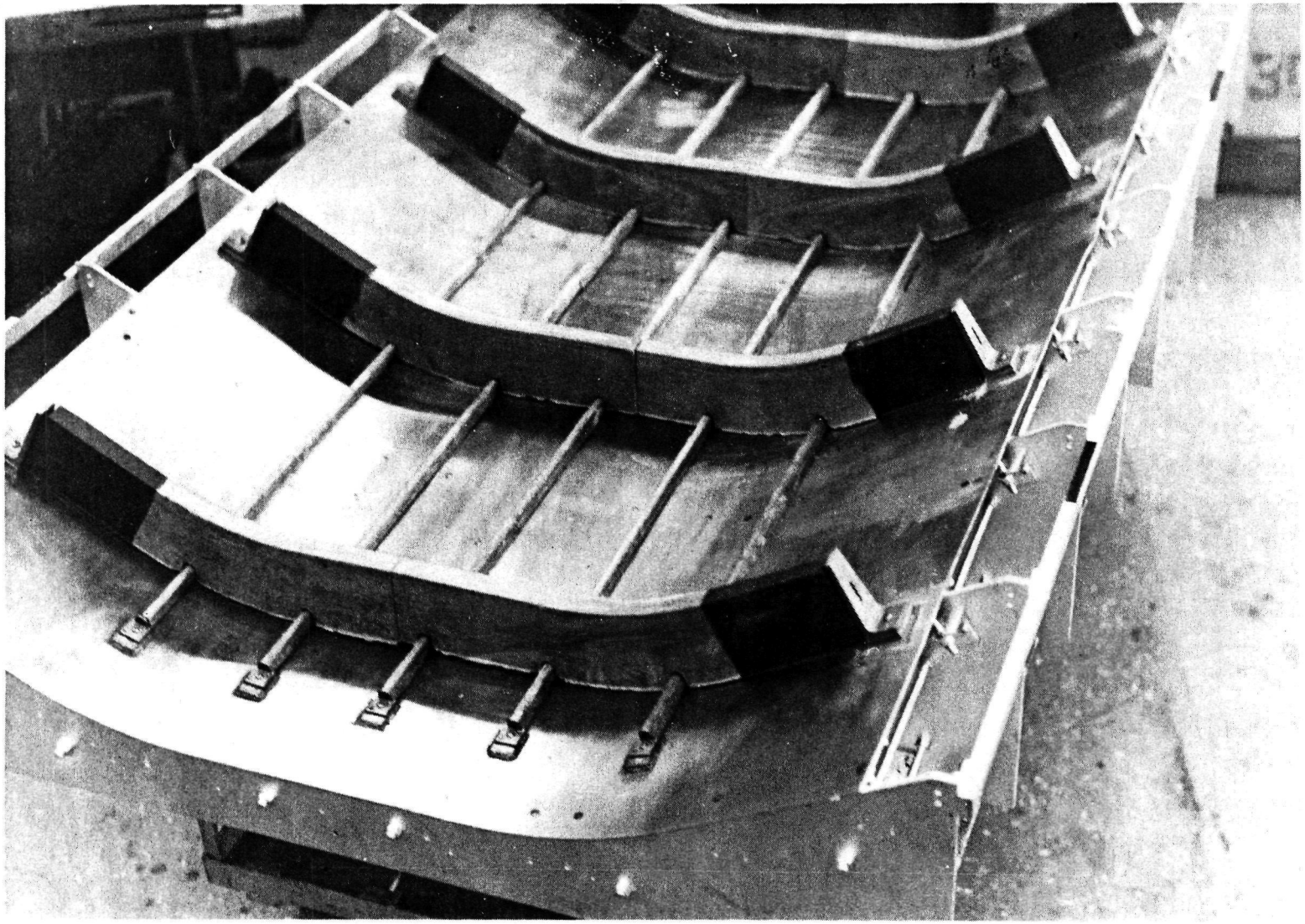

FIGURE 10. EWR 32381-T60 LAYUP TOOL WITH FOAM CORE FRAME AND STRINGER DETAILS IN POSITION.

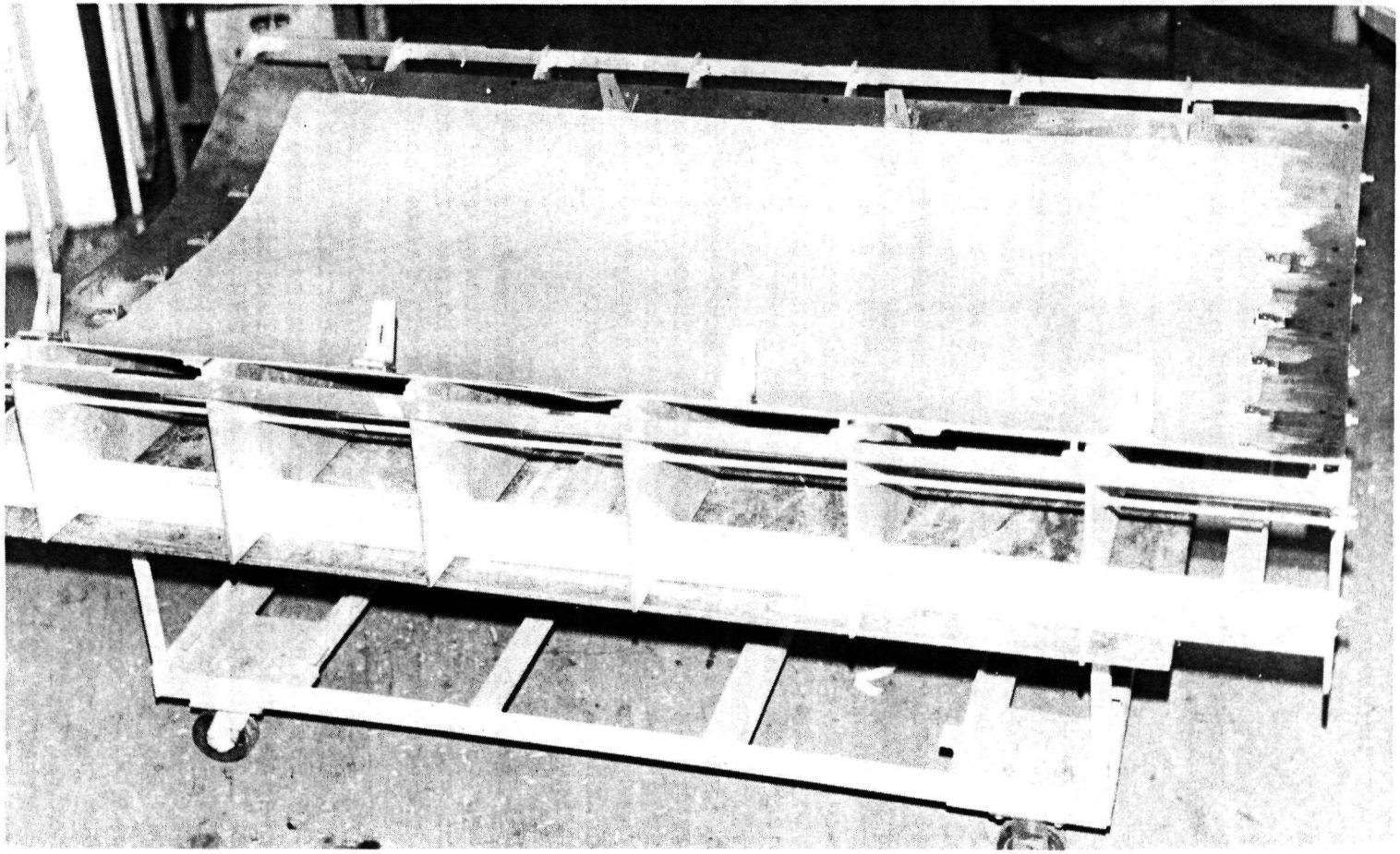

FIGURE 11. COMPLETED SKIN PLY LAYUP IN EWR 32381-T60 LAYUP TOOL.

forcement was placed in the contoured tool, it was found that the cap which had been pre-plied on a flat surface had developed wrinkles caused by forcing the 18 ply layup into the tool contour. The tack of the resin was apparently sufficient to prevent a shearing action to take place between the individual plies as they were warped into place on the tool. On all three remaining lower cap layups, the pre-plied cap laminates were placed on an electrically heated table and warmed to 35-43°C (95-100°F) before attempting to position them on the tool surface. This operation proved highly successful and eliminated any apparent fiber buckling. The completed skin and lower cap layup is shown in Figure 12. The -107 stringer foam details were then positioned on the layup and a pre-plied graphite/Kevlar stringer laminate positioned over the foam. When attempting to compact the laminate over the foam surface, excessive movement of the foam was encountered and as a result, the completed stringer layup was no longer positioned to receive the notched frame foam details. It was therefore necessary to remove and discard the first stringer assembly. Material for a replacement stringer was prepared and an alternate, improved procedure for the assembly of the stringer layup to the stringer foam was developed. Each stringer foam core detail was placed on the electrically heated table over a release paper slip-sheet. The composite pre-plied layup was then positioned over the foam and pin tacked in place. A vacuum bag was placed over the foam and composite layup. Heat was applied to the table to warm the layup to 35-43°C (95-100°F) and vacuum drawn on the bag. As the air was evacuated by the vacuum, the composite layup was drawn down over the foam. When the composite layup contacted the slip sheet placed under the stringer foam detail, it was mechanically squeegeed to conform to the foam contour producing a well compacted assembly of the layup and foam as shown in Figure 13.

The resulting assembly was removed after cooling to room temperature under vacuum, and successfully positioned on the skin layup. The procedure was repeated with the remaining stringer foam core details to produce the skin/stringer layup shown in Figure 14.

The next step in the sequential layup procedure involves the layup of the frame sections. All composite materials were prewarmed to 35-43°C (95-100°F) on the electrically heated table prior to layup to increase the tack and promote flexibility to enhance their drapability characteristics. One EWR 38321-105 frame foam detail was placed over the partially completed composite shell section layup and pinned to the frame locator angles. The pre-plied (2 ply) EWR 38321-108 inner end reinforcements were positioned and hand compacted. A 40 ply upper cap layup assembly, EWR 38321-104, was then positioned on the upper surface of the frame foam detail with no apparent difficulty (see Figure 15). Placement of the EWR 38321-102 web reinforcement plies was accomplished as follows:

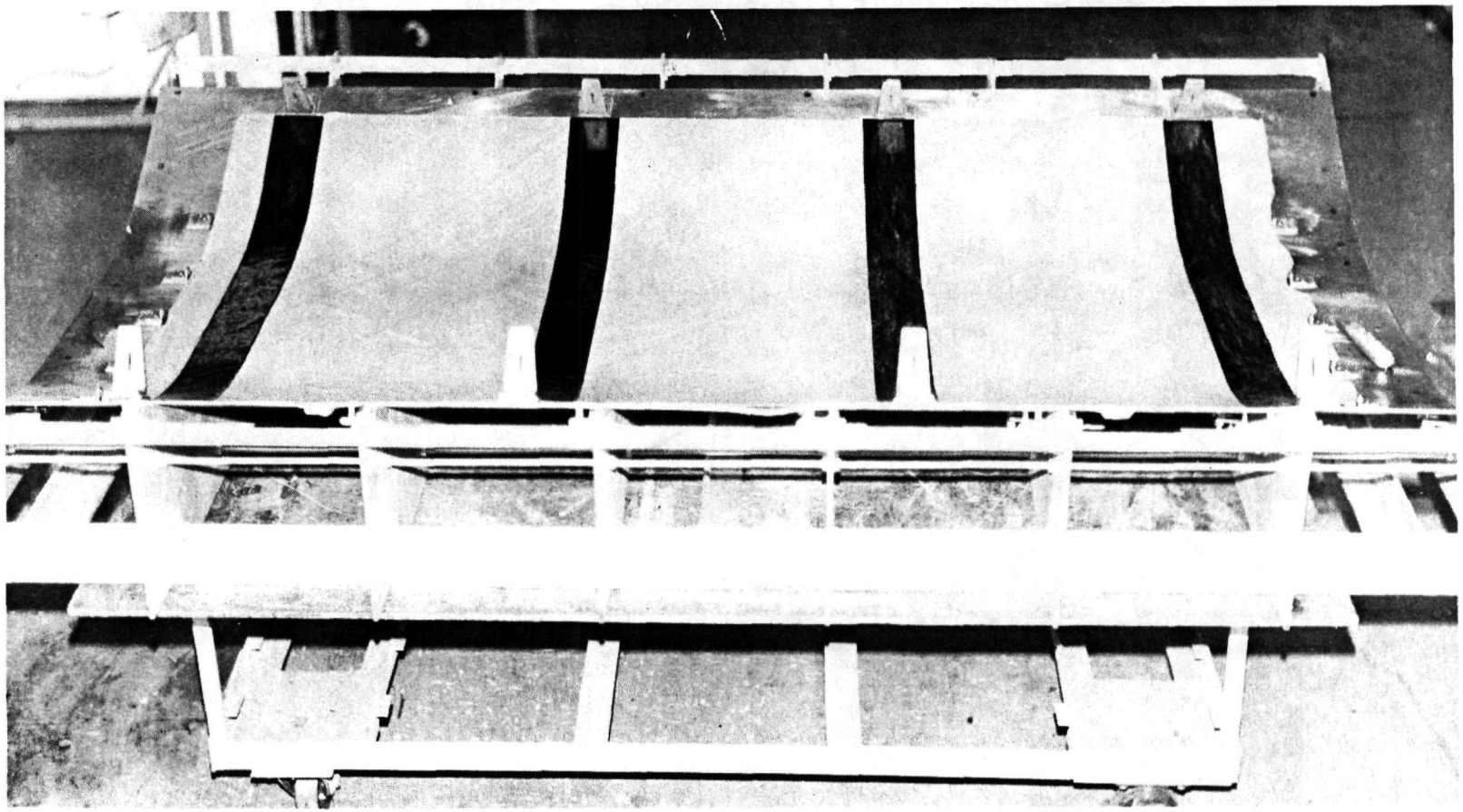

FIGURE 12. COMPLETED SKIN AND LOWER CAP LAYUP IN EWR 32381-T60 TOOL.

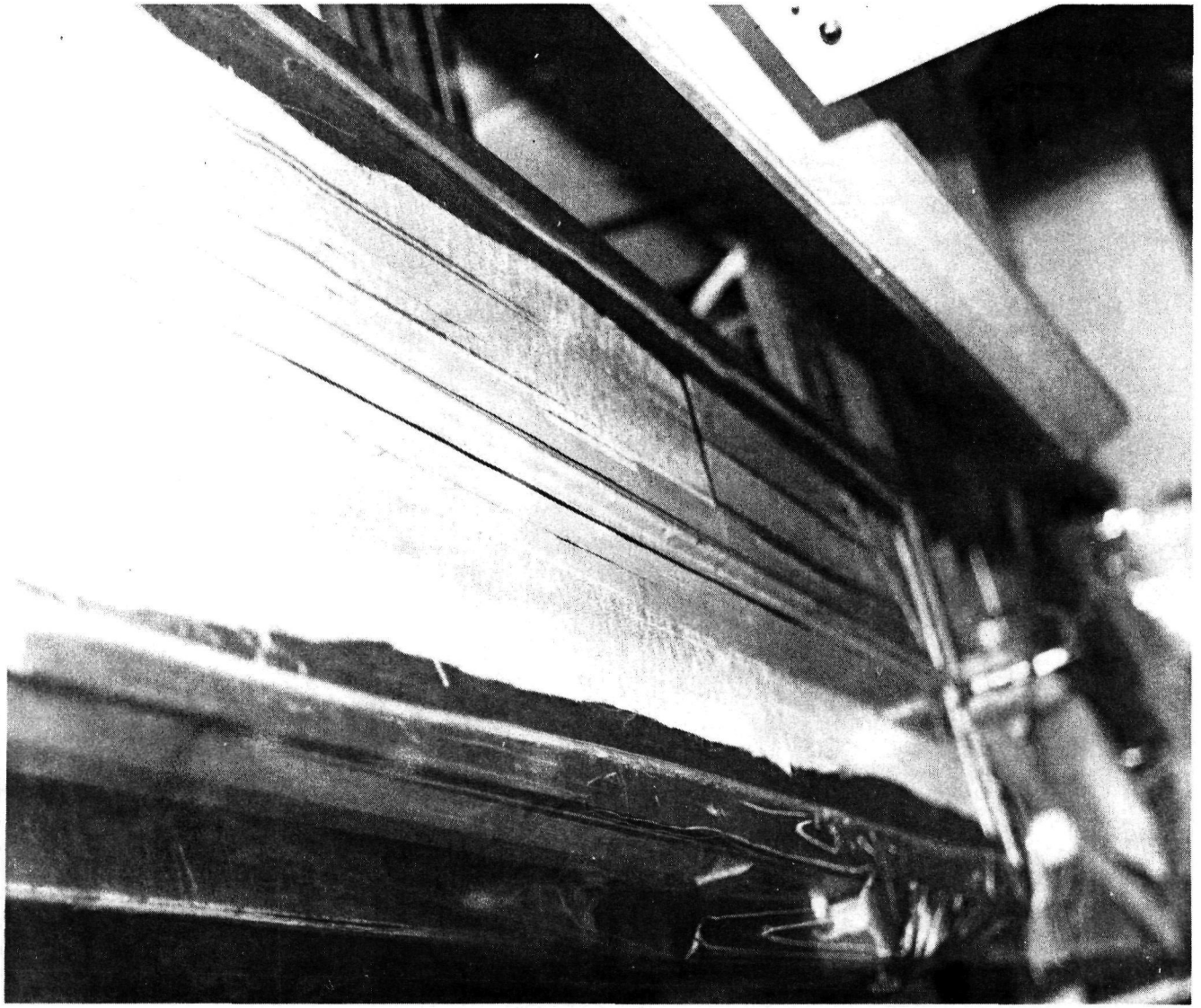

FIGURE 13. FORMED STRINGER LAYUP/STRINGER FOAM ASSEMBLY UNDER VACUUM ON ELECTRICALLY HEATED TABLE.

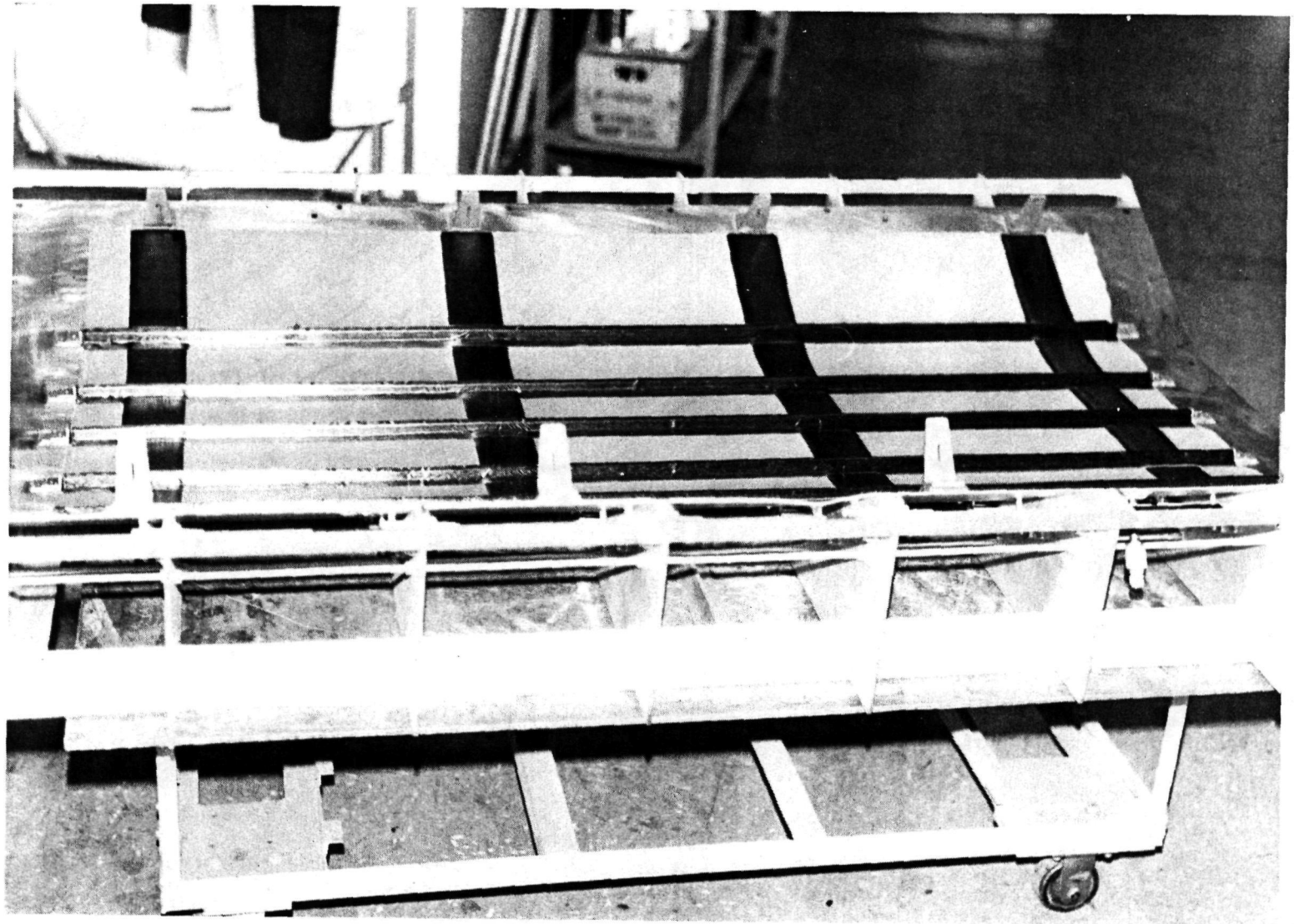

FIGURE 14. EWR 32381 COMPOSITE SHELL SECTION LAYUP, WITH SKIN, LOWER CAP, AND STRINGER LAMINATES IN POSITION.

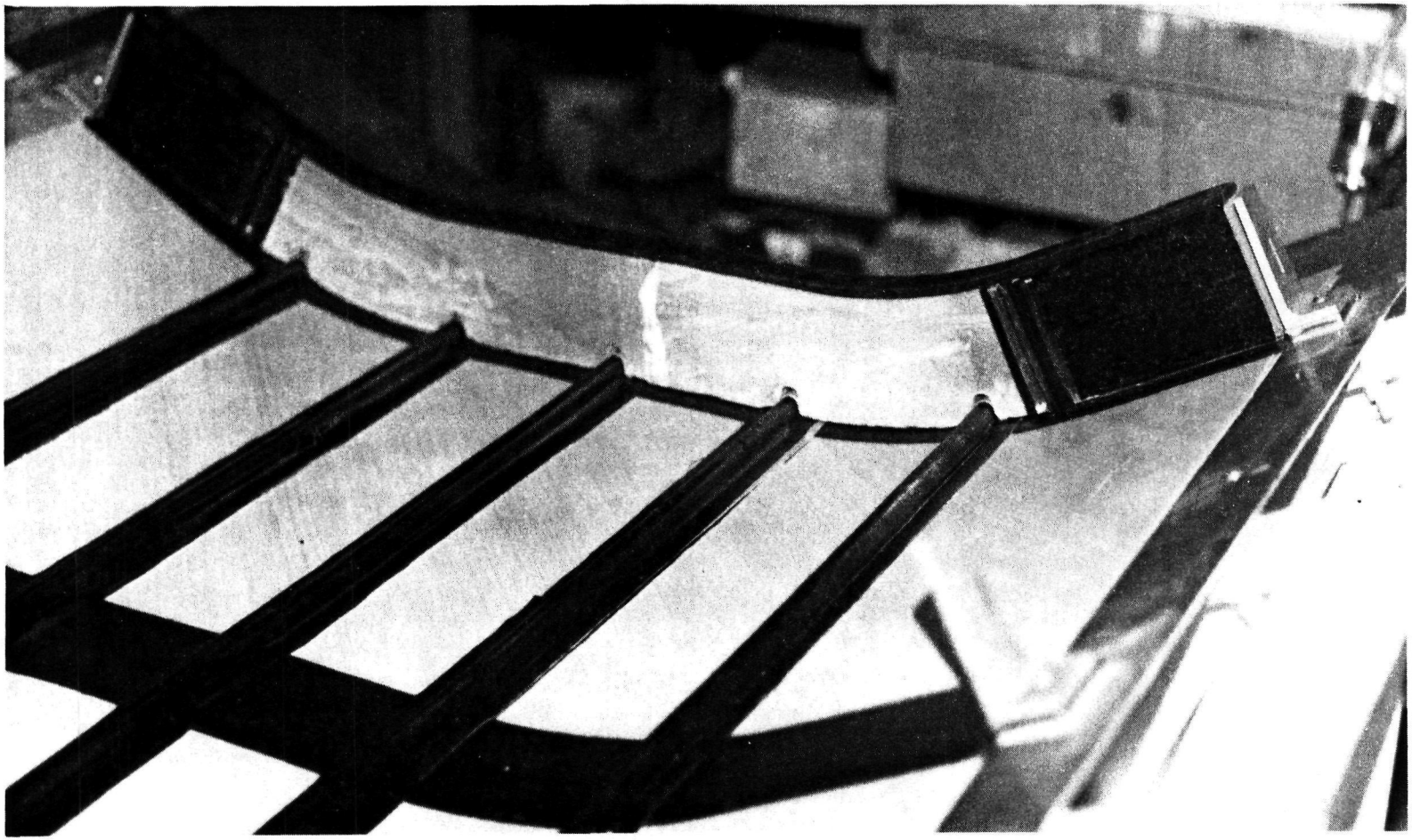

FIGURE 15. EWR 32381 COMPOSITE SHELL SECTION LAYUP, WITH INTERNAL FRAME END REINFORCEMENTS, AND UPPER CAP LAMINATE IN POSITION.

1) Remove separator paper from one surface of pre-plied two ply web reinforcements.
2) Place on heating table and allow to stabilize at temperature.
3) Transfer ply #1 and #2 to tool, align center line coordinator markings with locator angle center lines and squeegee to contact upper surface of cap laminate.
4) Remove paper separator from upper surface.
5) Work web reinforcement into position from center of layup out towards end of frame.
6) Compact web layup by squeeging to surface of frame foam.
7) Trim excess material from flanges at frame skin intersection and slit at frame/stringer juncture.
8) Repeat until frame web laminate is completed.

The EWR 38321-109 outer end reinforcements were positioned and compacted completing the layup of the first frame of the composite fuselage shell section. Figure 16 shows the completed layup of the first frame. A release fabric was fitted to the partially completed layup, a nylon film vacuum bag sealed to the tool surface and vacuum applied. The part was allowed to remain under vacuum overnight to pre-compact the partially completed layup (see Figure 17). Layup of the remaining frame sections continued until the composite fuselage shell section layup was completed.

The completed layup was prepared for cure by placing a tailored porous teflon coated release fabric over the entire layup surface, a nylon peel ply over the release ply and style #181 glass bleeder plies in the ratio of one bleeder ply to each five composite plies over the peel ply as shown in Figure 18. A film type nylon vacuum bag was sealed to the periphery of the layup tool and vacuum drawn. The completed composite fuselage shell section was cured in an autoclave utilizing the cure cycle developed for the Narmco 5209 resin system in Phase I of the program, with the exception that vacuum was released and the bag vented to the atmosphere at the beginning of the autoclave cycle. The completed cured part is shown in Figure 19.

5.3 SPECIMEN PREPARATION, FRAME SECTION

End reinforcements incorporated into the ends of each frame detail during the one-step cure process on the composite shell section were designed to react the anticipated loads developed in a realistic airframe splice joint area. The test loads imposed during the spectrum fatigue test of each frame specimen are approximately five times greater than those calculated for the aircraft splice joint area. Therefore, it was necessary to reinforce the end attachment areas of each frame speciment to accept the test attachment hardware and to insure failure in the test area of the specimen. To accomplish this, tapered graphite doublers were laminated to the end areas of each frame test specimen in a subsequent cure operation. The laminated doublers

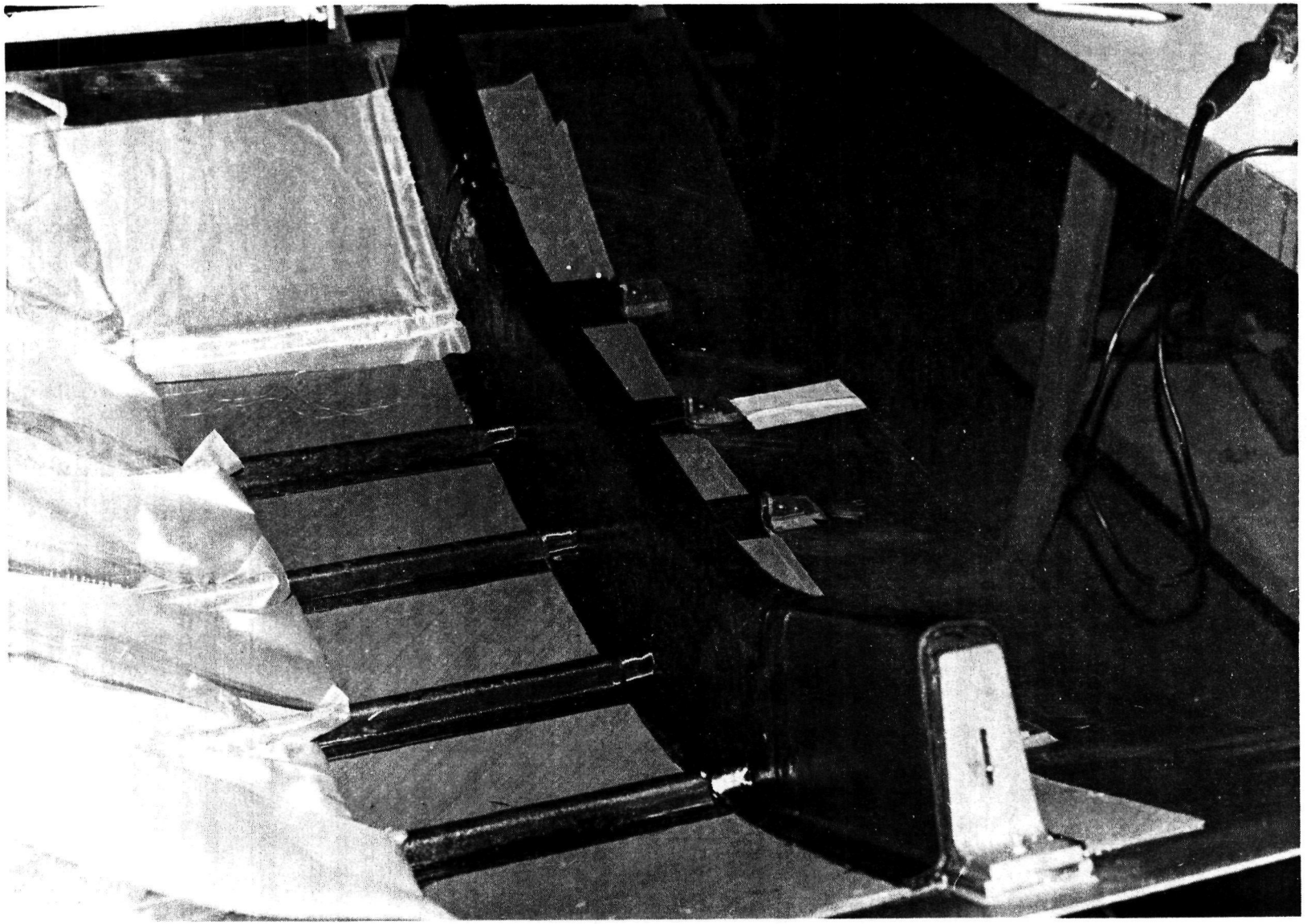

FIGURE 16. COMPLETED #1 FRAME LAYUP, WITH RELEASE FABRIC PARTIALLY IN POSITION.

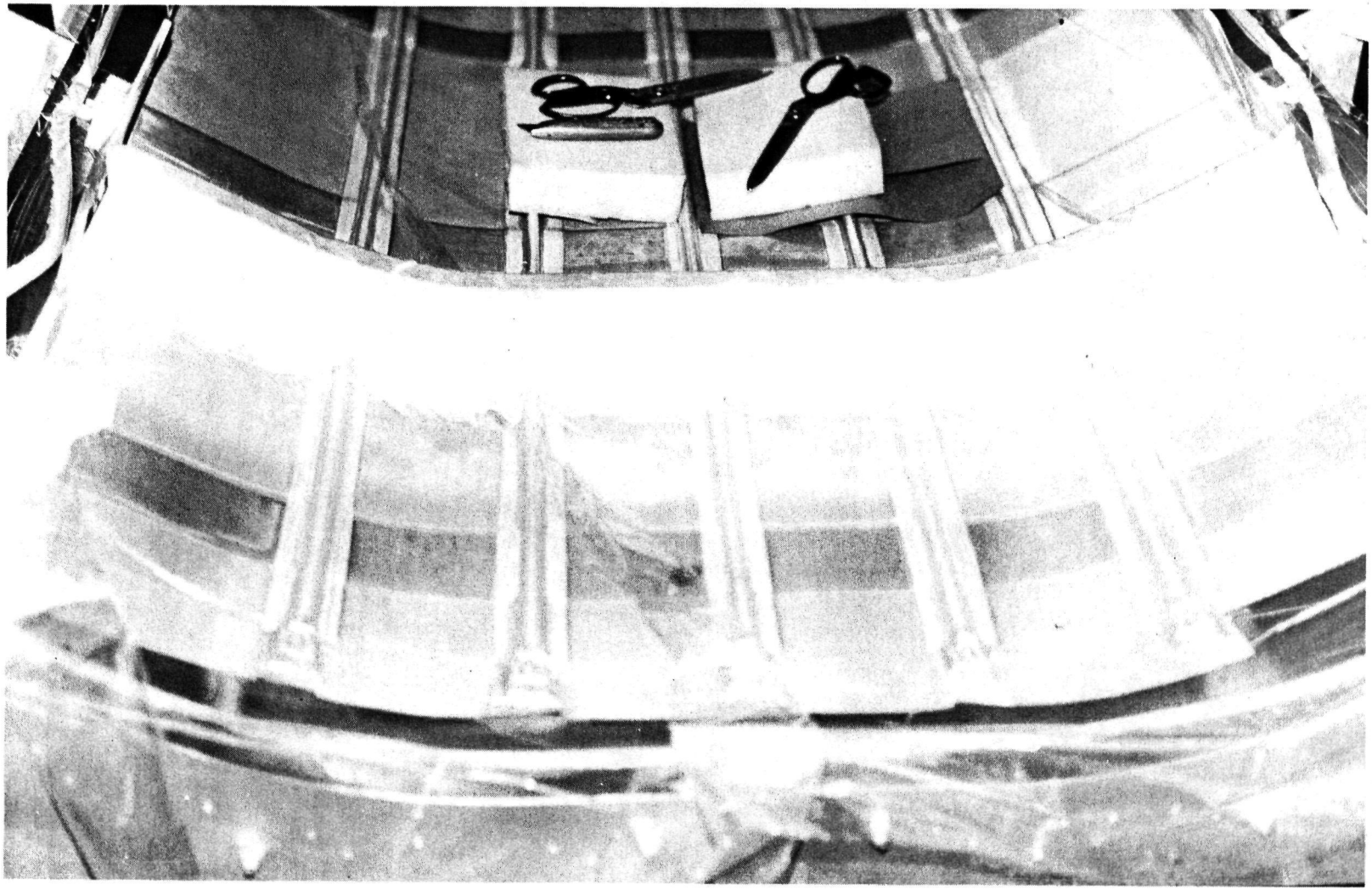

FIGURE 17 . #1 FRAME SECTION UNDER VACUUM DURING PRECOMPACTION STAGE.

FIGURE 18. COMPLETED EWR 32381 FUSELAGE COMPOSITE SHELL SECTION BEFORE CURE, SHOWING GLASS BLEEDER FABRIC IN POSITION.

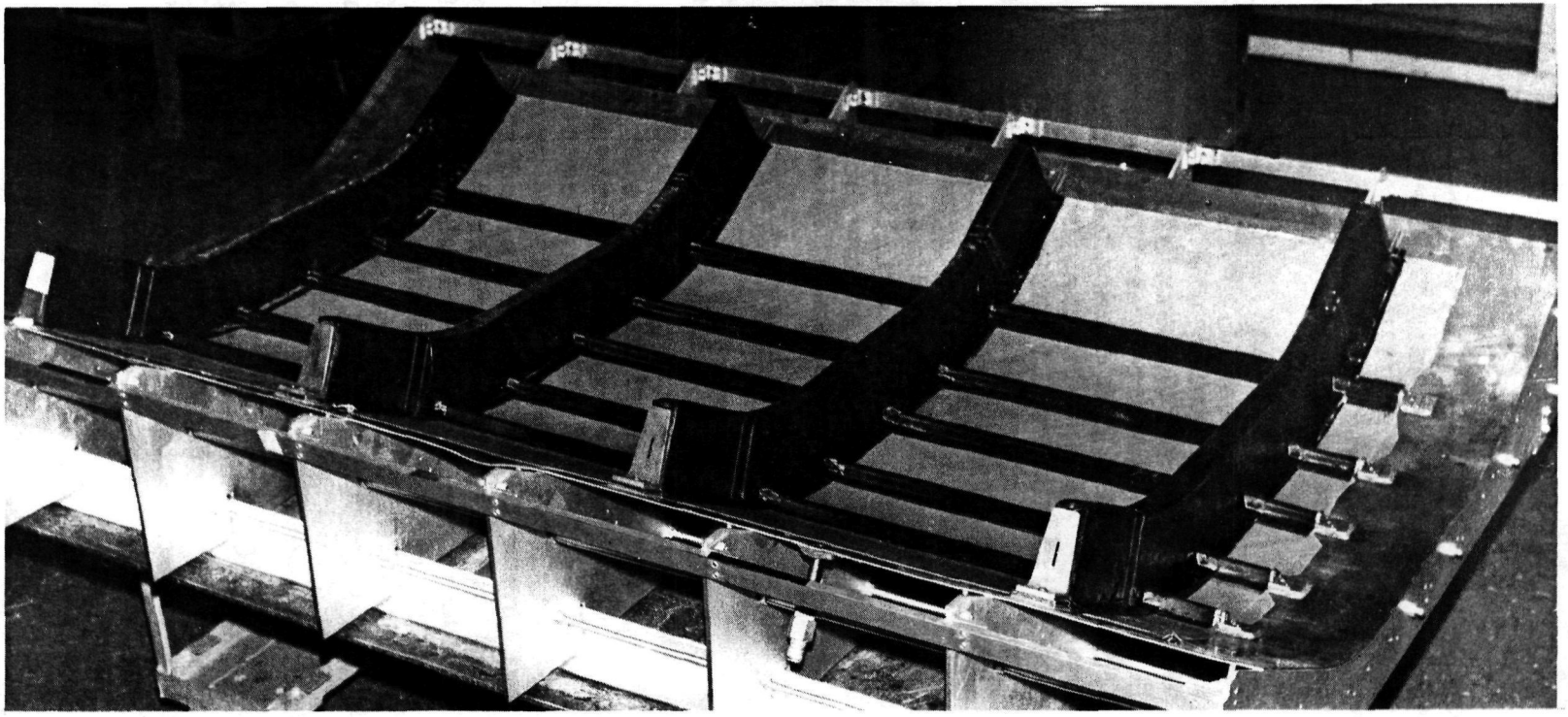

FIGURE 19. COMPLETED EWR 32381 FUSELAGE COMPOSITE SHELL SECTION.

are similar to those developed in the analytical portion of Phase I and proven successful during the static test portion of Phase I. The doubler configuration consists of a series of forty-four patterned plies applied to each end of the frame specimen to produce a tapered reinforced area as shown in Figure 20.

Individual specimens were cut from the composite shell section panel on a Bay State Model #41A Cutoff Saw, utilizing an eight inch diamond wheel with a 100-120 grit cutting surface. Tap water flood coolant was applied during the entire cutting operation. All cut edges were acceptable as cut.

The upper surface of the laminated end doublers required machining to produce a surface and dimension suitable for insertion into test end fittings. Surface machining was accomplished on a conventional J head Model #17390 Bridgeport Milling Machine utilizing a six toothed three inch diameter carbide end mill. The test end fittings were then located and clamped to the frame specimen. Drilling of the frame to test end fitting holes was accomplished by utilizing the predrilled holes in the end fittings as alignment and locator bushings for drilling the frame specimens. Drilling was performed on a Carlton three foot radial drill as shown in Figure 21. Conventional cobalt steel drills were used to produce all holes. The machine speed was 124 rpm with a feed rate of 0.006 inch/revolution. After drilling, all holes were final sized to 0.003 inch diameter over the bolt diameter by machine reaming with a conventional four fluted spiral reamer.

5.4 IMPROVED FRAME SPECIMEN

An unexpected static failure of the number one frame fatigue specimen in the curved portion of the specimen during limit load application and the subsequent failure analysis, as discussed further in Section 6.2, indicated certain design modifications were required to be incorporated into the present composite frame design. To verify the effects of these projected improvements, a decision was made to fabricate an additional frame specimen, incorporating all of the calculated design improvements. In addition to the changes made in the design of the frame section, suggested fabrication improvements were also evaluated. Semi-flexible caul plates were fabricated and utilized to improve surface definition and contours on the frame outer surfaces.

A caul plate assembly, consisting of 0.020 inch perforated fiberglass laminates for the cap and end areas of the frame, and perforated steel (0.010 inch thick) caul plates for the straight sides of the frame was fabricated as shown in Figure 22. The design improvements to be incorporated into this specimen involved a rearrangement of the cap and web laminate plies. With the exception of these changes and a modification to the sequential layup procedure, fabrication of the improved frame specimen

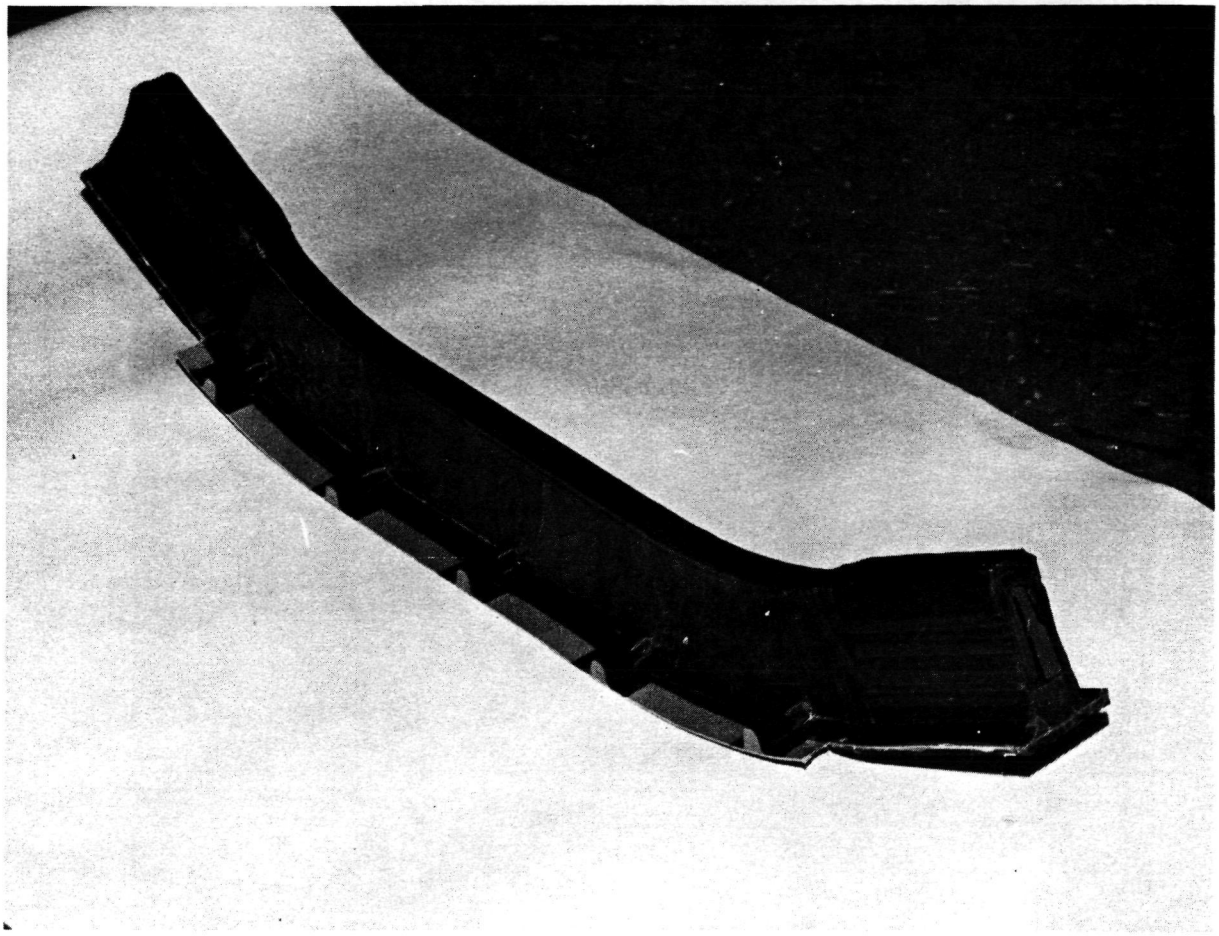

FIGURE 20 . COMPLETED EWR 32381 FRAME CYCLIC FATIGUE TEST SPECIMEN.

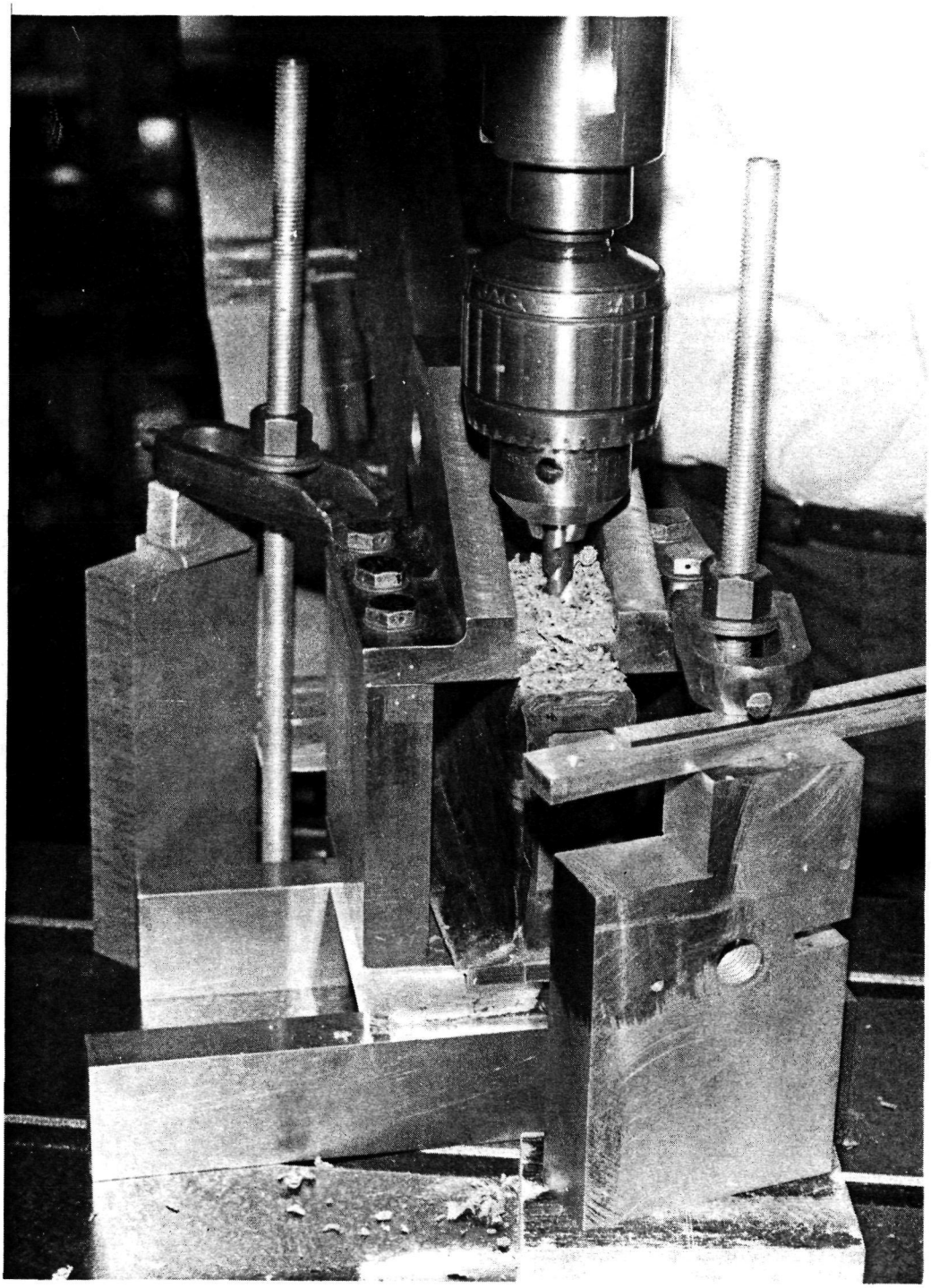

FIGURE 21. EWR 32381 FRAME FATIGUE SPECIMEN DRILLING OPERATION FOR EWR 44092 TEST END FITTING ATTACHMENT.

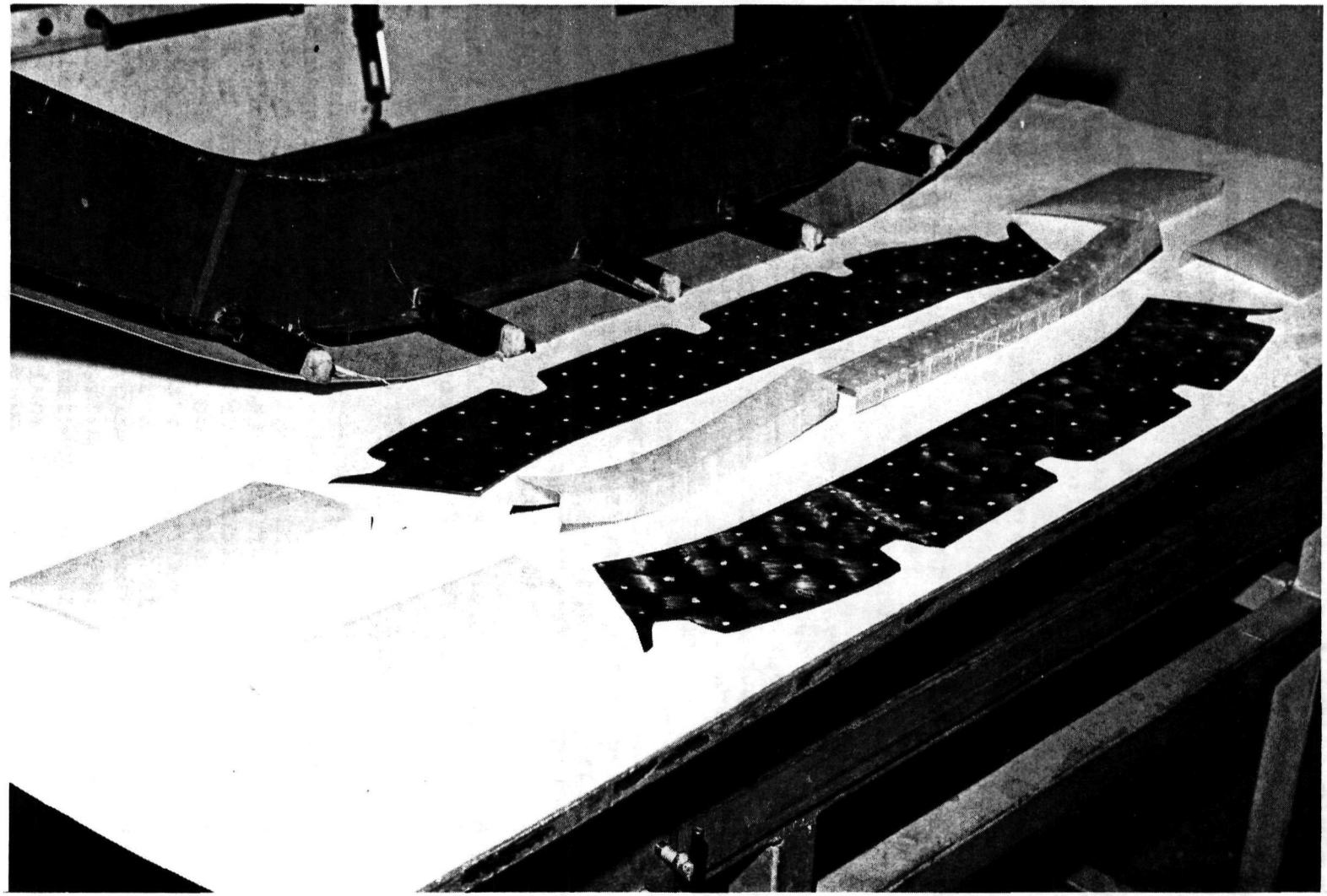

FIGURE 22. EWR 32381 IMPROVED FRAME SPECIMEN WITH CAUL PLATE ASSEMBLY.

was identical to that of the completed EWR 32381 frame specimens. The fabrication procedure was modified as follows:

- The lower cap unidirectional plies were pre-plied into two ply assemblies and placed on the skin layup in nine individual operations.

- Six frame web plies were laid up on the frame foam core detail before application of the upper cap laminate layup.

- The upper cap unidirectional plies were pre-plied into two ply assemblies and placed on the frame web layup in twenty individual operations.

- The remaining web and reinforcement plies were added to complete the layup.

- After completion of the layup, the caul plate assembly was applied to the frame surface and the glass fabric bleeder plies positioned over the caul plate assembly.

The cure of the improved frame specimen was accomplished in accordance with the cure cycle developed in the Phase I study. The initial dwell period of 45 minutes under vacuum only was re-instituted to produce additional resin bleedout and reduce porosity in the cured laminate.

The completed specimen seen in Figure 23 shows the improvement gained in surface finish. In Figure 24, a comparison of a section removed from the improved frame specimen to one removed from the original composite shell section shows the improvement on cross-sectional definition and upper cap uniformity imparted by the use of semi-flexible caul plates during the cure cycle.

Preparation of the improved frame specimen for test was identical to that of the original EWR 32381 frame specimen.

5.5 FRAME SPLICE JOINT FUSELAGE SECTION

A fuselage section was fabricated with frame splice joints incorporated to provide three frame splice attachment specimens for spectrum fatigue test evaluation. The individual frame splice joint specimens differ from those previously fabricated in that two fuselage frame stub sections are connected by a composite splice channel. A Fuselage Composite Shell Section, consisting of a skin, three frame sections and two stringer sections, was required for this portion of the program. Fabrication of the shell section was conducted on the existing EWR 38381-T60 shell mold. All design and manufacturing modifications evaluated on the improved frame specimen were incorporated into the fabrication of the frame joint shell section.

FIGURE 23. AUTOCLAVE CURED EWR 32381 IMPROVED FRAME SPECIMEN.

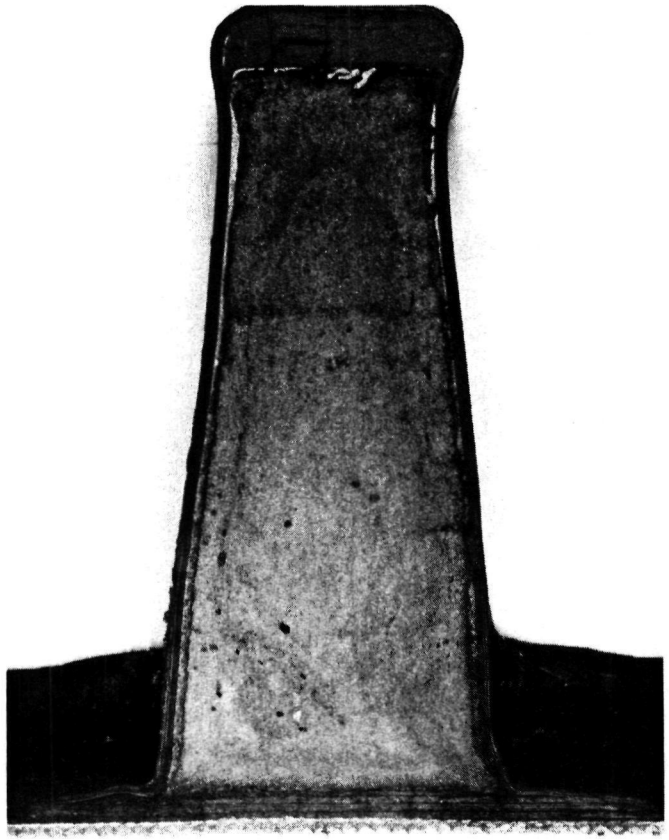

(a) ORIGINAL FRAME SECTION. POOR DEFINITION AND COMPACTION OF UPPER CAP.

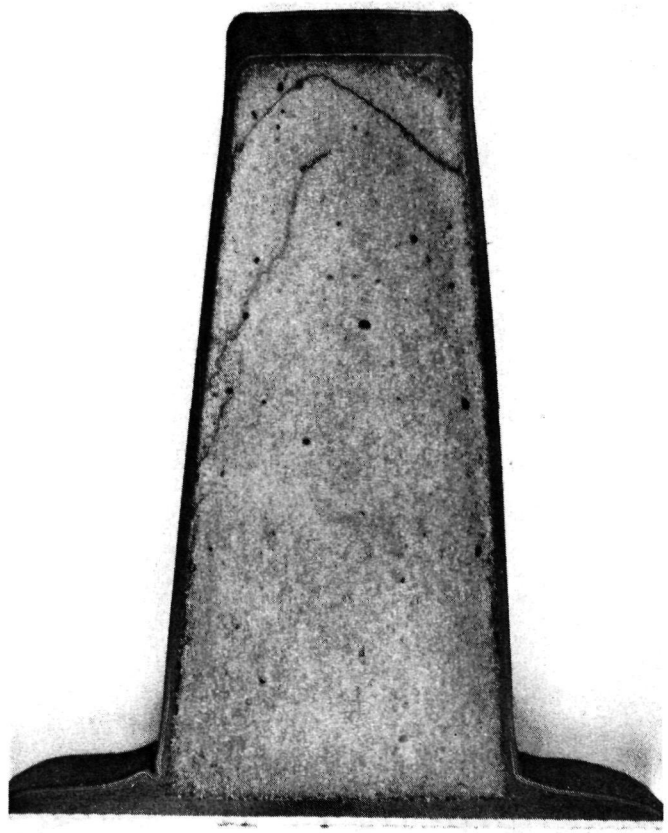

(b) IMPROVED FRAME SECTION. EXCELLENT DEFINITION OF CROSS SECTION AND COMPACTION OF UPPER CAP.

FIGURE 24. SECTION VIEWS OF ORIGINAL SHELL SECTION FRAME AND IMPROVED FRAME.

Individual foam core details were fabricated for each of the six frame half sections required to produce the three fatigue specimens. Foam sections were cast as previously detailed, removed from the foaming tool, cut to size and replaced in the tool. Syntactic foam mechanical attachment spacers were cast to both ends of the foam frame core. The completed foam core details were then fitted to the layup tool with the aircraft attachment ends butting at the center of the tool. The frame shell section was fabricated in accordance with the basic fabrication procedure previously described in detail except that the aircraft attachment reinforcements were laid up at the center of each frame. Caul plates, similar to those developed for the improved frame specimen, were utilized on all three frame details.

The composite splice channel, shown installed on the frame splice joint specimen in Figure 25, was fabricated on an aluminum male tool provided in Phase I of this program.

5.6 SPECIMEN PREPARATION, FRAME SPLICE JOINT SECTION

To eliminate the requirement for special alignment fixturing during the machining of the splice channel to frame attachment holes, each frame was incorporated into the fuselage shell section with the foam half sections butted at the center of the frame, and the splice joint occurring at the center of the frame. The layup was positioned over the two sections as though it were a continuous single frame. Therefore, when a splice channel was positioned on each frame section in the correct location, drilling could be accomplished on both frame section segments at one time in a single machine setup, as shown in Figure 26. To eliminate splintering at the entry and exit surfaces of the spliced channel during the drilling operation, the fiberglass bleeder plies were not removed until after the drilling operation was completed. A backup support plate on the exit surface, also shown in Figure 26, was provided to prevent deformation and possible fiber splitting. Machine speed and feed rate was the same as used in the drilling of the test end fitting holes on the frame specimens. Holes were reamed to produce an .001 in. - .003 in. diametral clearance between the hole and bolt diameters. Upon completion of the splice channel attachment holes, each frame section was cut at its centerline on a Bay State Model 41A Cutoff Saw with a diamond wheel. Test end fittings were then located and attached to the frame half sections in an identical procedure to that developed during the preparation of the full frame specimens for test. The frame half sections were joined with the splice channel using bolts. The bolts were installed with SS 81-011 aluminum taper shim washers bearing against the composite surface, and torqued to 150 in./lb to prevent any localized deformation of the composite structure.

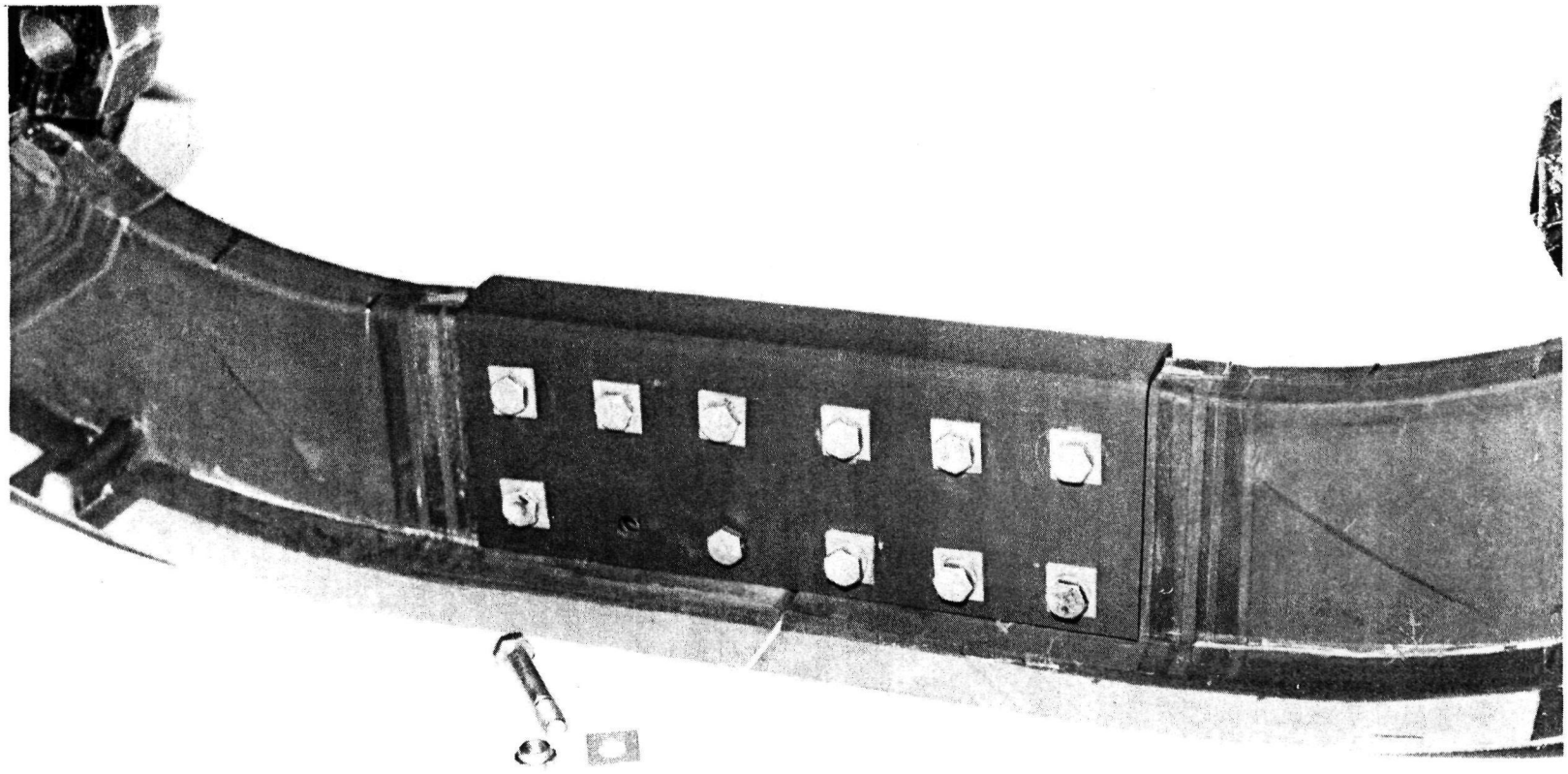

FIGURE 25. EWR 39411-113 COMPOSITE SPLICE CHANNEL INSTALLED ON EWR 32381 FRAME SPLICE JOINT SPECIMEN.

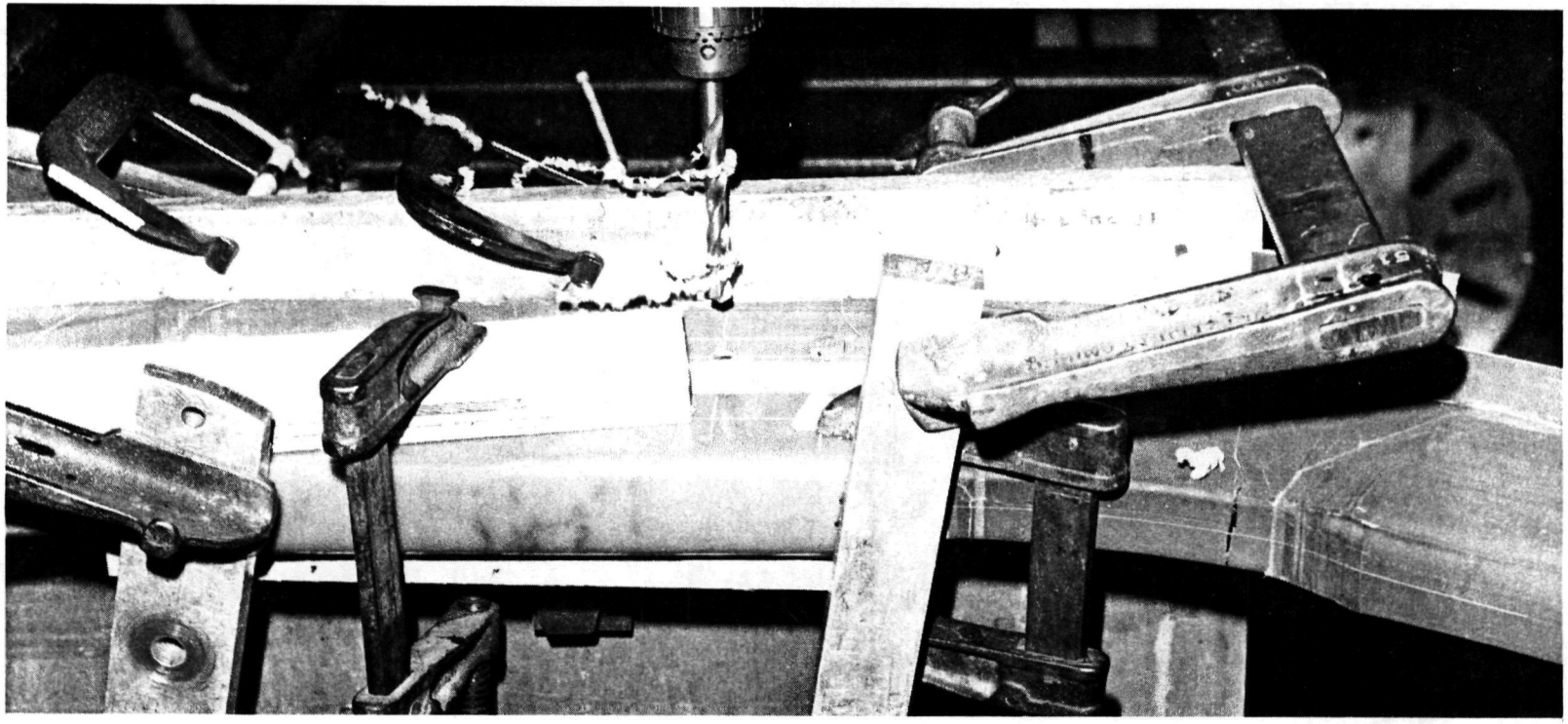

FIGURE 26. COMPOSITE FRAME SPLICE JOINT, ATTACHMENT HOLE MACHINING.

THIS PAGE INTENTIONALLY LEFT BLANK.

6.0 SPECTRUM FATIGUE TEST, EQUIPMENT AND PROCEDURES

In Phase I of this program, static axial and bending tests were conducted on short sections of representative frame, frame joint stringer and stringer joint specimens to substantiate the strength and stability characteristics of these members. Test results indicate the single cure process, as developed, has significant potential for fabrication of large airframe sections.

The test procedures developed for this, the Phase II effort of the program, were intended to evaluate the structural integrity of frame and frame joint sections in a realistic fatigue environment and to determine the residual static strength of each structure after completion of the spectrum fatigue tests.

6.1 TEST EQUIPMENT

The test equipment shown in Figure 27 was prepared specifically for the spectrum fatigue testing of the composite frame and frame splice sections fabricated in this program. The equipment consists of a test fixture designed to provide a stable base for the specimen/load cylinder assembly. Loads are inputted to the specimen being fatigue tested through a load programmer/controller specifically designed for this test. Individual load chips, representing the randomized loading spectrum for the 4000 hour accelerated fatigue test were prepared and stored in the programmers memory banks. Based on the randomization selected, the programmer provides the command signal which actuates an electrohydraulic servo cylinder. The electrohydraulic servo cylinder presents the load selected to the hydraulic load cylinder connected to the section being tested. Control of the load input is maintained through a closed loop circuit utilizing the load cell connected to the load input cylinder to provide a load feedback signal. The load programmer/controller is shown in Figure 28 with a schematic drawing of the program/load control system. To monitor acoustic indications of damage, the equipment shown in Figure 29 was utilized. Three electric condenser microphones were isolation suspended from the test fixture in areas of anticipated damage accumulation. These areas were determined by the failure analysis of the first frame specimen. The microphones were connected through a sound level meter and preamplifiers to individual tape recorders. All specimens were prepared for test by the addition of test end fittings shown in Figures 30 and 31. The load cylinder and load cell were attached between the pin ends of the end fittings. The specimens were suspended in the test fixture by means of elastic shock cords to preclude any extraneous load reactions. Specimen behavior during the spectrum fatigue test was monitored by a digital strain indicator and dial indicators installed to measure both vertical and horizontal displacement.

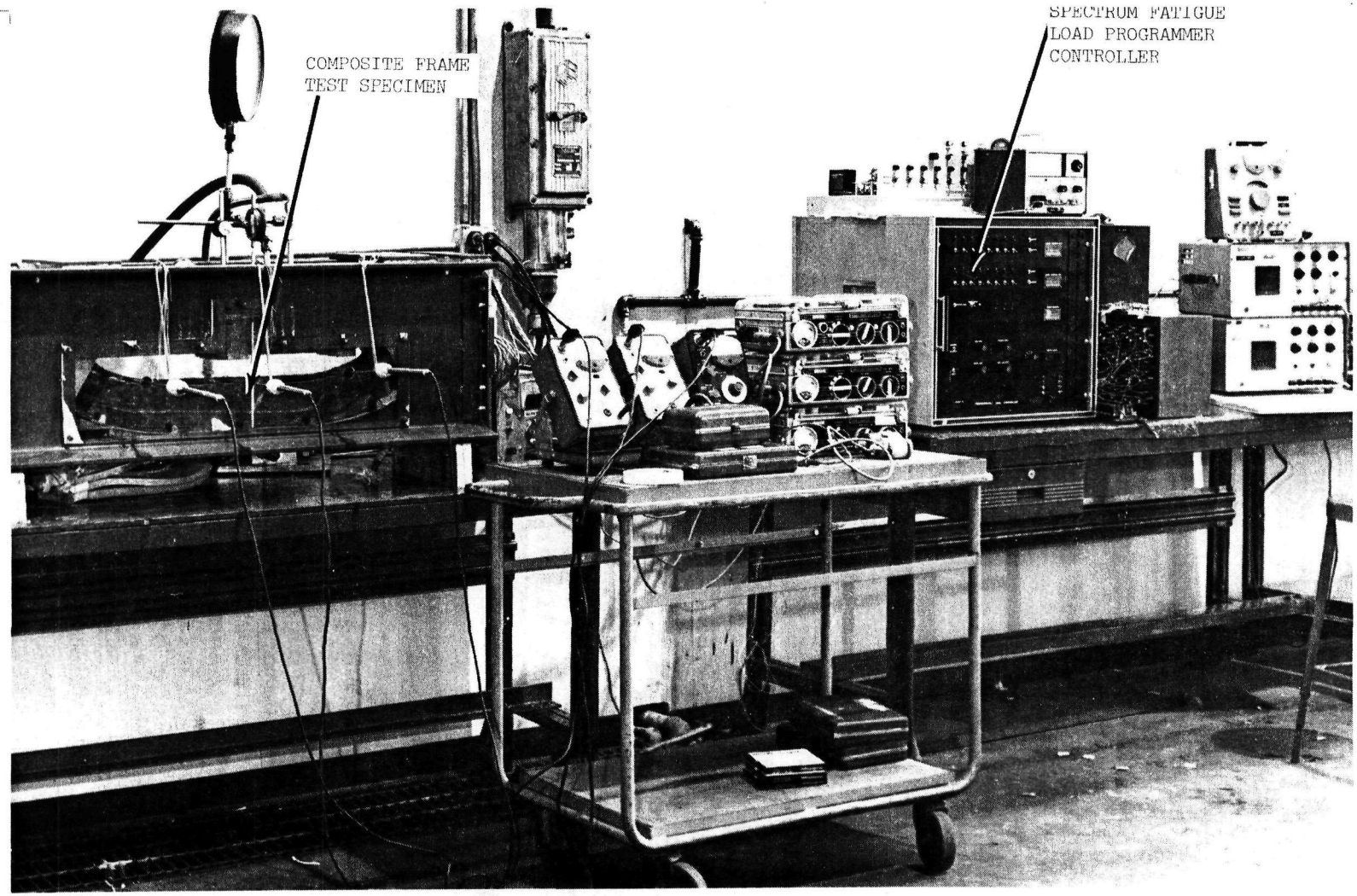

FIGURE 27. COMPOSITE FUSELAGE FRAME AND FRAME SPLICE JOINT SPECTRUM FATIGUE TEST FACILITY.

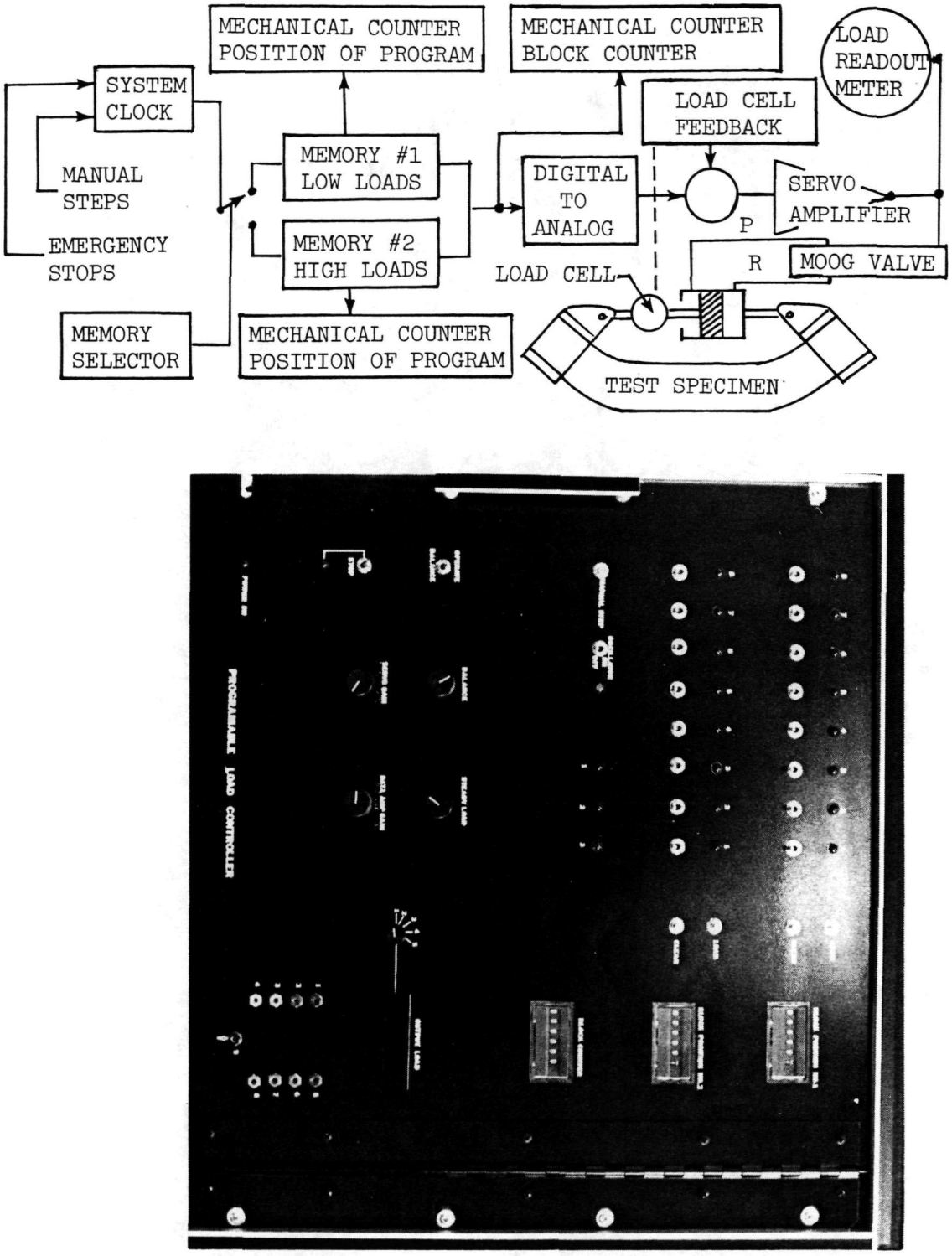

FIGURE 28 . COMPOSITE FUSELAGE FATIGUE TEST PROGRAMMABLE LOAD CONTROLLER CONSOLE WITH SCHEMATIC ARRANGEMENT DIAGRAM.

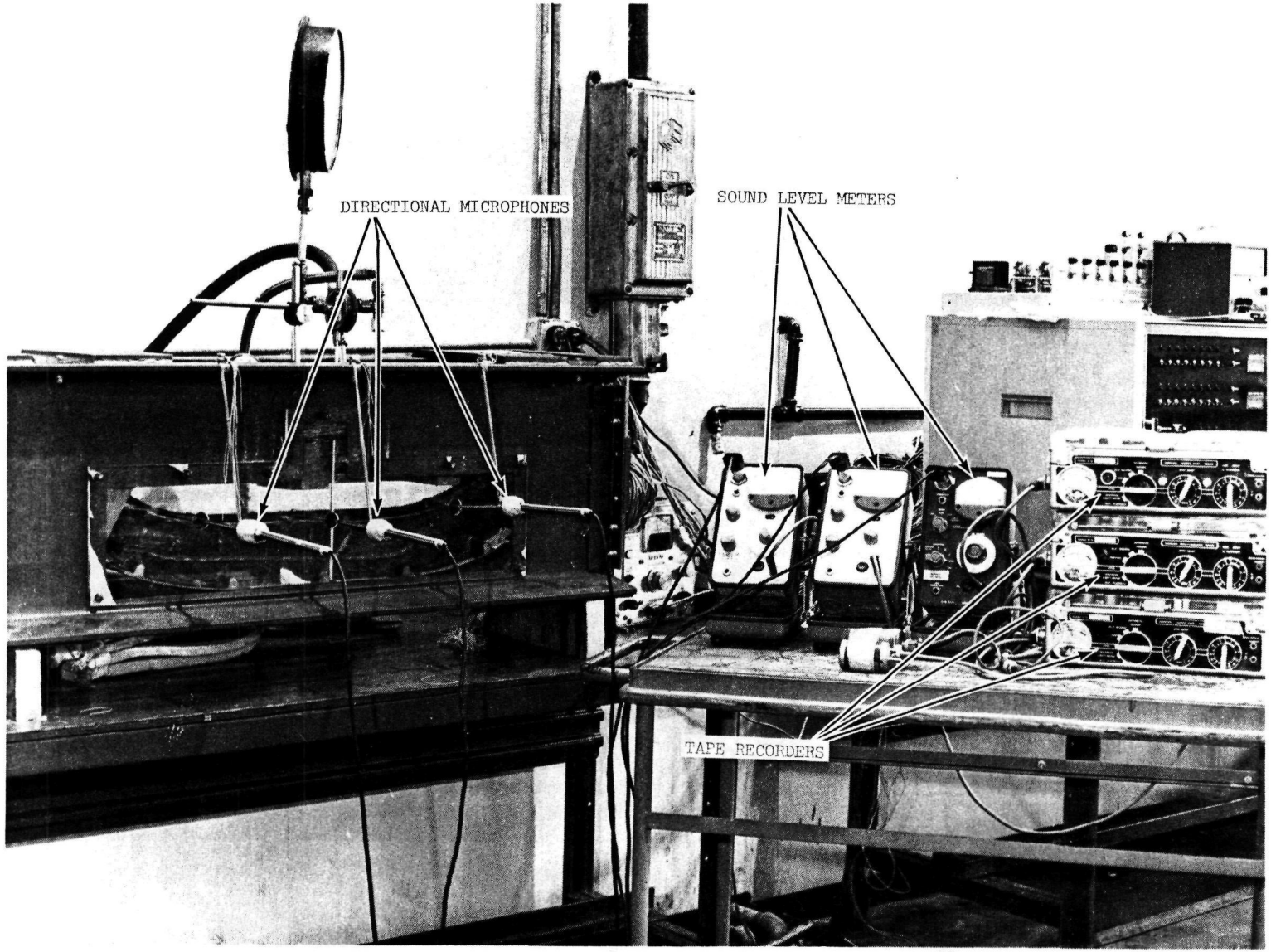

FIGURE 29. ACOUSTIC MEASUREMENT EQUIPMENT INSTALLED ON COMPOSITE FUSELAGE FRAME SPECIMEN IN POSITION FOR FATIGUE TEST.

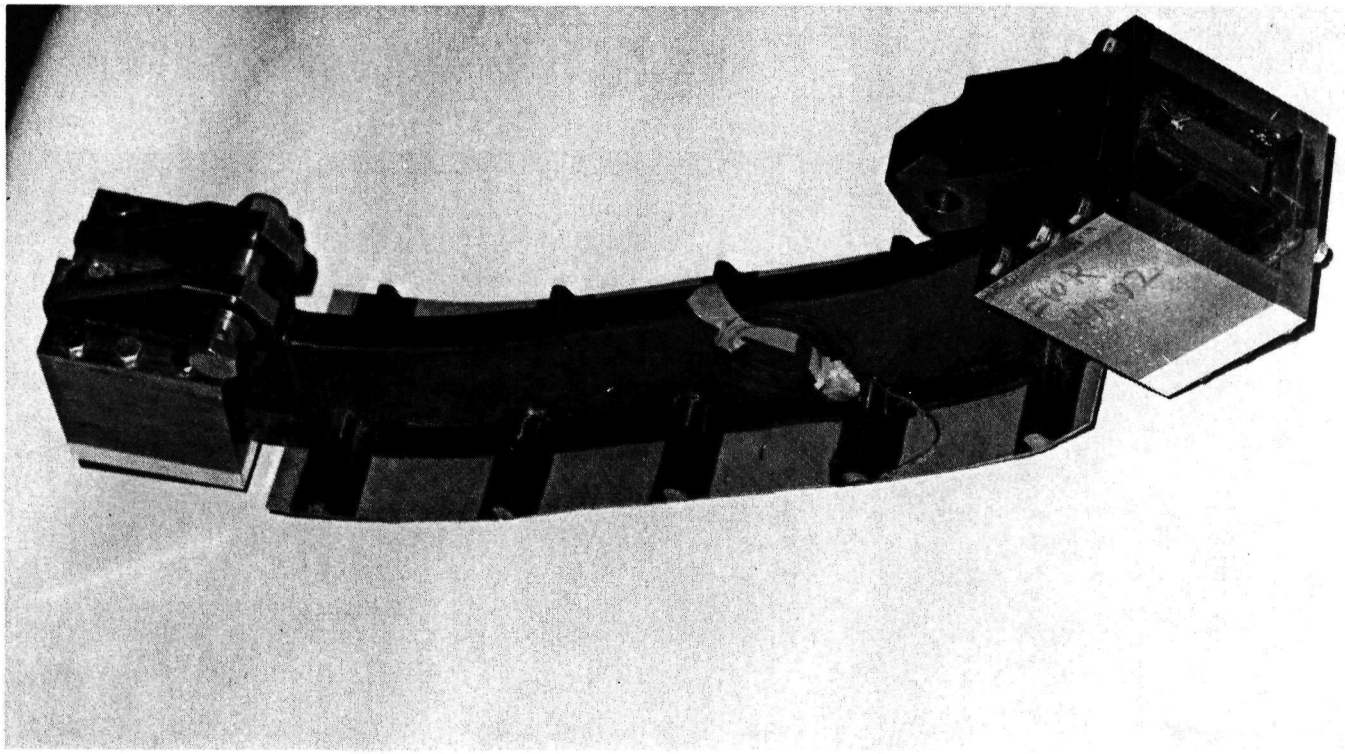

FIGURE 30 . FRAME FATIGUE SPECIMEN WITH TEST END FITTING INSTALLED.

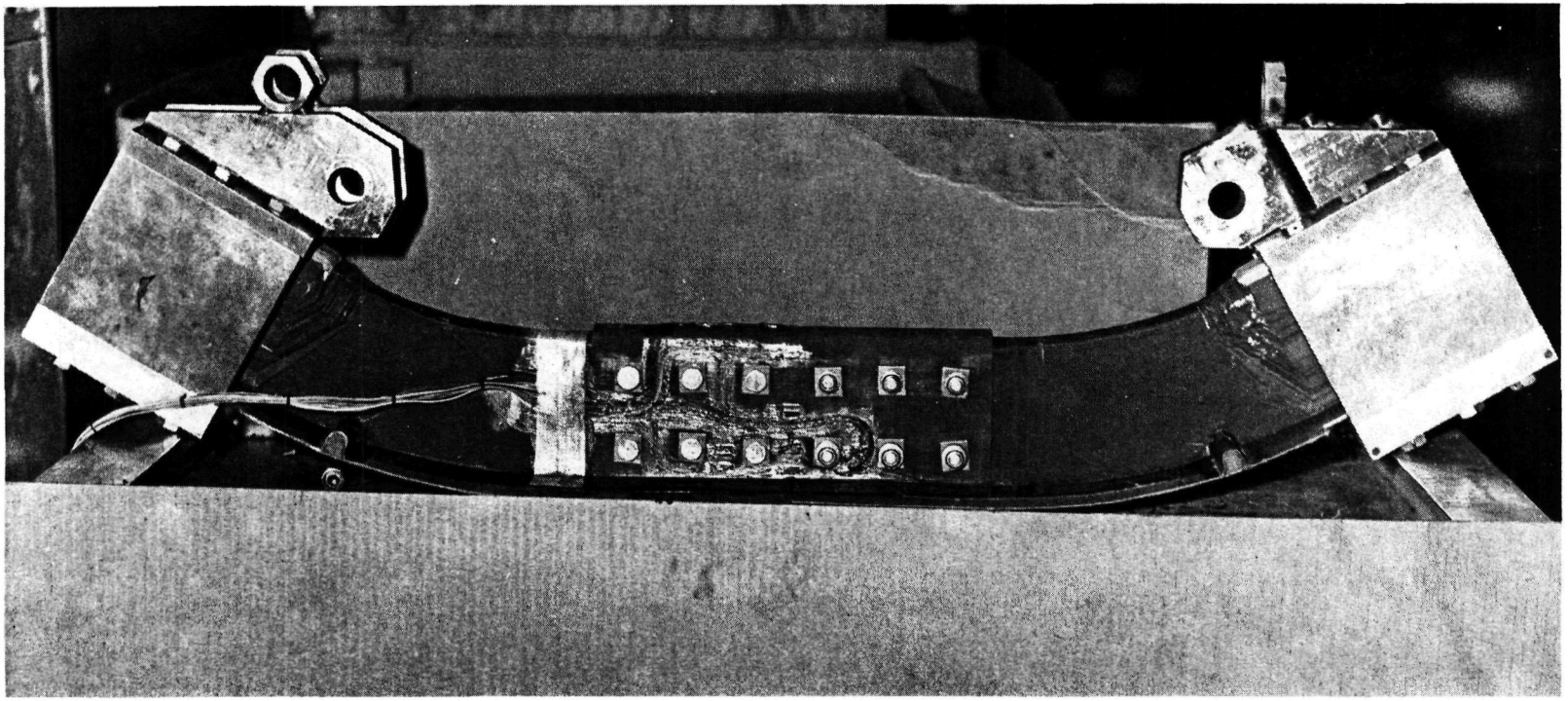

FIGURE 31. FRAME SPLICE JOINT SPECIMEN WITH TEST END FITTING INSTALLED.

6.2 TEST PROCEDURES

The test procedures developed for this program are based upon the requirement of an airframe fatigue life of 4000 hours. The applied loads generated for the fatigue test of the frame and frame splice joint sections are the design loads used for the CH-53 aircraft, and are representative of the loads found in heavy frames during maneuver, gust or landing conditions encountered during the service life of the aircraft. In a typical heavy frame, a limit frame bending moment of 7.45 kN•m (66,000 in.-lb) and a compression axial load of 49.3 kN (11,100 lb) was used. The limit loads were based on a limit load factor of 3.0 x gravity and the remaining applied loads obtained by the ratio of their respective load factors to the limit load factor. The test load spectrum shown in Table I consisted of 200 blocks of 155 cycles each representing load conditions 1 through 5 in Table I, and 102 additional cycles representing load conditions 6 through 10 in Table I. Load conditions within each block were randomized. Each specimen was instrumented with bonded electrical resistance strain gauges located in areas of anticipated maximum strain. One cycle of load condition 10 (limit load) was applied to the specimen at the start of each test in 4.4 kN (1000 lb) increments with strain, horizontal and vertical deflection measurements, recorded at each load increment to determine the spring rate of each specimen. Following the static limit load test, each specimen was subjected to the load spectrum shown in Table I. Periodic records of strain and displacement were taken during the spectrum fatigue test using a direct printout oscillograph. Upon successful completion of the load spectrum fatigue testing, each specimen was statically loaded to failure. Load was applied in 4.41 kN (1000 lb) increments with strain, vertical and horizontal deflection measured at each load increment. Failure analysis was conducted on each specimen tested.

TABLE I. 4000 HOUR LOAD SPECTRUM, COMPOSITE FUSELAGE FRAME SPECIMEN.

Load Condition	N_z (g)	Maneuver Cycles	Gust Cycles	Landing Cycles	Total Cycles	Bending Moment kN.m (In. Lb)	Axial Load kN (Lb)
1	1.2	0	14,000	2500	16,500	3.01(26,600)	19.6 (4,400)
2	1.4	8000	2000	500	10,500	3.51(31,100)	23.0 (5,180)
3	1.6	2000	300	90	2390	4.01(35,500)	26.2 (5,900)
4	1.8	500	45	27	572	4.52(40,000)	29.4 (6,600)
5	2.0	175	7	8	190	5.02(44,400)	32.9 (7,400)
6	2.2	60	1	3	64	5.51(48,800)	36.2 (8,140)
7	2.4	24	0	0	24	6.02(53,300)	39.1 (8,800)
8	2.6	8	0	0	8	6.53(57,800)	42.7 (9,600)
9	2.8	3	0	0	3	7.03(62,200)	46.3(10,400)
10	3.0	1	0	0	1	7.52(66,600)	49.4(11,100)

SECTION 7.0 SPECTRUM FATIGUE TEST RESULTS AND FAILURE ANALYSIS

The failure analysis conducted in Phase II of this program involves the investigation and determination of failure modes of four individual frame specimens prepared from one composite fuselage shell section, an individual frame specimen incorporating modifications described herein, and fabricated specifically to evaluate these modifications, and three individual frame splice joint specimens prepared from a second composite fuselage shell section.

7.1 FRAME FATIGUE SPECIMENS

Test #1, Frame S/N 1

The first EWR 32381 frame fatigue specimen, Figure 30, was installed in the test fixture and loaded with the upper cap in compression. Load was applied in 4.45 kN (1000 lb) increments to determine the spring rate of the specimen. At 43.6 kN (9800 lb) or approximately 60 percent of design ultimate load, the specimen failed suddenly and catastrophically in the area of the 50.8 cm (20 in.) radius adjacent to the built up test fixture doublers as shown in Figure 32. The frame specimen was separated at the fracture to inspect the damage which had occurred. Sections were cut from the specimen as shown in Figure 33 to determine the extent of damage. Figure 34 shows the fracture surface (Figure 34a) and the damage at a point 5.08 cm (2 in.) away from the fracture surface (Figure 34b). In the area of fracture, the upper cap laminate was completely separated from the web laminate, and forced downward approximately 2.54 cm (1.0 in.) into the foam core causing localized crushing of the foam. The web laminate was buckled on both sides of the frame section and had completely separated from the stabilizing foam core. Examination of sections cut from the frame specimen in areas C&D (Figure 33) shows a separation of the shear webs from the stabilizing foam core and indications of cap/web separation. No damage was apparent in the center portion of the frame specimen (Sections E, F, G, H, I (Figure 33). In Sections J, K, L (Figure 33), the curved area opposite the primary fracture area of the specimen, a separation of the shear web from one side of the foam core was found. A longitudinal crack extending from the shear web to foam separation was discovered in the upper cap laminate extending to the cap to web interface. From these preliminary observations, no conclusions to determine the mode or sequence of failure could be established. To provide the information necessary to thoroughly understand the premature failure of this first specimen, five separate areas of investigation were established.

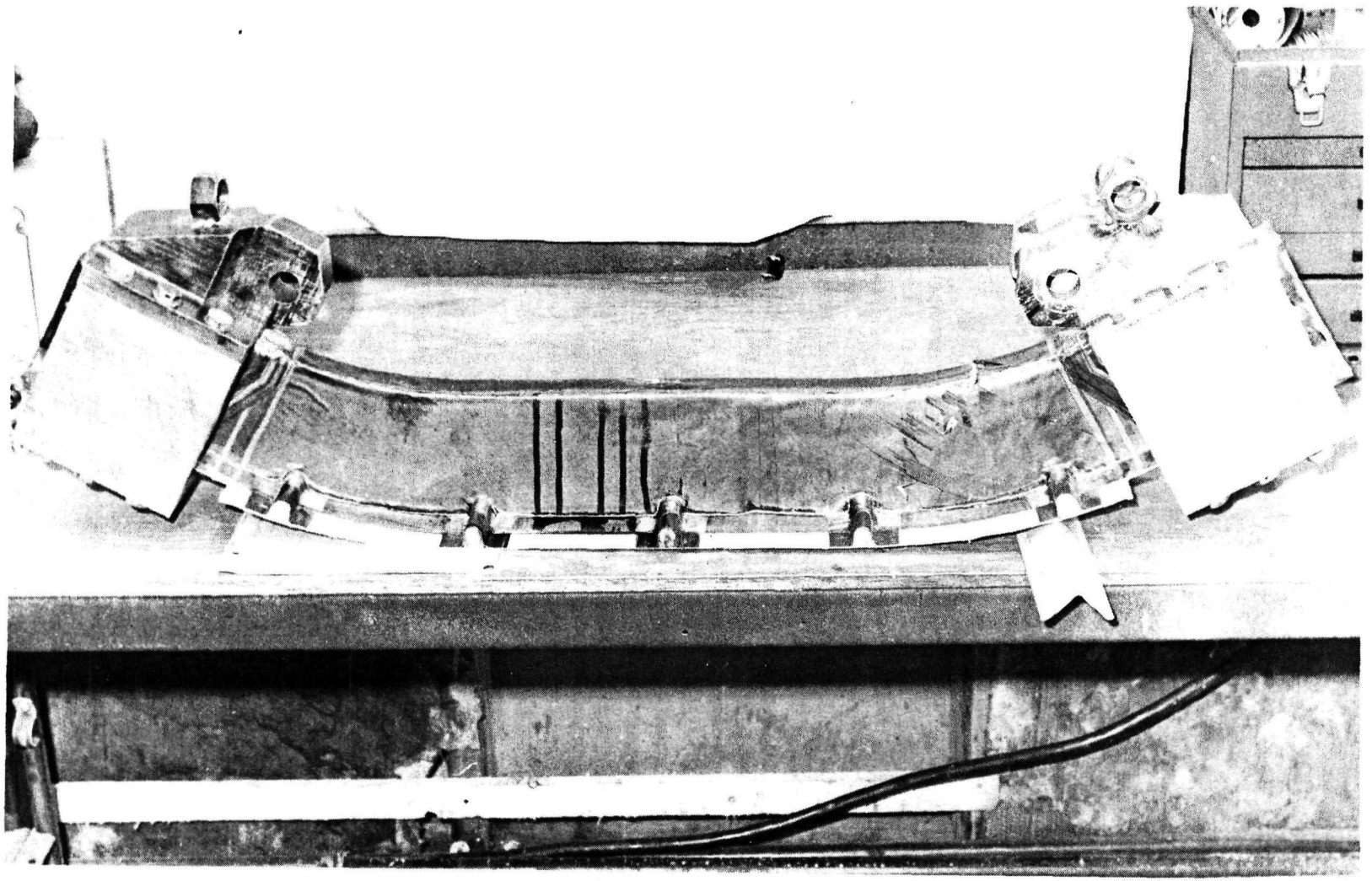

FIGURE 32. TEST #1, FRAME S/N 1; FAILURE OCCURRED IN CURVED AREA BETWEEN 4TH AND 5TH STRINGER, RIGHT HAND END.

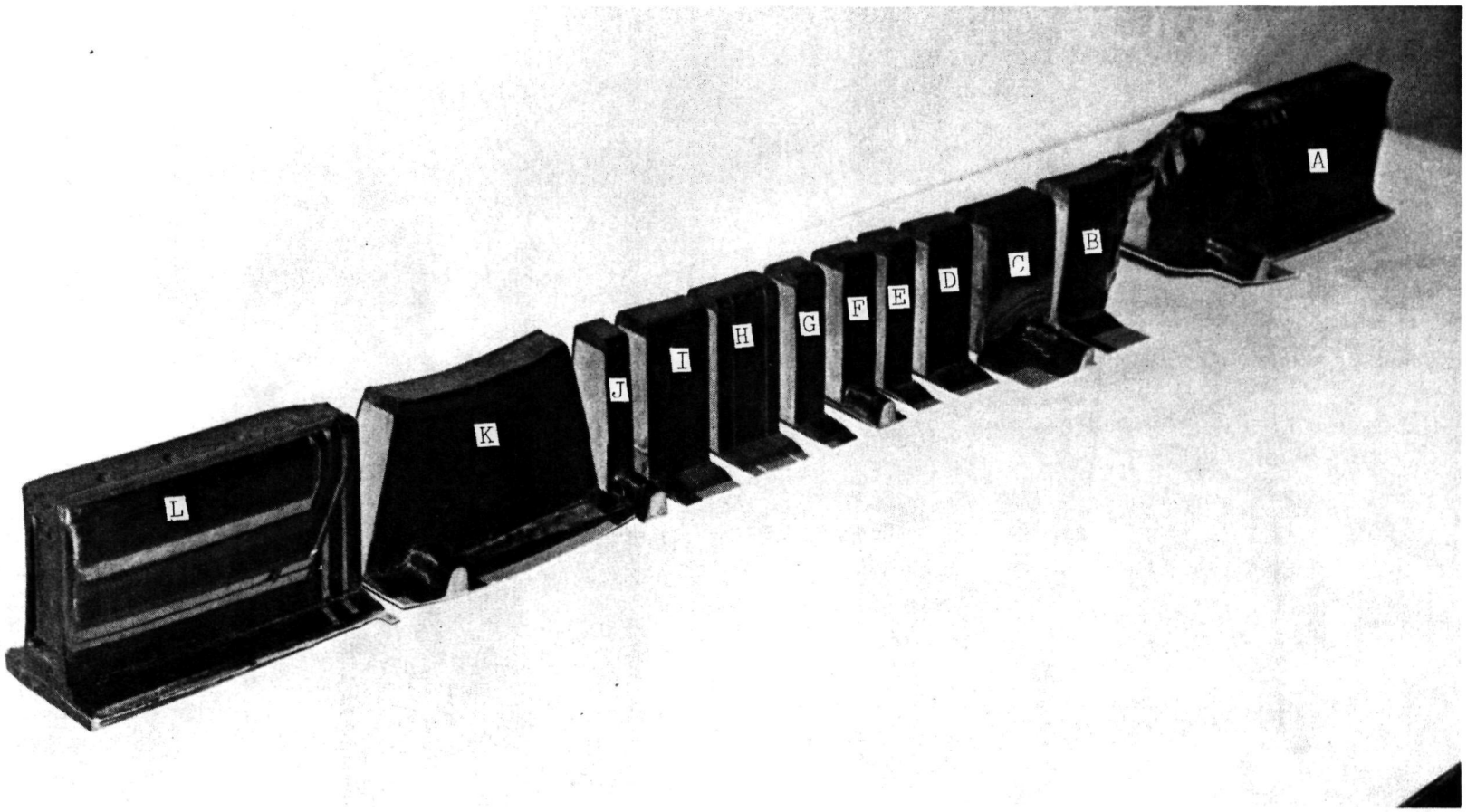

FIGURE 33. FAILED FRAME SPECIMEN #1; SECTIONED FOR FAILURE ANALYSIS AND MATERIAL PROPERTY IDENTIFICATION.

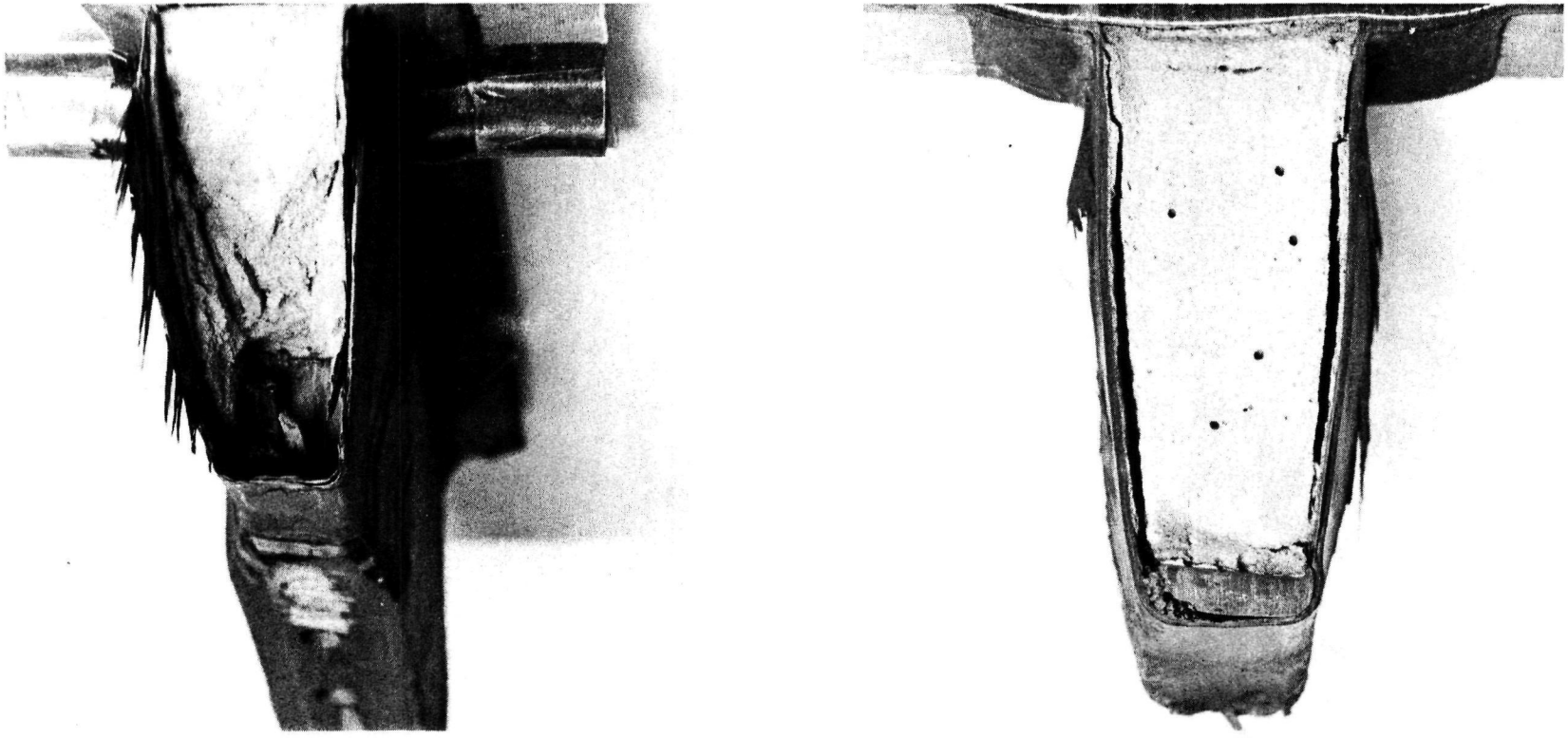

(a) SECTION 5.08 CM (2 IN.) AWAY FROM FRACTURE SURFACE

(b) FRACTURE SURFACE

FIGURE 34. FAILED FRAME SPECIMEN #1; VIEWS OF THE INTERIOR FAILURE.

1. Calibration of Test Loading System and Conditions

In order to verify the validity of the loads imposed on the first frame specimen, the test system was recalibrated and found to be accurate.

2. Material Evaluation and Substantiation

To determine the quality of the first frame test specimen, materials evaluation specimens were removed from the areas where no damage was apparent. These areas represented by letters F and K in Figure 33 were further machined to provide short beam shear and photomicrograph specimens of the upper cap laminate and foam compression specimens of the frame core. Shear properties of the upper cap laminate were found to average 87.5 MPa (12,700 psi), which is above the calculated minimum acceptable value of 86.2 MPa (12,000 psi). Examination of the upper cap photomicrographs revealed small voids running longitudinally, but not of sufficient size or magnitude to be considered a contributory factor in the static failure of the frame specimen. Foam compression samples prepared from area F (Figure 33) were within the nominal density range of 221 Mg/m^3 (8.0 lb/ft^3) and produced an average room temperature compression strength of 1.38 MPa (200 psi) at 10 percent deflection, which is above the design requirement for the core material.

3. Verification of Predicted Stresses on Fully Calibrated Specimen

To investigate the distribution of strains in both the curved and straight areas of the frame specimen as originally designed, the second specimen S/N #2 was instrumented with fifty strain gauges, located in the test area and the curved areas at both ends of the specimen. The specimen was statically loaded to 15.6 kN (3500 lbs) in 4.4 kN (1000 lb) increments. The recorded strain gage readings were as anticipated in both the straight and curved sections. No excessive strain readings were observed. The compression strains in the cap were as predicted, and the compression strains in the curved web sections were substantially below the predicted capability of the material.

4. Re-evaluation of Loads in Frame Section

The original analysis reported in Phase I (Reference 1) did not address the curved frame section. Subsequent analysis indicates that due to the method of loading, radial kick

loads of up to 8 percent of the applied compression load exist in the curved areas of the frame. This is equivalent to 3.56 kN (800 lb) radial kick load at the failure load of frame #1.

5. Attempted Reproduction and Simulation of Observed Failure

In an attempt to better understand the failure observed in the first frame specimen and possibly duplicate the effect of the radial or kick load in the curved portion of the specimen, small specimens, as shown in Figure 35a and 35b, were prepared from sectioned areas E, G, H and I (Figure 33). The specimens shown in Figure 35a prepared from areas E and G Figure 33 were tested in pure compression. The average failure load on a 2.54 cm (1 in.) wide section was 10.67 kN (2400 lb). Both specimens failed identically, with the failure occurring initially as a separation of the cap/web interface followed by a buckling of the web, separation from the foam core and an extension of the initial cap/web separation. The origin of failure appeared at the junction of the web, cap and foam core. The analytical calculations predict the radial or kick load in a 45.7 cm (18.0 in.) radius at design ultimate load to be 2.58 mN/m (1475 lb/in); therefore proving the adequacy of the basic foam supported frame concept when completely stabilized. The crushing strength of the foam is 0.49 mN/m (280 lb/in.).

To determine the cap/web interface integrity, two specimens shown in Figure 35b prepared from areas H and I Figure 33 were tested. The first specimen failed at 2.82 kN (634 lb), a load substantially below the 10.67 kN (2400 lb) achieved by the pure compression specimens, but approximately equal to the calculated radial load of 1.4 mN/m (800 lb/in.) in the curved section of the first frame specimen at the actual static failure load. The failure observed in this specimen also originated at the junction of the web, cap and foam core, and propagated along the foam interface until the web buckled. The crack also propagated upwards into the 0° cap laminate. Inspection of the second specimen revealed pre-existant damage sustained during the static loading of the full-scale frame specimen. The damage appeared as a slight separation of the shear web from the side wall of the foam stabilizing core. When tested to determine its residual load carrying capabilities, the specimen would not sustain load above 1.56 kN (350 lb) because of the significant deflection of the pre-existing separation. Comparison of the pre-existant failure observed in this specimen under load with the generated failure in the first specimen tested reveals an identical failure pattern and location as shown in Figure 36.

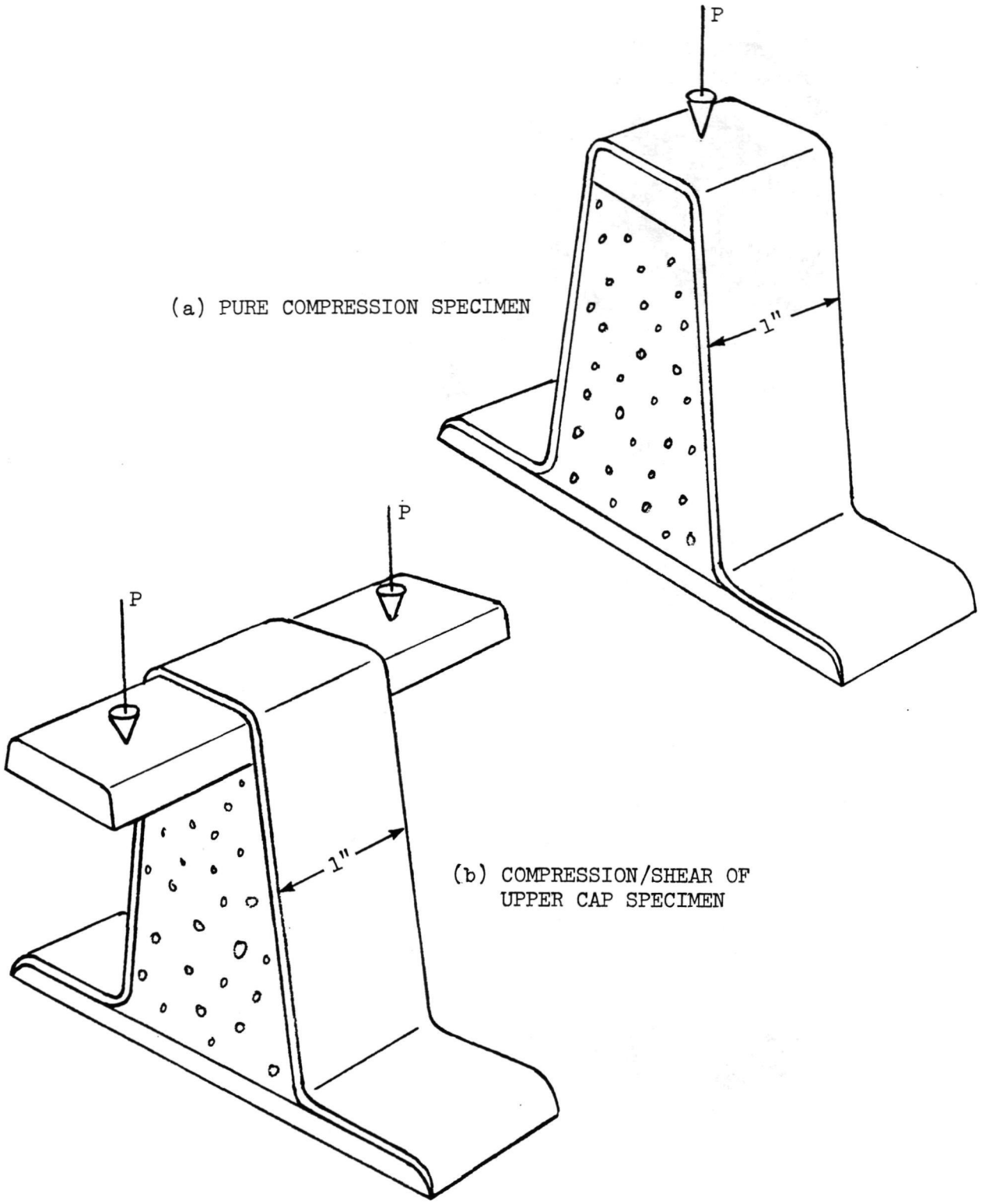

FIGURE 35. COMPRESSION TEST SPECIMENS REMOVED FROM FIRST FRAME SPECIMEN.

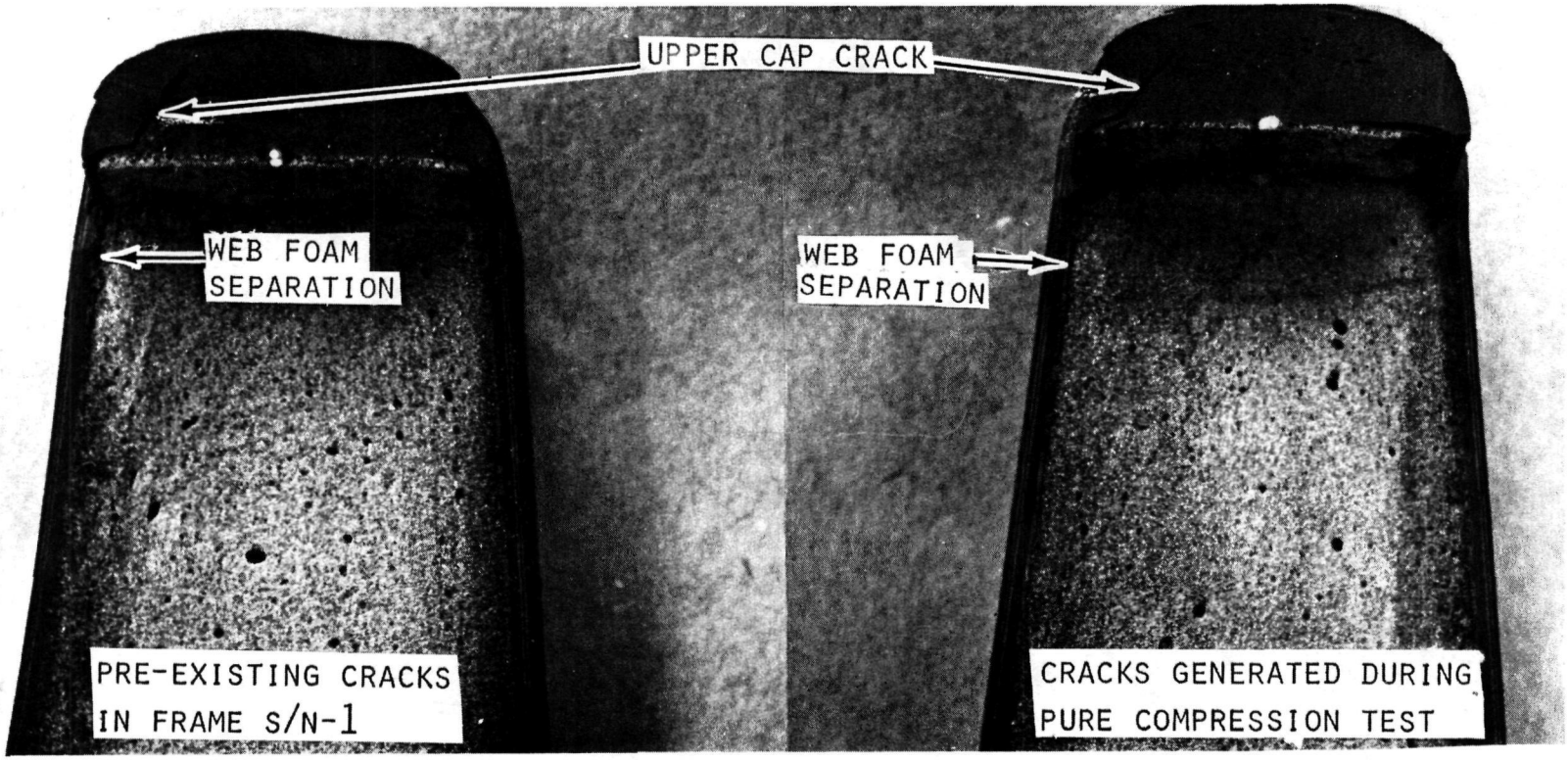

FIGURE 36. FULL SCALE FAILURE MODE DUPLICATED BY SPECIMEN TESTS.

Because the small specimen failure mode and load in terms of the radial or kick load duplicates that calculated to exist in the first full-scale frame test specimen at the time of static failure, it is concluded that the design configuration and not the material quality was the primary cause of the premature static failure.

The design configuration was predicated on the utilization of low cost manufacturing concepts which necessarily involved trade-offs relative to structural optimization. A guiding principal was to reduce labor cost by minimizing the steps to accomplish the composite "lay-up". This is illustrated by the frame cap configuration in which the unidirectional (0^{o}) material is pre-plied into a 40 ply assembly and placed as an entity on the foam core. This permits the "lay-up" of the subsequent web plies ($\pm 45^{o}/0^{o}/90^{o}$) to be applied without interruption or special pattern preparation. Although this is a desirable manufacturing technique, the interlaminar shear stresses between the 0^{o} cap and the web material will be significantly higher than with a configuration where the 0^{o} cap material is interlaminated between the web plies.

Test #2, Frame S/N 4

To preclude a large schedule slippage, the second specimen frame was prepared from the #4 frame element of the fabricated composite fuselage shell section. Test doublers identical in laminate configuration and stacking sequence but extended to provide a complete stabilization of the curved areas at both ends of the frame specimen where failures were originating were laminated to the frame specimen. The doublers, as extended, were installed to provide additional support in the curved sections of the frame specimen and promote failure in the center or straight test area of the specimen. Upon successful completion of the 4000 hour spectrum fatigue test, the specimen was incrementally loaded to its design limit load to determine whether any spring rate changes had occurred during the cycle fatigue test. No deterioration in stiffness was observed. The specimen was statically loaded to fracture to determine residual strength. Fracture occurred at 60.9 kN (13,700 lbs) in compression and 92.8 kN.m (82,200 in-lb) in bending, or 83 percent of the design ultimate load. Fracture occurred in the center of the test area of the frame specimen as shown in Figure 37. The spectrum fatigue test of this specimen was conducted at the same time failure analysis, fracture mode and material properties were being evaluated to determine the cause of the premature failure of the first frame specimen.

FIGURE 37. TEST #2, FRAME S/N 4; VIEW OF STATICALLY INDUCED FRACTURE, AFTER SUCCESSFUL COMPLETION OF 4000 HOUR SPECTRUM FATIGUE TEST.

When the frame specimen was sectioned to evaluate the extent of damage and determine the failure mode, separation between the supporting core foam and the frame web was discovered. The separation extended from the web fracture to the beginning of the extended doublers on one end of the specimen for a length of approximately 20.3 cm (8.0 in.). The upper cap was cracked in this area to a point 25.4 cm (10.0 in.) from the origin of web fracture. The cracks appearing in the upper cap, the separation of the web from the stabilizing foam and the web from the upper cap duplicated exactly, although to a much lesser extent, the failure observed in the first statically loaded specimen. A partial fracture of the upper cap occurred in the curved area of the specimen 25.4 cm (10.0 in.) from the center of the specimen.

Test #3, Frame S/N 3

On the third frame fatigue specimen, the existing short composite doublers were modified by laminating additional doubler material to each end of the frame to provide the same configuration as that successfully fatigue tested on the previous frame fatigue specimen. Equipment to measure acoustic emission from the specimen was installed at this time. The frame specimen was then subjected to static limit load of 49.4 kN (11,100 lbs) to verify the spring rate of the specimen. During load application, there were several acoustic indications in the form of loud reports or cracking sounds, indicative of damage occurring in the specimen. Although no visual indications of damage were apparent, erratic strain readings obtained during the spring rate check verified that some damage had occurred. The cyclic fatigue test was initiated and the specimen continued to produce acoustic indications of cumulative damage. After 1600 hours of simulated flight spectrum fatigue loading, the test was stopped and the spring rate of the specimen rechecked. A 50 percent reduction in stiffness of the specimen was determined.

At this time the specimen was coin tapped to determine the location of areas of delamination or separation. The suspect areas were identified and when compared to the recorded acoustic emission data, revealed a close correlation to the areas where increased acoustic indications were recorded. The cyclic fatigue test was resumed and at the third load cycle of 46.3 kN (10,400 lbs), the specimen fractured in the center of the test area. At the time of fracture, the frame had successfully completed 18,232 cycles at load levels ranging between 40 percent and 67 percent of limit load and 58 high load cycles consisting of 38 cycles at 73 percent of design limit load, 15 cycles at 80 percent of design limit load, 2 cycles at 86 percent of design limit load, and 3 cycles at 94 percent of design limit load. The load at fracture was 44.9 kN (10,100 lbs) or 61 percent of the design theoretical ultimate load.

Failure occurred in the center portion of the test area as shown in Figures 38a and 38b and Figure 39. The specimen was sectioned into 5.04 cm (2 in.) pieces cut at right angles to the length of the frame. Longitudinal cracks were observed in the upper cap throughout the entire length of the specimen. A complete fracture of the upper cap was found in the curved section under the extended doublers at a point 17.8 cm (7 in.) away from the externally visible web failure. At the point of fracture, the upper cap was separated from the web and had been driven into the supporting foam core approximately 0.32 cm (0.125 in.). A 38.0 cm (15 in.) separation of the web from the supporting core foam was observed extending along the frame to a point 19.0 cm (7.5 in.) on each side of the externally visible fracture. Examination of the sectioned pieces removed from the frame specimen show the failure to be identical to that experienced in the first statically loaded specimen. As demonstrated by the static tests conducted during the failure analysis of the first frame, the failure initiated at a point where the upper cap, the shear web cover and the supporting foam core meet (see Figure 40). The failure was initiated by separation of the web laminate from the foam core at this point. Separation at the web/foam interface propagated downward to the lower cap. Loss of adhesion between the supporting foam and the web caused a buckling of the web laminate. The additional deflection caused by the loss of stability of the web during cyclic loading then induced cracking in the upper cap still bonded to the continuous web. At this point, the opposite side stabilizing web separated from the foam core and the upper cap to web bond separated. With no support, the upper cap laminate was driven into the foam core with each cyclic loading until fracture occurred.

Test #4, Frame S/N 2

The fourth frame fatigue specimen was prepared for test by extension of existing doublers, instrumented with strain gages and installed in the test fixture. Based on the reliable correlation between the information derived during the failure analysis on the preceeding frame specimen and the acoustic indications of damage monitored during the cyclic fatigue test of the frame specimen, a decision was made to monitor the acoustic emission generated by the specimen during application of static limit load and if sufficient indication of damage was recorded, the specimen would be removed from the test fixture and sectioned to quantify the accumulated damage.

No acoustic indications of damage were recorded during the application of the static limit load. The spring rate was checked and stiffness measurements found to be comparable to the first spectrum fatigue specimen which successfully completed the spectrum fatigue test. The cyclic fatigue loading of the frame

(a) FRACTURE SURFACE, RIGHT SIDE.

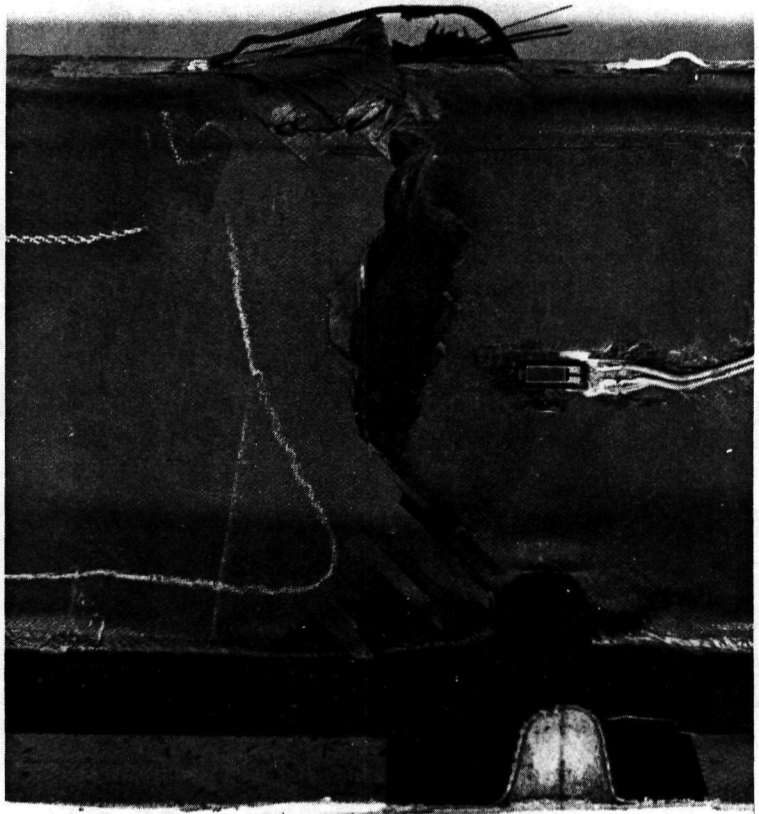

(b) FRACTURE SURFACE, LEFT SIDE.

FIGURE 38. TEST #3, FRAME S/N 3; FAILURE OCCURRED IN CENTER TEST AREA.

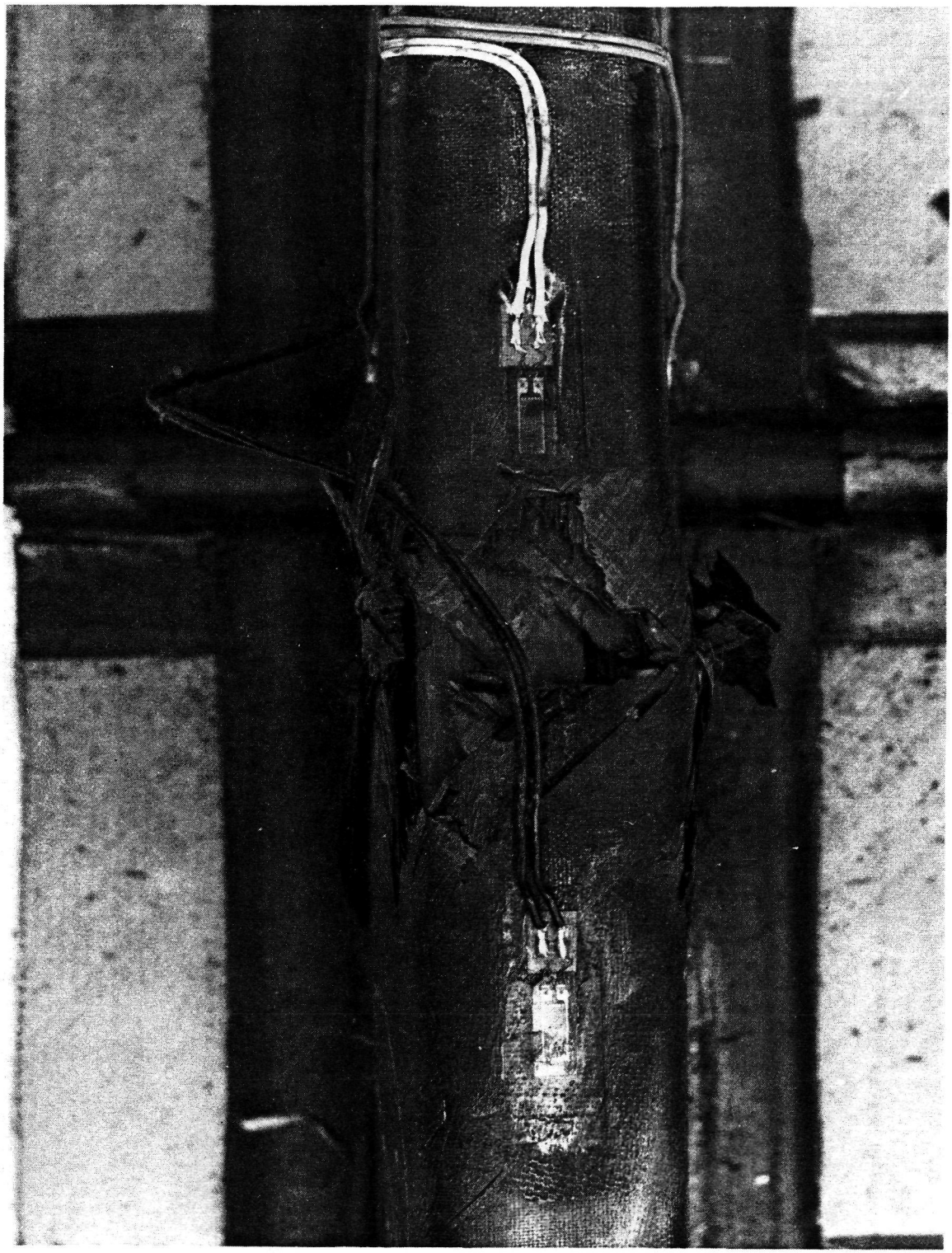

FIGURE 39. TEST #3, FRAME S/N 3; TOP VIEW OF FATIGUE FAILURE SHOWING FRACTURE OF SHEAR WEB AND UPPER CAP.

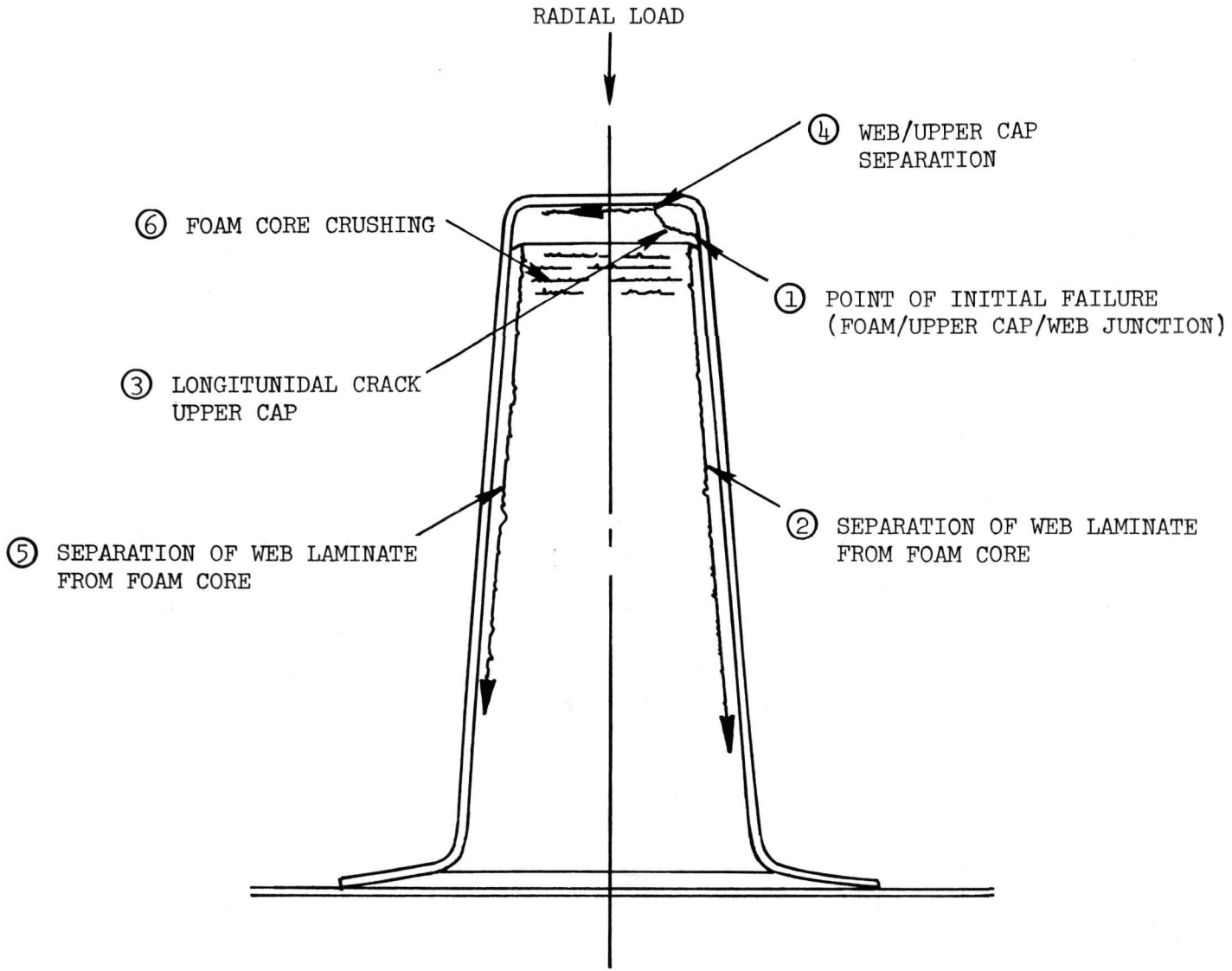

FIGURE 40. CROSS SECTION OF FRAME SPECIMEN, POINT OF INITIAL FAILURE, AND SEQUENCE OF FRACTURE.

specimen was initiated and the specimen reacted loads quietly with no acoustic indications of damage recorded. With 40 percent of the cyclic fatigue test completed, acoustic indications of internal damage were recorded, increasing in both frequency and intensity until the specimen failed catastrophically 51 percent through the spectrum fatigue test. The fracture occurred in the center of the test area as shown in Figure 41, and externally duplicated the fractures experienced on the first two frame fatigue specimens. The fractured frame specimen was sectioned as shown in Figure 42 to permit a detailed failure analysis. Examination of the section removed from the test area of the specimen show the same failure pattern observed in all three previously tested specimens. Again, web to foam separation was observed on both sidewall webs, accompanied by longitudinal cracks in the upper cap and separation of the cap from the web laminate. On this specimen, an additional failure had occurred for the first time. A separation of the web laminate from the lower cap laminate originating at the center frame/stringer intersection and extending to a point 10.16 cm (4 in.) towards the left end of the specimen was discovered. In this area a more severe degradation of the upper cap in the form of longitudinal delamination and cracking was observed. The left end of the frame was sectioned revealing the damage shown in Figure 43. At the beginning of the curved section 17.8 cm (7.0 in.) from the center of the specimen complete separation of the upper cap from the web was apparent. Total separation of the upper cap into small fiber bundles had occurred in the curved area beginning at the second stringer/frame intersection 17.8 cm (7.0 in.) from the center of the frame specimen and ending outboard of the first stringer/frame interesection, 38 cm (15.0 in.) from the center of the specimen. Complete fracture of the upper cap was observed at a point 26.7 cm (10.5 in.) from the center of the frame specimen. At the point of upper cap fracture, the supporting foam core was depressed and powdered to a depth of 3.8 cm (1.5 in.). The point of fracture in the upper cap occurred in the center of the curved area of the frame section. No evidence of separation between the web laminate and the supporting foam core in the curved portion of the specimen was observed.

Primary failure of the fourth frame fatigue specimen occurred 40 percent into the spectrum fatigue test in the curved section at the left hand side of the frame specimen. At that time the upper cap separated from the shear web. Buckling of the shear web in the curved portion of the specimen was prevented by the additional stabilization provided by the extended doublers in that area. With each additional cyclic loading, the upper cap no longer restrained from independent deflection by the web to cap bond was driven into the supporting foam core until complete separation into small fiber bundles had occurred. Failure of the upper cap proceeded as individual fiber bundles fractured with each load application until a point 51 percent through the cyclic fatigue

FIGURE 41. TEST #4, FRAME S/N 2; VIEW OF FRACTURE OF SHEAR WEB AND UPPER CAP.

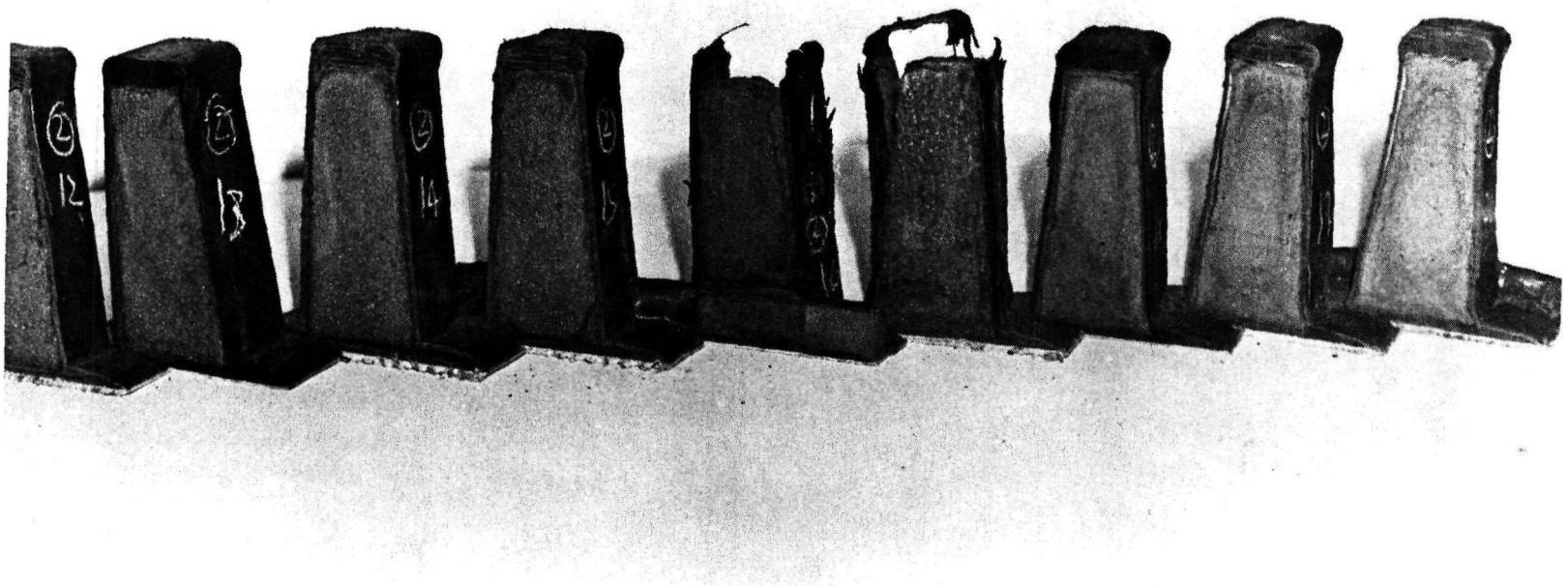

FIGURE 42. TEST #4, FRAME S/N 2; FRACTURE ANALYSIS SECTIONS CUT FROM CENTER TEST AREA OF FRAME.

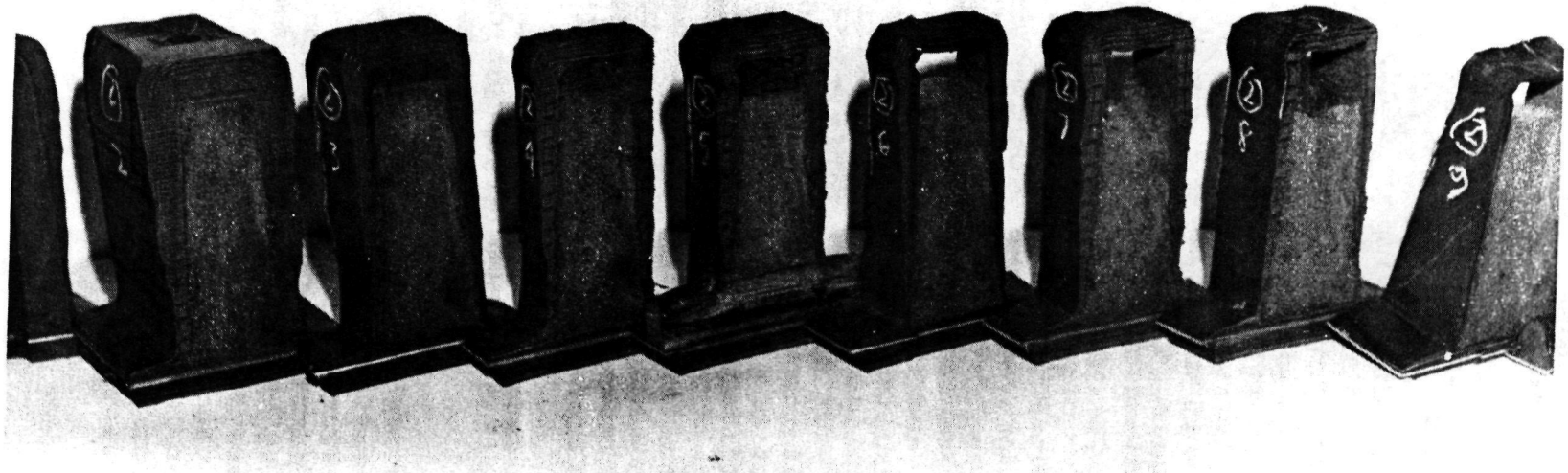

FIGURE 43. TEST #4, FRAME S/N 2; FRACTURE ANALYSIS SECTIONS CUT FROM LEFT CURVED AREA OF FRAME.

test. At that time the cumulative damage previously described in the center or test area of the specimen could no longer react the imposed loads and the apparent failure shown in Figure 41 occurred.

7.2 IMPROVED FRAME SPECIMEN

To substantiate the design improvements developed during the analysis of the premature failure which occurred on the first frame specimen during application of static limit load, a single frame section was fabricated in the EWR 32380-T60 tool. This frame, although externally identical to the four frame specimens prepared from the original composite shell section, had incorporated into it a design modification which consisted of the encapsulation of the upper cap laminate between the shear web plies i.e.: In all previous specimens, the upper cap (40 ply unidirectional graphite) was laid directly on the upper surface of the supporting foam core, and the shear web plies consisting of $+45^{\circ}/-45^{\circ}/0^{\circ}/90^{\circ}/0^{\circ}/90^{\circ}+45^{\circ}/+45^{\circ}/-45^{\circ}$ were placed over the cap layup. In this improved frame specimen, the first six shear web plies, $+45^{\circ}/-45^{\circ}/+45^{\circ}/-45^{\circ}/0^{\circ}/90^{\circ}$, were laid up on the supporting foam core, the upper cap layup positioned on the partially completed web layup, and the remaining four shear web plies, $0^{\circ}/90^{\circ}/+45^{\circ}/-45^{\circ}$, then applied over the upper cap and previously positioned shear web plies. Fabrication details of this specimen are presented in Section 5.4. This modification was developed to provide a reinforcement under the unidirectional (0°) cap laminate to resist the radial loads in the curved section of the frame. This modification was proven by the fabrication of a short section of a frame which was sectioned into one inch wide frame section specimens, similar to those shown in Figure 35 a and b, which were then subjected to static compression loads. Results of these tests showed an improvement of up to 100% over the original configuration in radial load buckling resistance.

In order to duplicate the test conditions under which the first frame specimen failed during static load application, original short configuration doublers were laminated to the ends of this specimen. The specimen was instrumented with strain gauges, installed in the test fixture, and statically loaded in compression and axial bending. Load was applied in 4.4kN (1,000 lb) increments to failure. Fracture of the improved frame specimen occurred in the curved area of the frame as shown in Figure 44, at a load of 57.82 kN (13,000 lb). Damage to the specimen consisted of fracture of the upper cap laminate at a point 35.5 cm (14.0 in.) from the center of the specimen, fracture of the shear web along the web/foam cap interface, and separation of the shear web from the supporting foam core beginning at the point of fracture of the upper cap and extending 10.2 cm to 15.2 cm (4 to

FIGURE 44. IMPROVED FRAME SPECIMEN, FAILURE AREA BETWEEN FOURTH AND FIFTH STRINGER RIGHT CURVED AREA OF FRAME.

6 in.) towards the centerline of the specimen. The location of sections removed from the improved frame specimen are shown in Figure 45a. Delamination of the shear web laminate shown in Figure 45b occurred between the plies separating the upper cap from the foam core and the plies covering the upper cap.

The fracture initiation point, similar to all specimens previously tested, appears to be the point at which the upper cap and the sidewall web plies intersect. In this specimen separation or delamination of the sidewall web laminate preceded the catastrophic failure of the frame, and the additional support provided by the web plies under the upper cap laminate permitted the specimen to sustain load until 57.82 kN (13,000 lb), an improvement of 33 percent over the original configuration, or approximately 79 percent of the axial compression design ultimate.

7.3 FRAME SPLICE JOINT FATIGUE SPECIMENS

In Phase I of this program, static test results proved the splice channel design to be conservative. To provide a spectrum fatigue test more representative of the actual capabilities of the splice channels, the fatigue load spectrum was revised to produce load inputs to the first frame splice joint specimen at a load level of 125 percent of the calculated limit load for all spectrum conditions. Based on the results of the spectrum fatigue tests, and the residual static fracture strength of the first frame splice joint specimen, the fatigue spectrum loads for the second and third specimen would be adjusted accordingly. The 4000 hour load spectrums for the first frame joint test is presented in Table II.

Test #1 Frame Splice Joint S/N 1

The first frame splice joint specimen was prepared for test with strain gauges bonded to the splice channel in areas of maximum anticipated strain. The specimen was installed in the test fixture and the simulated 4000 hour spectrum fatigue test initiated. Cyclic loads were applied to the specimen in accordance with the 4000 hour loading spectrum shown in Table II. No visual or acoustic indications of damage were apparent at the completion of the 4000 hour test. Fracture occurred during the residual strength test at a compression load of 32.47 kN (7,300 lbs). Fracture initiated at the lower or free edge of the splice channel, immediately below the bolt hole closest to the centerline of the splice channel, as shown in Figure 46. The fracture extends from the lower edge of the splice channel to the upper bolt hole closest to the centerline of the channel on both sides of the channel. The lower bolt hole through which the fracture propagated was incorrectly drilled. When the specimen was set up for drilling the first hole drilled was at right angles to

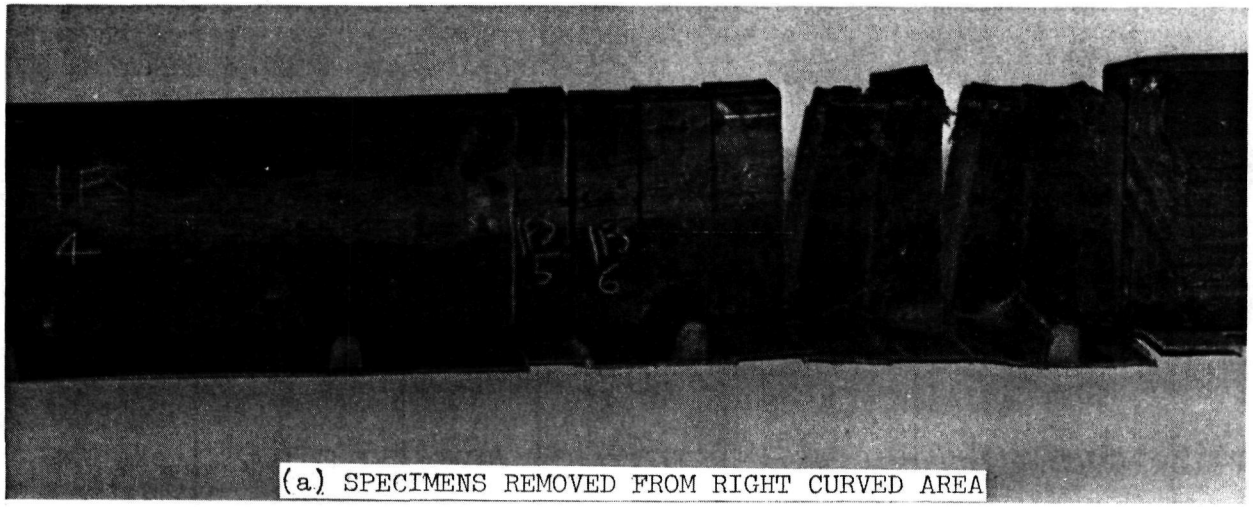

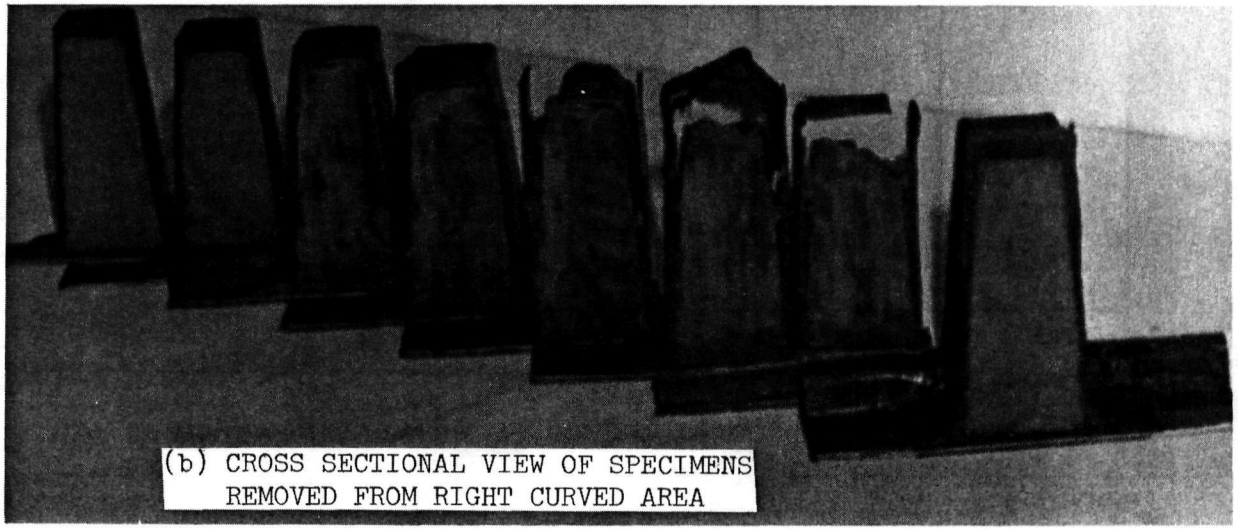

FIGURE 45. FAILURE ANALYSIS SPECIMENS CUT FROM IMPROVED FRAME SPECIMEN.

C-2

TABLE II. 4000 HOUR LOAD SPECTRUM, FRAME SPLICE SPECIMEN LOAD ACCELERATION @ 125% OF DESIGN LIMIT LOAD.

Load Condition	N_z (g)	Total Cycles	Bending Moment @ 125%		Axial Load @ 125%	
			kN.m	(in.lb)	kN	(lb.)
1	1.2	16,908	7.59	(6,720)	4.98	(1,120)
2	1.4	10,757	8.88	(7,860)	5.83	(1,310)
3	1.6	2,449	10.17	(9,000)	6.67	(1,500)
4	1.8	586	11.39=	(10,080)	7.47	(1,680)
5	2.0	195	12.67	(11,220)	8.32	(1,870)
6	2.2	66	13.96	(12,360)	9.16	(2,060)
7	2.4	24	15.18	(13,440)	9.96	(2,240)
8	2.6	8	16.47	(14,580)	10.81	(2,430)
9	2.8	3	17.62	(15,600)	11.56	(2,600)
10	3.0	1	18.98	(16,800)	12.45	(2,800)

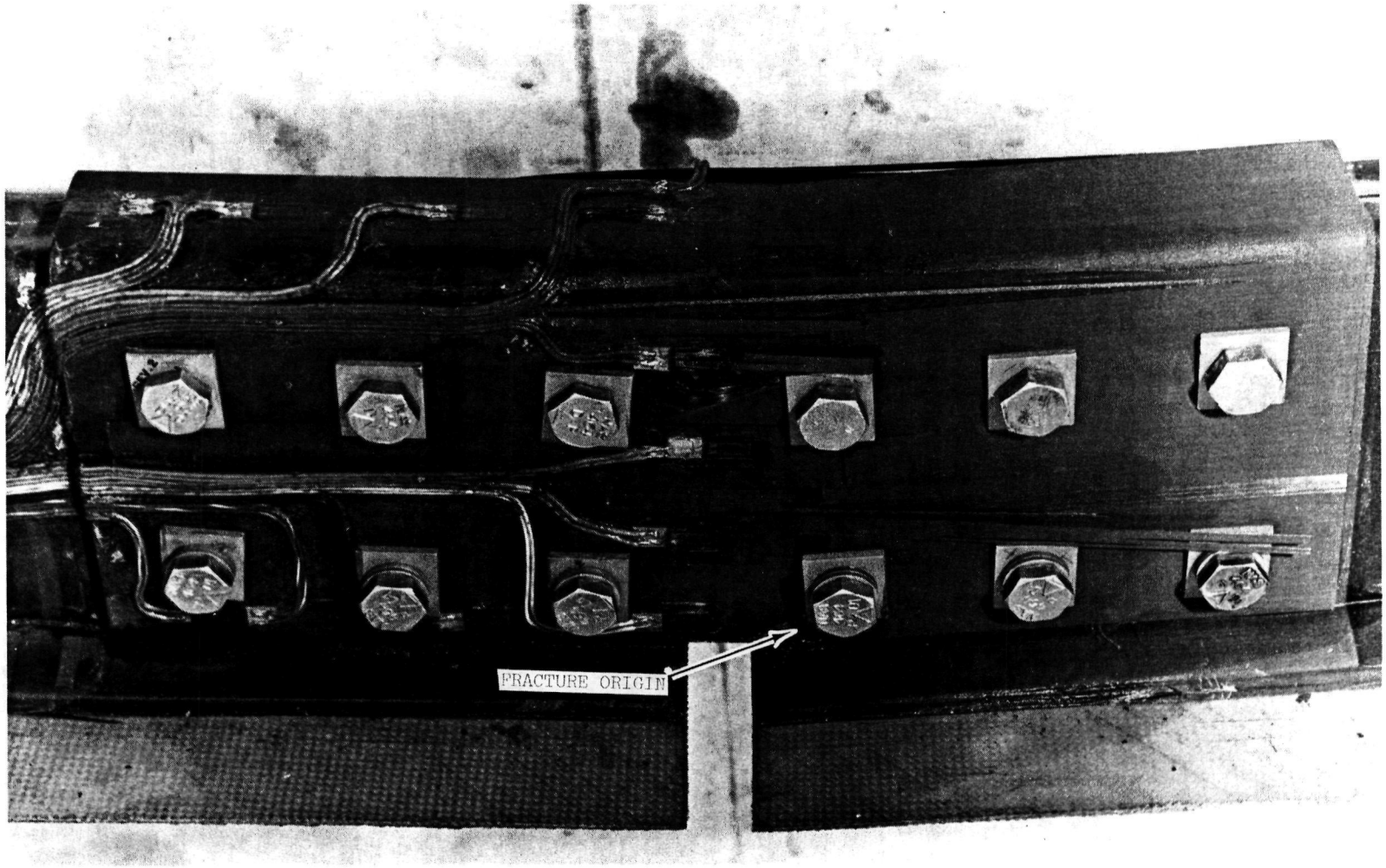

FIGURE 46. #1 FRAME SPLICE JOINT FATIGUE SPECIMEN, STATIC FRACTURE OF SPLICE CHANNEL INITIATED AT FREE EDGE BELOW BOLT HOLE CLOSEST TO SPECIMEN CENTER LINE.

the face of the splice channel causing an angular displacement of the hole on the exit side of the channel of 0.15 cm (0.060 in.), thus reducing the edge distance from the bolt hole to the free edge of the specimen. It was at this misdrilled hole where the fracture occurred.

Test #2, Frame Splice Joint S/N 2

Spectrum fatigue loads were revised upward for the cyclic fatigue test of the second frame splice joint specimen. The fatigue loading spectrum shown in Table III was revised to increase the limit load to 200 percent of the calculated theoretical limit load. All intermediate loads were increased by the same ratio. The second specimen was subjected to the revised design limit load, 19.7 kN (4,440 lbs) and then to the simulated 4000 hour spectrum fatigue test. After successful completion of the spectrum fatigue test, the specimen was statically loaded to fracture Fracture occurred in the curved area of one of the frame sections at a compression load of 44.9 kN (10,100 lbs). The fracture shown in Figure 47 is similar to those encountered during the testing of the frame specimens, and although a valid fracture of the splice channel was not obtained, the test does prove the capability of a properly drilled splice channel to exceed the fracture load at which the first splice joint specimen failed through the mislocated attachment bolt hole. Upon microscopic examination of the bolt holes on this specimen, no damage was apparent other than a slight burnishing of the holes in areas corresponding to the direction of load application during the cyclic fatigue test.

Test #3, Frame Splice Joint S/N 3

The third frame splice joint specimen was prepared for test. The load spectrum for the third specimen duplicated that for the second specimen. After application of static design limit load, 19.7 kN (4,440 lbs), the specimen was exposed to, and successfully completed the simulated 4000 hour spectrum fatigue test. Fracture occurred at 48.9 kN (11,000 lbs) in the center of the splice channel. The fracture shown in Figure 48 is an exact duplicate of the fracture which occurred on the first frame splice joint specimen. The fracture initiated at the lower edge of the specimen directly under the bolt hole closest to the center of the splice channel. Failure of the splice channel at this point was anticipated since the analysis conducted in Phase I of the program indicates that the two lower bolts located closest to the ends of the frame sections, (the center of the splice channel), are the most highly loaded bolts, subject to a tensile bending stress imposed by the loads introduced at the four bolts located on the outboard sides of each of these center bolts.

TABLE III. 4000 HOUR LOAD SPECTRUM, FRAME SPLICE SPECIMEN LOAD ACCELERATION @ 200% OF DESIGN LIMIT LOAD.

Load Condition	N_z (g)	Total Cycles	Bending Moment @ 125%		Axial Load @ 125%	
			kN.m	(in.lb)	kN	(lb.)
1	1.2	16,908	12.07	(10,680)	7.92	(1,780)
2	1.4	10,757	14.10	(12,480)	9.25	(2,080)
3	1.6	2,449	16.07	(14,220)	10.54	(2,370)
4	1.8	586	18.10	(16,020)	11.88	(2,670)
5	2.0	195	20.07	(17,760)	13.17	(2,960)
6	2.2	66	22.10	(19,560)	14.50	(3,260)
7	2.4	24	24.13	(21,360)	15.83	(3,560)
8	2.6	8	26.10	(23,100)	17.12	(3,850)
9	2.8	3	28.20	(24,960)	18.50	(4,160)
10	3.0	1	30.10	(26,640)	19.75	(4,440)

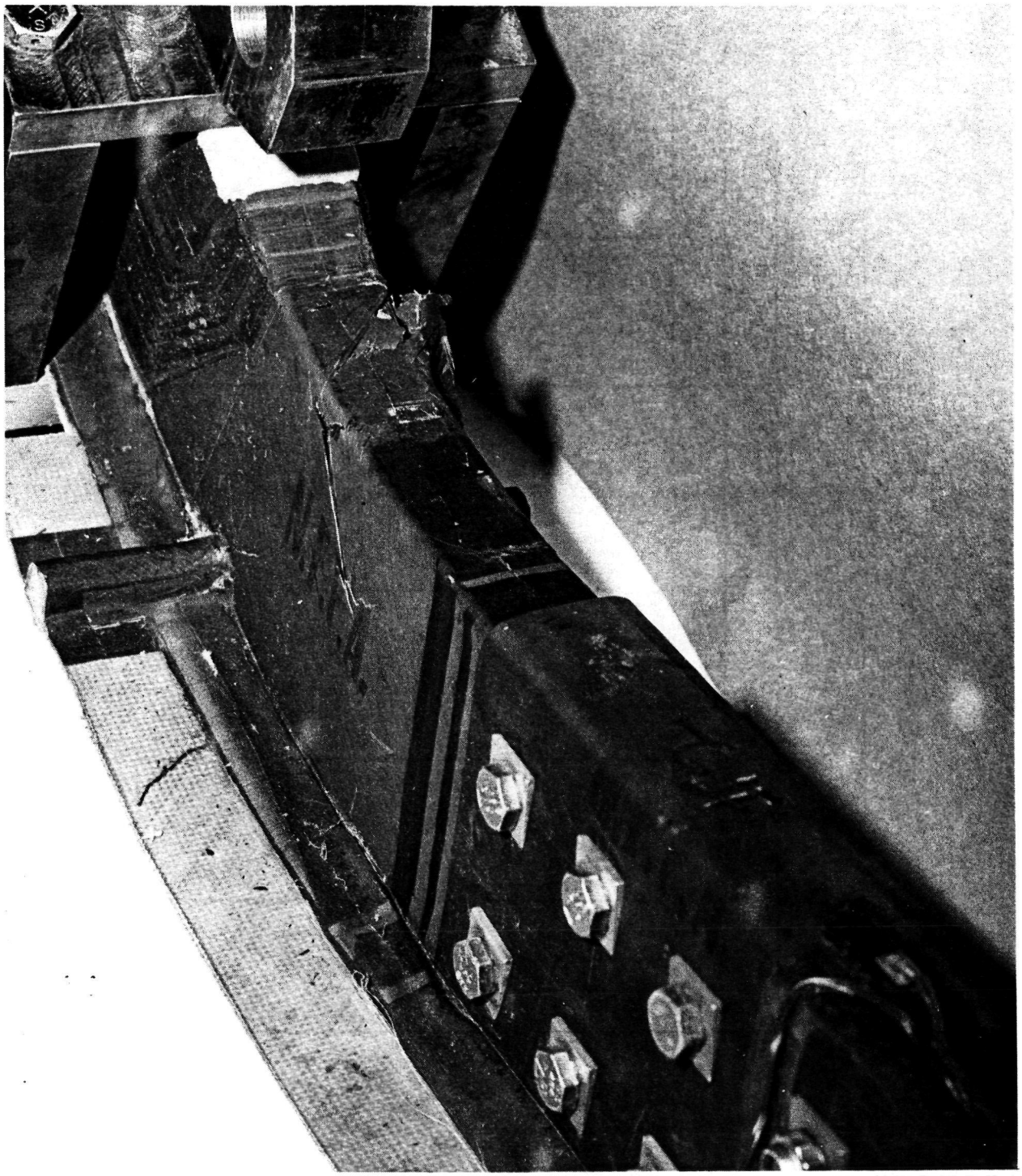

FIGURE 47 FRACTURE OF THE #2 FRAME SPLICE JOINT FATIGUE SPECIMEN OCCURRED IN THE CURVED AREA OF THE FRAME SECTION.

FIGURE 48. #3 FRAME SPLICE JOINT FATIGUE SPECIMEN, STATIC FRACTURE OF SPLICE CHANNEL INITIATED AT FREE EDGE BELOW BOLT HOLE CLOSEST TO SPECIMEN CENTER LINE.

7.4 SUMMARY OF TEST RESULTS AND FAILURE ANALYSIS

The comparison of actual failure loads vs design predictions are presented in Table IV. It is to be noted that only one frame specimen (S/N 2) successfully completed the 4000-hour accelerated spectrum fatigue test, and that the failure load for that specimen when statically tested to fracture after completion of the fatigue spectrum was below the design ultimate load for the frame section. All frame specimens when sectioned for failure analysis revealed the primary or initial failure to be in the curved areas of the frames. It has been shown that the failures are directly related to the radial loads which exist in the curved areas under the loading conditions experienced. These loads were omitted from the original analysis of the frame section because the curved areas were incorporated into each end of the frame test specimens only to demonstrate the fabricability of curved frame members in the manufacture of low cost composite fuselage shell sections. In actual design practice, the curved areas of the frames would be the areas of attachment between the manufactured composite shell sections and in these areas the design loads are typically 25 to 50 percent lower than those in the straight sections.

In Table IV the test failure loads are compared by ratio to the design ultimate load for all specimens tested in both Phase I and Phase II. Although the ratios shown indicate an apparent design deficiency in the basic frame section, all failures occurred at loads equal to or above those anticipated for frame areas where splice joints would occur. With this in mind, and the realization that certain frame sections, i.e., transmission support, sponson support, ramp support, etc., would be subject to uniformly higher loads throughout the frame, the improved frame was developed as a first generation modification effort to produce a frame capable of reacting these increased loads over the entire frame. As noted in Table IV, the basic straight frame, tested in Phase I of this program (Reference 1), met the design ultimate requirements established for the straight area of the frame. The first frame specimen (S/N 1) tested in this Phase II effort failed at approximately 60 percent of the design ultimate load in the curved section. Both specimens were of the same laminate construction and equal in manufacturing quality. Therefore, it is anticipated that this frame too would have met the design ultimate load requirement if test loads were restricted to only the straight section of the frame. The improved frame specimen incorporating only the design changes and fabrication improvements described in the fabrication section of this report, successfully reacted loads to 13,000 lbs before fracture. Again, fracture occurred in the curved area of the specimen. However, this specimen showed a 33 percent improvement over the initial frame specimen. Therefore, if each of the frames prepared from

the original composite shell section can be considered adequate in the straight portion, then the improvement derived from a simple rearrangement of materials in the improved frame specimen provides the mechanism by which radial loads can be successfully reacted in critical curved areas of highly loaded frame members. In addition, the original design concept was developed with cutout areas in the frame web laminate at the intersection of each stringer with the frame member. This was done as a theoretical approach to simplification of the fabrication procedure. Zero degrees and 90° plies extending over the entire surface of the frame member were incorporated into the design to compensate for the reduced shear web in these areas. In actual fabrication practice, it has been found through the experience gained during the fabrication of specimens in this program that rather than cut out the web laminate plies at the stringer intersections, it was feasible to slit and lay up each frame web ply in such a manner as to produce a composite flange extending onto each stringer. With the cutouts no longer necessary, it now becomes possible to relocate and/or reorient the 0° and 90° plies to the curved areas in highly loaded frames to provide additional structural capabilities in these areas at no weight increase. The frame splice joints, already conservatively designed, are capable of reacting loads much higher than those anticipated in splice joint areas. When coupled with frames incorporating the above mentioned improvements, it is anticipated that a practical solution exists whereby all structural considerations can be incorporated into the low cost composite fuselage concept.

THIS PAGE INTENTIONALLY LEFT BLANK

TABLE IV.

COMPARISON OF ACTUAL FAILURE LOADS VERSUS DESIGN PREDICTIONS

Structure	Specimen Configuration	Design Ultimate Load	Predicted Failure Load Zero Margin of Safety	Test Failure Load	Ratio of Test to Predicted Failure Load	Ratio of Test to Design Load	Residual Strength % of Design Ultimate	Time to Failure (Fatigue Specimen)	Comments
Frame - Axial Compression & Bending	Phase I Straight Section	73.84 kN (16,600 lb) 11 291 N.m (100,000in.lb)	85.67 kN (19,260 lb) 13 505 N.m (116,000in.lb)	67.61 kN (15,200 lb) 11 066 N.m (98,000 in.lb)	.84	.98	-	Static Test	Straight frame section with 4" long test area.. Reported results are average of two specimens.
Frame Composite Shell Section Axial Compression & Bending	#1 Frame	73.84 kN (16,600 lb) 11 291 N.m (100,000in.lb)	85.67 kN (19,260 lb) 13 505 N.m (116,000in.lb)	43.59 kN (9,800 lb) 6 638 N.m (58,800in.lb)	.51	.59	-	0 Hours (Static Test)	Straight frame area 14" long with unreinforced curved areas at each end. Fracture occurred in curved area during initial application of static limit load prior to initiating spectrum fracture test.
	#2 Frame	"	"	60.94 kN (13,700 lb) 9 280 N.m (82,200in.lb)	.71	.82	82%	4000 Hrs. (No Failure)	Doublers added to curved frame areas to attempt to stabilize and force failure mode into straight section. Failure initiated in curved area. Specimen successfully completed 4000 hour spectrum fatigue test. Failure occurred during static residual load test.
	#3 Frame	"	"				Failed During Fatigue Test	2400 Hrs.	Second configuration of doublers added to curved areas. Specimen failed during 4000 hour spectrum fatigue test. Failure originated in curved area. Specimen failed after successfully completing static limit load application (11,100 lb) and 58% of spectrum fatigue high load cycles.
	#4 Frame	"	"				Failed During Fatigue Test	2000 Hrs.	Same configuration as #3 above. Specimen failed during 4000 hour spectrum fatigue test. Failure originated in curved area. Specimen failed after successfully completing static limit load application (11,100 lb) and 50% of spectrum fatigue high load cycles.
Improved Frame Specimen		"	"	57.82 kN (13,000 lb) 8 805 N.m (78,000in.lb)	.67	.78	-	Static Test	Improved frame section, with interlaminated web and cap plies and changes in fabrication procedures. No reinforcement in curved areas. Fracture occurred in curved area. Specimen loaded statically to fracture. Loads 33% higher than original #1 frame with unreinforced curved section.
Frame Splice Axial Compression & Bending	Phase I Straight Specimen	14.68 kN (3,300 lb) 2 258 N.m (20,000in.lb)	23.93 kN (5,380 lb) 3 681 N.m (32,600in.lb)	35.76 kN (8,040 lb) 5 587 N.m (49,470in.lb)	1.49	2.43	243%	Static Test	Phase I specimen; failure occurred in splice channel. Fracture initiated at lower edge of splice below bolt subjected to highest load.
Frame Splice Composite Shell Section Axial Compression & Bending	1	"	"	32.47 kN (7,300 lb) 4 945 N.m (43,800in.lb)	1.35	2.21	221%	4000 Hrs. (No Failure)	Splice joint fatigue tested at 125% acceleration over flight spectrum loads. Specimen successfully completed 4000 hour spectrum fatigue test. Fracture initiated at lower edge of splice below bolt subjected to highest load during residual static load test.
	2	"	"	44.92 kN (10,100 lb) 6 841 N.m (60,600in.lb)	1.88	3.06	306%	4000 Hrs. (No Failure)	Splice joint fatigue tested at 200% acceleration over flight spectrum loads. Specimen successfully completed 4000 hour spectrum fatigue test. Fracture occurred in curved area of frame section during residual static load tests.
	3	"	"	48.93 kN (11,000 lb) 7 451 N.m (66,000in.lb)	2.04	3.33	333%	4000 Hrs. (No Failure)	Splice joint fatigue tested at 200% acceleration over flight spectrum loads. Specimen successfully completed 4000 hour spectrum fatigue test. Fracture initiated at lower edge of splice below bolt subjected to highest load during residual static load test.

SECTION 8.0 COMPOSITE VS CONVENTIONAL VEHICLE WEIGHT AND COST DATA ANALYSIS

This section details the weight and cost comparisons between conventional and composite construction for a CH-53D aircraft. Comparisons are conducted for both the prototype and production vehicles. A cost effectiveness analysis is presented for a 600 aircraft fleet, operating for a ten year period.

8.1 WEIGHT COMPARISON

As summarized in Table V, the composite airframe is 503.9 Kg (1,111 lbm) or 18 percent lighter than the conventional CH-53D airframe. A detailed breakdown of the material utilization for the composite airframe is shown in Table VI. Also shown in Table VI are the unit costs of the various composite materials calculated for the 1980 time frame. The weight savings projected as a result of this study are within 3.17 Kg (7.0 lbm) of those originally published in Reference 3. However, the detail studies conducted in both the design of the specimens and the fabrication of test hardware during Phases I and II of this program produced significant changes in the utilization of the component composite materials. These changes are detailed in the following paragraphs.

In the frames and beams for an all composite airframe in the original Reference 3 study, the structural weight for the foam core materials for frames and beams was calculated utilizing a foam density of 96.1 Kg/m^3 (6.0 lb/ft^3). As determined experimentally in Phase I of the program, 128.1 Kg/m^3 (8.0 lb/ft^3) density foam was required to provide stabilization for the structures during the fabrication cycle. This produces a 109.3 Kg (241 lbm) weight increase in the foam utilized for stringer and beam construction.

Where the composite stringers intersect the frames, simple cutouts were thought to be adequate in the preliminary Reference 3 study. Further analysis indicated the desirability of additional 0^o and 90^o plies to reinforce the cutout areas in the graphite/epoxy shear webs. This modification added a total of 77.1 Kg (170 lbm) additional weight to the frame webs.

With the changes discussed in the preceeding paragraphs, the foam supported frame concept utilized in this study is 16 percent heavier than originally projected, but still shows a 19 percent weight advantage over conventional built-up construction aluminum frames. Likewise, in the detail design and fabrication of the composite stringers, it was found necessary to incorporate 128.14 Kg/m^3 (8 lb/ft^3) density foam in place of 96.1 Kg/m^3 (6 lb/ft^3) foam, and add one ply of woven Kevlar-49/epoxy to the 0^o graphite/epoxy stringer laminate to provide a shear capability in the stringer web. This resulted in an increase of 35.4 Kg (78 lbm) over the figures projected for stringers in the original Reference 3 study.

TABLE V

COMPOSITE AIRFRAME IS 503.9 kg (1,111 lbm) OR 18% LIGHTER THAN CONVENTIONAL CH-53D

Type of Structure	Conventional Airframe kg (lbm)	Composite Airframe kg (lbm)	Weight kg (lbm) Difference	% Difference
Skin/ Stringers	837.6(1847)	635.9(1402)	-201.7(-445)	-24
Frames	922.4(2034)	745.3(1643)	-177.1(-391)	-19
Beams	317.1(699)	269.4(594)	-47.7(-105)	-15
Longerons	38.1(84)	23.6(52)	-14.5(-32)	-38
Fairings	62.6(138)	46.7(103)	-15.9(-35)	-25
Fittings	150.1(331)	141.5(312)	-8.6(-19)	-6
Misc. Hardware	428.2(944)	54.4(120)	-373.8(-824)	-87
Misc. Joints	--	254.5(561)	+254.5(+561)	
Adhesive	--	81.2(179)	+81.2(+179)	
Total Airframe Weight	2756.1(6077)	2252.5(4966)	-503.9(-1.111)	-18

TABLE VI

CONVENTIONAL VS COMPOSITE CH-53D AIRFRAME
MATERIAL USAGE AND UNIT COST

Material	Conventional Airframe Wt. kg (lbm)	Composite Airframe Wt. kg (lbm)	Material Cost $/Unit
Graphite/ Epoxy	-	541.5(1194)	55.00/ kg (25.00/lbm)
Kevlar 49/ Epoxy	-	576.9(1270)	2.97/m^2 (2.50/Yd^2
Fiberglass	185.5(409)	79.8(176)	7.70/ kg (3.50/lbm)
Foam	-	145.6(321)	6.60/kg (3.00/lbm)
Aluminum	2438.1(5375)	227.2(501)	2.20/kg (1.00/lbm)
Steel	7.25(16)	17.7(39)	0.55/kg (0.25/lbm)
Titanium	13.1(29)	391.4(863)	15.45/kg (7.00/lbm)
Aluminum Honeycomb	-	45.8(101)	110/kg (50.00/lbm)
Adhesive	-	81.6(180)	10.76/m^2 (9.00/Yd^2)
Misc.	112.5(248)	144.7(319)	-
Weight Totals	2756.5(6077)	2252.2(4966)	-

For the composite skins, it was found that a four ply 0.001 mm (0.040 in.) thick woven Kevlar-49/epoxy laminate, oriented at $+45^{o}$ provided a better combination of mechanical strength and impact resistance at a lower cost and weight than the original skin concept, which was composed of graphite/epoxy skins, surfaced with a protective ply of Kevlar-49/epoxy. For the all Kevlar-49/epoxy skins, a weight savings of 163.3 Kg (360 lbm) was realized.

Originally the attachment concept considered for both frame and stringer joints was that of a bonded mechanical fitting at the end of each composite member. These mechanical connectors were considered to be of titanium. To simplify joint design, comparable weight composite splice fittings were designed and successfully tested for both the frame and stringer joints. Even though the composite frame attachment joint was demonstrated to be overdesigned by 233 percent, a reduction in weight has not been assumed, and conservatively, no weight advantage was utilized.

8.2 PROTOTYPE AND PRODUCTION VEHICLE COST COMPARISON

The Reference 3 cost study was used as the starting basis for the costs developed herein. The major differences in costs developed during this study and that of Reference 3 is an update to the 1980 time frame to account for inflation plus the differences in materials utilization and manufacturing concepts developed under the current study. The materials utilization for the composite vehicle is discussed under Section 8.1, and Table VI includes reference to the material costs. The following assumptions were made in the updating of the cost data to a 1980 time frame: Airframe cost increases are based on a 50 percent material and labor rate increase, a 39 percent engineering rate increase, a 140 percent increase in computer rate, and an increase in the tooling rates of 16.2 percent for the prototype, and 21.6 percent for the production airframes.

The 50 percent increase in non-airframe acquisition cost reflects a 6 percent annual inflation. The non-airframe acquisition cost was obtained by applying an average 6 percent annual inflation rate between 1973-1980 to the conventional vehicle total acquisition cost, estimated in 1973 to be $3,290,000, to obtain the 1980 cost of $4,949,000. The airframe cost was deducted from this value to obtain the non-airframe cost, which is assumed to be the same for both aircraft.

Prototype Vehicle Cost Comparison

The cost comparison between prototype composite and conventional material vehicles is presented in Table VII and Figure 49.

TABLE VII

PROTOTYPE COMPOSITE VEHICLE COST VS
CONVENTIONAL PROTOTYPE VEHICLE COST
(TABULATED VALUES ARE IN $1000 UNITS)

	Composite Vehicle	Conventional Vehicle (Ref)
Engineering	9,120	8,000
Material	453	204
Labor	3,164	3,600
Tooling	8,437	8,437
Miscellaneous	1,210	1,210
Total Airframe	22,384	21,456
Non-airframe Acquisition Cost	4,071	4,071
Total Vehicle	26,455	25,522

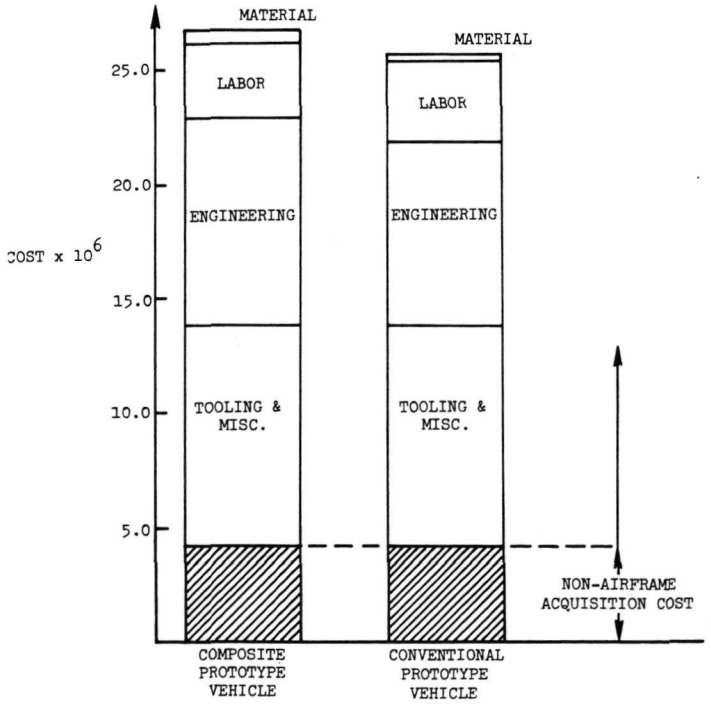

FIGURE 49. COMPOSITE PROTOTYPE VEHICLE COSTS 3.6% MORE THAN PROTOTYPE CONVENTIONAL DESIGN.

From the cost breakdown shown in Figure 49, it is apparent that a major source of the 3.6 percent higher cost for the composite vehicle is the higher engineering cost. This is introduced by the additional design and analysis effort which would be required for prototype design using composite materials. This cost increase together with the higher composite material costs is offset only slightly for the prototype by the reduction in fabrication labor costs using composite materials. Although the single cure concept has been proven feasible and will reduce the cost of tooling for major airframe components, the additional cost for tooling to produce composite hardpoints or attachments is unknown. Therefore, the conservative estimate is made that the tooling costs are the same.

Production Vehicle Cost Comparison

The cost comparison for conventional and composite production vehicles is presented in Table VIII and Figure 50, and is based on production of 600 vehicles starting in 1980.

The small saving in composite vehicle acquisition cost (approximately 0.3 percent) is shown by the cost breakdown of Figure 50 to be largely attributable to the increased cost of composite materials compared with the metals used in the current vehicle. This increase is offset by the reduction in labor cost for fabrication using composite materials.

The material costs presented in Table VI are calculated on the basis of projected production technology advancements and reflect quantity procurement. Manufacturing costs used in this study are projected on the basis of data obtained in the manufacture of the tooling and composite shell sections generated in this Phase II study. Development and utilization of automated equipment for specific manufacturing tasks as developed during a risk reduction program to optimize production techniques and evaluate cost effective manufacturing trade-offs is assumed. The cost of such a program has been included in the cost for the composite prototype.

The largest single cost savings item gained from the investigations conducted in Phase I and II of this program has been the incorporation of the skin/stringer/frame members into a single step fabrication concept, cured in a single operation. Elimination of the requirement for fabrication and assembly of separate skin and frame/stringer details produces a 25 percent reduction in labor costs of a composite vehicle vs a conventional vehicle which more than offsets the greater material costs of the composite vehicle.

TABLE VIII

PRODUCTION COMPOSITE VEHICLE COST COST/UNIT FOR
TOTAL PRODUCTION OF 600 VEHICLES
(TABULATED VALUES ARE IN $1000 UNITS)

	Composite Vehicle	Conventional Vehicle (Ref)
Material	291.70	122.30
Labor	552.40	735.00
Tooling	18.49	18.49
Miscellaneous	2.31	2.31
Total Airframe	864.90	878.10
Non-airframe Acquisition Cost	4,070.90	4,070.90
Total Vehicle	4,936.00	4,949.00

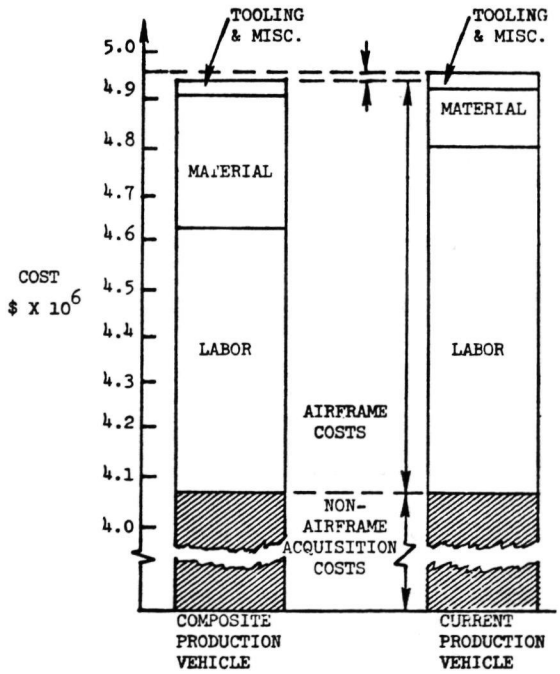

FIGURE 50. COMPOSITE PRODUCTION VEHICLE COSTS 0.3% LESS THAN CURRENT PRODUCTION VEHICLE.

8.3 TEN-YEAR LIFE CYCLE COST FOR PRODUCTION VEHICLE

A cost effectiveness analysis was conducted for the CH-53D on the basis of a 600-vehicle fleet with an average utilization of 500 hours per vehicle per year. The fleet operation consists of the primary transport mission role, with 30 percent troop and 70 percent cargo usage. For this role, the average gross weight is 18,490 kg (40,770 lbm). The increased productivity of the composite aircraft coupled with its reduced acquisition cost, results in a reduced fleet cost of $401,000,000 over a ten year service life.

The cost effectiveness analysis of Reference 3 has been updated to reflect the latest technical and cost changes. The weight of the composite vehicle has been increased by 3.18 kg (7.0 lb). The cost of both the composite and current conventional CH-53D has been increased to reflect changes in inflationary expectations which are assumed to be 6 percent annually for all costs except fuel. Fuel cost in 1980 is projected to be 300 percent of the 1973 costs. The complete revised analysis of Reference 3 is presented herein to provide clarity.

In comparing current and composite designs, the two are evaluated for mission performance and fleet cost. Performance is measured on the basis of aircraft mission productivity expressed in kg.m/s (ton-knots). Cost is measured on the basis of fleet cost to maintain a constant fleet effectiveness.

To determine mission productivity representative of the conditions in which the CH-53D operates in its primary transport mission, a probabilistic mission environment was established and 1000 simulated missions were flown. The mission environment used in the simulation was defined by the cumulative probability distributions of the following parameters:

1. sea level temperature (standard altitude lapse rate was assumed)
2. take-off pressure altitutde
3. sortie radius
4. cruise altitude elevation above take-off
5. percentage of outbound payload carried inbound
6. required payload
7. down time per sortie
8. hover time per sortie
9. take-off hover power margin (fraction of hover out-of-ground-effect power actually required)

Take-off pressure altitude was based on 20 percent of time take-off is at sea level, 50 percent of time take-off is at 153 m (500 ft) or less, 90 percent of time at 762 m (2500 ft) or less, and 100 percent of time at 3,045 m (10,000 ft) or less. This is representative of land area from shore to 92.6 km (50 n.mi) in-

land typical of CH-53D operations. Sea level temperature distribution is based on an average world-wide temperature distribution of 298°K (76°F) for potential areas of engagement on or near coastlines; 85 percent of time temperature is 302°K (83°F) or below, and 100 percent of time temperature is at 322°K (120°F) or below. This distribution also approximates the sea level temperature distribution for regions of anticipated operation. Cruise pressure altitude above take-off is estimated to average 610 m (2000 ft) with 90 percent of time flying 762 m (2500 ft) or less, and 100 percent flying 1830 m (6000 ft) or less above take-off pressure altitude.

Required payload, a demand function independent of capability, is based on carrying troops 30 percent of the time and cargo 70 percent of the time. Cargo distribution is based on redeployment of air-cargo from C-130 and C-141 for 30 percent of cargo loadings, and redeployment of 2268 kg (2.5 ton) and 4536 kg (5 ton) truck cargo for 70 percent of cargo loadings. Required payload-out average 15,240 kg (16.8 ton). This requirement exceeds the CH-53D payload capability. Therefore, any increase in payload capability will produce an increase in productivity.

Inbound payload averages 12 percent of outbound payload with 50 percent of flights returning empty. Sortie radius average is 46.3 km (25 n.mi) with 50 percent of missions being 27.8 km (15 n.mi) or less and 90 percent of missions being 92.6 km (50 n.mi) or less. Take-off power margin range is .60 to 1.0 with an average value of .75. Hover time per sortie averages 1/3 minute, with two minutes maximum hover time per sortie. Down time per sortie averages two minutes, with 90 percent of time less than seven minutes and 100 percent of time less than 30 minutes.

Other inputs to the mission analysis include CH-53D rotor parameters, engine performance, basic operating weight, and constraints imposed by maximum gross weight, drive system rating, speed limit, and fuel capacity. The CH-53D parameters are:

Rotor Diameter	22.0 m (72 ft 2.7 in.)
Total Blade Area	43.5 m^2 (469 sq ft)
Basic Operating Weight (includes 725 lbs (329 kg) of fixed useful load)	11,000 kg (24,210 lbm)
Engines	T64-GE-41
Drive System Maximum Power	0.523 MW (7,000 hp)
Maximum Gross Weight	19,060 kg (42,000 lbm)
Red Line Speed Limit	87.3 m/s (170 kts)
Fuel Capacity	2.39 m^3 (630 gal)

Simulation of the current CH-53D in the established mission environment yielded the following results:

Average Take-Off Gross Weight	18,493 kg (40,770 lbm)
Average Outbound Payload	6,630 kg (14,620 lbm)
Average Fuel Flow	1,036 kg/hr (2285 lbm/hr)
Average Sortie Time	0.362 hr
Average Mission Productivity	173,500 kgm/s (372.8 ton/kts)

Comparison of the existing and composite airframe designs on the basis of weight and cost for a single prototype flight vehicle and production vehicle cost for a fleet of 600 aircraft are given in Table IX.

TABLE IX

CH-53D WEIGHT AND COST COMPARISON OF COMPOSITE AIRFRAME WITH CURRENT DESIGN

	Current CH-53D Airframe	Composite CH-53D Airframe
Prototype Cost ($)	25,522,000	26,455,000
Production Cost ($)	878,100	864,900
Weight Kg	2746	2252.5
(lbm)	(6077)	(4966)

For a single prototype aircraft, the increased cost is $933,000 to achieve 503.9 kg (1,111 lbm) of weight savings by use of composites. For a 600-aircraft fleet, the cost is reduced to reflect a savings of $26.2/kg ($11.9/lbm) of weight saved. In order to relate the impact of the candidate design characteristics on aircraft performance and cost, it is necessary to evaluate the operational changes in aircraft productivity and mission effectiveness achieved by the use of composites. Change in fleet cost of the composite design to maintain the same fleet effectiveness as the current design is used to evaluate the impact of cost and technical factors.

Table X compares the two designs, considering (a) performance in the CH-53D primary transport mission role and (b) the total system cost over the expected 10-year service life to maintain a constant fleet effectiveness of 600 baseline aircraft flying an average 500 hours per aircraft annually.

TABLE X

CH-53D COST EFFECTIVENESS SUMMARY

	Current CH-53D	Composite CH-53D	Change	Percent Change
Acquisition Cost (Million $) Per Aircraft	4.949	4.936	- .013	- .03
Weight Empty kg (lbm)	10,650 (23,485)	10,149 (22,374)	-504 (-1,111)	- 18
Mission Availability	.909	.909	0	0
Mission Reliability	.992	.992	0	0
Average Aircraft Productivity kg.m/s (ton-knots)	173,500 (372.8)	184,950 (397.2)	+11,450 (+24.4)	+6.5
Operating Cost per Flight Hr($)	1,138	1,138	0	0
Fleet Size	600	563	-37	-6.2
Fleet Life Cycle Cost (Million $)	6,383	5,982	-401	-6.3

Current aircraft acquisition cost, estimated at $3,290,000 in 1973, has been escalated an average of 6 percent per year between 1973 and 1980 to reflect inflationary expectations. The revised cost estimated at $4,949,000 includes flyaway cost, initial spars, ground support equipment (GSE), and training costs. Initial spares and GSE cost are assumed unchanged from the current CH-53D. The use of Kevlar-49 in the outer cover of the airframe is considered to provide a damage tolerance level similar to that of the current aluminum structure. For this reason, no change is considered in MMH/FH, so the incremental cost to train maintenance personnel is zero. Changes in flyaway cost are obtained from Table BI for the production aircraft, adjusted for amortization of composite aircraft non-recurring cost and are added to the current CH-53D acquisition cost to obtain the composite aircraft acquisition cost.

Weight empty of the current CH-53D is based on specification SD 552-1-3. The composite CH-53D empty weight is obtained by adding to the current aircraft the incremental change due to the composite design obtained from Table V.

Mission availability is based on a down-hour rate of 1.6 per flight hour for the current CH-53D. The use of composite materials may reduce this rate through reduction of corrosion and related inspection. However, in the absence of service experience in this area, the rate is considered unchanged, giving the same availability for the composite CH-53D as for the current vehicle. Mission reliability is based on an abort rate of 23 per thousand flight hours and an average mission time of .362 hour. For the composite vehicle mission, reliability is considered unchanged due to lack of service information.

Average mission productivity of the current CH-53D is obtained from the mission simulation previously discussed. The mission capability of the composite CH-53D is obtained by adding to the current aircraft value the incremental change in productivity due to the incremental change in weight. The partial derivative of mission productivity with respect to weight is -22.6 kg.m/s/kg (-.022 ton-knots/lb).

Operation cost of the current CH-53D, estimated at $357,500 annually in 1973, has been increased to $569,200. This increase reflects a 6 percent annual inflation rate to 1980 for all costs except fuel which is assumed to have increased 300 percent. Operation cost includes maintenance, replacement spares, replacement GSE, replacement training, fuel, and crew costs. Replacement spares, replacement GSE, and crew costs are assumed not to change. Change from the current aircraft maintenance cost and replacement training cost of maintenance personnel is a function of the incremental MMH/FH change for the composite aircraft. As mentioned previously, the MMH/FH are considered unchanged for the

composite vehicle compared with the current CH-53D. Therefore, maintenance and replacement training costs do not change. The effect of composite design on annual fuel cost is obtained from the incremental fuel flow due to change in aircraft weight empty 0.8 kg fuel/hr (1.8 lbm/hr) times the cost of fuel 2.24 cents/kg of fuel (5.55 cents/lb) times the annual 500 flight hours, i.e., $50 annually, is considered negligible. Therefore, the operating cost of the composite CH-53D is considered to be the same as the current CH-53D.

Fleet size of the composite CH-53D is based on the number of aircraft required to maintain the fleet mission effectiveness of the current CH-53D, where mission effectiveness is defined as the product of productivity, availability, and reliability.

Fleet life cycle cost is the summation of acquisition cost, assuming that the basic aircraft development cost has been amortized, plus operating cost for the required fleet size flying an average of 500 hours a year per aircraft over a 10-year service life.

The increased productivity of the composite aircraft coupled with its reduced acquisition cost results in a reduced fleet cost of $401,000,000 over a 10-year service life. The results of a 10-year life cycle cost of operation analysis are summarized in Table X.

From Table X it can be seen that the 0.3 percent savings in vehicle acquisition cost coupled with a 6.5 percent greater productivity than the current vehicle produces a 6.3 percent reduction in fleet life cycle cost.

THIS PAGE INTENTIONALLY LEFT BLANK

SECTION 9.0 CONCLUSIONS AND RECOMMENDATIONS

The single cure concept, as developed, provides an economical approach to the fabrication of large helicopter airframe sections utilizing composite materials. The application of composite materials to these airframe components can produce a significant savings in weight through the use of selective reinforcement, providing the designer with a new freedom not before available.

9.1 CONCLUSIONS

1. Fabrication of multi-element frame/stringer/skin sections by the single or one step cure concept as developed has been proven feasible and with automated equipment for cutting of composite materials and the layup of these materials, provides the potential for significant manufacturing savings.

2. A revised weight analysis, utilizing the data derived from the actual fabrication of the fuselage shell sections confirms an 18 percent projected weight savings in the fabrication of a complete composite airframe.

3. The acquisition cost of a production composite vehicle in the 1980 time frame is decreased by only 0.3 percent which is largely attributable to the increased cost of composite materials. However, when measured against the increased vehicle productivity and reduced fleet size requirements, a savings of 6.3 percent is realized in the 10 year life cycle costs to provide comparable mission capabilities.

4. Fatigue testing of frame and frame attachment specimens confirms the adequacy of the basic section in a fatigue environment In the curved sections, however, the radial loadings must be properly analyzed and acounted for by the introduction of additional stabilizing laminates if required.

5. The improved frame specimen incorporating the upper cap plies between the web plies provides a significant improvement in resistance to separation at the point of initial fracture.

6. The tooling concept utilizing lightweight shell tooling to the outside contour of the aircraft has shown good potential for low cost tooling for large composite airframe sections.

9.2 RECOMMENDATIONS

1. A detailed finite element analysis should be included in all future programs to provide design information for the selective reinforcement of frame elements in areas of complex combined loading such as joints or curved areas.

2. Additional investigations of highly loaded hardpoint attachment areas such as transmission and landing gear mounts should be accomplished.

3. Recent studies conducted by Sikorsky and others reveals the possibility that 121°C (250°F) cure Kevlar-49 and graphite/epoxy systems may be susceptable to moisture degradation in service. It is becoming apparent that 177°C (350°F) cure epoxies will be required for production systems. Preliminary investigation of 177°C (350°F) cure compatible core and laminate materials should be initiated.

SECTION 10.0 REFERENCES

1. Adams, K. M., and Lucas, J. J.: Study to Investigate Design, Fabrication and Test of Low Cost Concepts for Large Hybrid Composite Helicopter Fuselage - Phase I, NASA CR-132371, 1975.

2. Weiss, O. E.: Low Cost Manufacturing Using Advanced Composite Broadgoods, Third Quarterly Progress Report, AFML-F33615-74-C-5156, 1975.

3. Rich, M. J., Ridgley, G. F., and Lowry, D. W.: Application of Composites to Helicopter Airframe and Landing Gear Structures, NASA CR-112333, 1973.